PROTOCOL FOR CHANNELIZED DEBRIS FLOW SUSCEPTIBILITY MAPPING

By William J. Burns, Jon J. Franczyk, and Nancy C. Calhoun

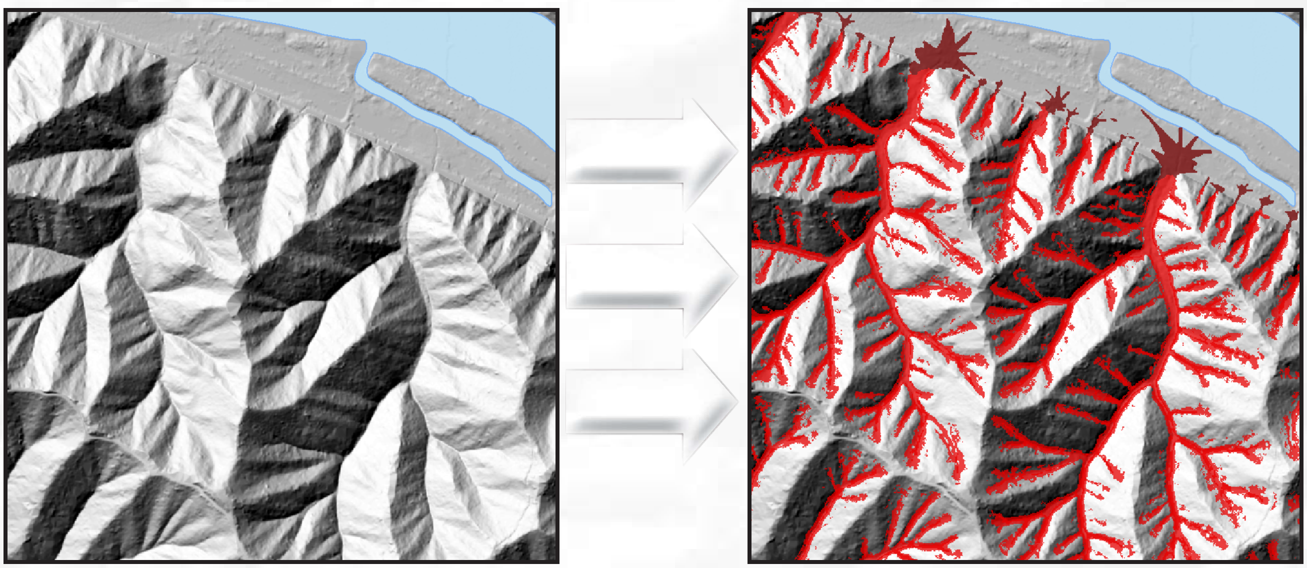

SPECIAL PAPER 53

2022

OREGON DEPARTMENT OF GEOLOGY AND MINERAL INDUSTRIES

State of Oregon
Oregon Department of Geology and Mineral Industries
Ruarri Day-Stirrat, State Geologist

SPECIAL PAPER 53

PROTOCOL FOR CHANNELIZED DEBRIS FLOW SUSCEPTIBILITY MAPPING

by

William J. Burns, Jon J. Franczyk, and Nancy C. Calhoun

2022

Oregon Department of Geology and Mineral Industries, 800 NE Oregon Street, Suite 965, Portland, OR 97232

DISCLAIMER

WHAT IS IN THIS REPORT?

The objective of this paper is to provide a protocol for developing channelized debris flow susceptibility maps that consistently categorize the potential for channelized debris flow into four categories: none-very low, low, moderate, or high. The datasets produced following this protocol include a channelized debris flows (CDF) inventory, as well as future CDF initiation susceptibilities, transport susceptibilities, overall basin susceptibilities, and inundation susceptibilities. The protocol is intended for internal use at Oregon Department of Geology and Mineral Industries (DOGAMI), as well as for use by the larger scientific community. By following this protocol, users can produce standardized maps relatively quickly and consistently. These maps can improve awareness of CDF hazards, which will help communities to design strategies that can better mitigate their landslide risks.

The intended audiences for this paper include those in government, industry, and academia who are interested in producing standardized landslide hazard maps. In addition, others may be interested in understanding how DOGAMI CDF susceptibility maps are made.

Expires: 1/1/2023

Oregon Department of Geology and Mineral Industries Special Paper 53
Published in conformance with ORS 516.030

For additional information:
Administrative Offices
800 NE Oregon Street, Suite 965
Portland, OR 97232
Telephone (971) 673-1555
https://www.oregongeology.org
https://oregon.gov/DOGAMI/

CONTENTS

LIST OF FIGURES

LIST OF TABLES

ArcGIS Toolboxes

An ArcPRO toolbox and ArcGIS toolbox are included as part of the digital publication bundle.

DF_ArcPRO_Toolbox.tbx

Part 1_Base Maps

Part 2_Initiation and Transport

Part 3_ Basins

Part 6_Inundation Zones Post-Processing

DF_Growth_ArcGIS_Toolbox.tbx

Part 4_Debris-Flow Growth Pre-Processor

Part 5_Multi-Point Laharz_py

ArcGIS CDF Inventory Geodatabase and Pilot Areas GIS Results

See the digital publication folder for files. Geodatabase is Esri® version 10.1 format.
Metadata is embedded in the geodatabase and is also provided as separate .xml format files.

CDF_Inventory.gdb

Amazon.gdb

Dean.gdb

Letz.gdb

Appendix

Detailed Procedures for the ArcGIS Toolboxes Part 1, 2, 3, & 6

Story Map

Understanding CDF in Oregon Story Map Link to Story Map

1.0 REPORT SUMMARY

Landslides are one of the most significant natural hazards in Oregon, causing occasional fatalities as well as millions of dollars in damage annually. Identifying areas susceptible to landslides is a critical step in reducing landslide risk. This paper describes the protocol used by the Oregon Department of Geology and Mineral Industries (DOGAMI) to develop standardized channelized debris flow (CDF) susceptibility maps. By identifying areas prone to CDF, this protocol and products produced by following this protocol can be used to help Oregon communities become more resilient to landslide hazards.

The CDF susceptibility map protocol described here is based on a CDF inventory dataset, which is used to calibrate the model to the local conditions and to define four relative CDF susceptibility zones (none-very low, low, moderate, high) for each of the process subdivisions (initiation, transport, etc.):

- Initiation (none-very low, low, moderate, high)
    - Slope, curvature, distance to channel
- Transport (none-very low, low, moderate, high)
    - Gradient and confinement
- Overall Basin Susceptibility (none-very low, low, moderate, high)
    - Combination of initiation and transport
- Inundation Susceptibility (none-very low, typical, intermediate, extreme)
    - Multi-Point LAHARZ model

The protocol also provides an online story map for sharing the data online at a scale of 1:8,000.

2.0 INTRODUCTION

The Oregon Department of Geology and Mineral Industries (DOGAMI) systematically maps landslides and creates landslide inventories in Oregon following the lidar-based mapping method described in Burns and Madin (2009). Landslide maps are significantly improved using this method and lidar-based mapping techniques (Burns, 2007).

The landslide map and inventory can then be used to make a susceptibility model to show the areas that are most likely to experience landslides in the future. There are several landslide types that behave differently. For this reason, there are different landslide susceptibility models for different types of landslides. Burns and others (2012b) published a method for shallow landslide susceptibility mapping (less than 15 feet [4.6 m] deep); Burns and Mickelson (2016) published a method for deep landslide susceptibility mapping (greater than 15 feet [4.6 m] deep). In this paper, we develop another method for the mapping of channelized debris flow susceptibility. Channelized debris flows (CDF), sometimes also referred to as rapidly moving landslides (RML), are a type of landslide that tend to move rapidly and are particularly dangerous to life and damaging to property (**Figure 1;** Highland and others, 1997).

Figure 1. Photo of the Hausmann residence on Highway 38 between Reedsport and Scottsburg, Oregon, inundated by a channelized debris flow (CDF) on Nov. 18, 1996. The home was occupied at the time, but fortunately no major injuries occurred. Note the chaotic mix of woody debris, boulders, smaller rocks, and mud, characteristic of a debris flow. Photo provided by John Seward, Oregon Department of Forestry.

Several Oregon state agencies have modelled the initiation locations, transport zones, and/or the depositional areas of CDFs in Oregon using various Geographic Information Systems (GIS) based methods. These efforts include western Oregon debris flow hazard maps produced by the Oregon Department of Forestry (Robison and others, 1999) and a GIS overview map of potential RML hazards in western Oregon produced by DOGAMI (Hofmeister and others, 2002). These previous attempts used the National Elevation Dataset (NED), which is a 10 m (32 ft) resolution digital elevation model (DEM) grid. Instead, we use lidar-derived 3x3-ft (1x1-m) resolution DEMs, which more accurately images the surface of the ground.

The objective of this paper is to provide a protocol for developing CDF susceptibility maps that consistently categorize areas according to a CDF potential of “none-very low,” “low,” “moderate,” or “high.” The datasets produced following this protocol include: a CDF inventory (where CDFs have occurred in the past), as well as future CDF initiation susceptibilities (where CDFs are likely to start), transport susceptibilities (where CDFs are likely to move through), overall basin susceptibilities (which watersheds are likely to have CDFs), and inundation susceptibilities (where CDFs are likely to deposit).

The protocol is intended for internal use at DOGAMI to produce maps for the State of Oregon and its communities and citizens. It may also be used by other government entities, private companies, and academic institutions who seek to produce standardized CDF hazard maps. In addition, others may be interested in understanding how DOGAMI CDF susceptibility maps are produced. These maps can improve awareness of CDF hazards, which will help communities to design strategies that can better mitigate their debris flow risks and become more resilient to debris flow hazards.

This study was funded in part by grants from the U.S. Geological Survey (USGS) Landslide Hazards Program and the Federal Emergency Management Agency (FEMA). DOGAMI plans to publish CDF susceptibility maps developed using this protocol for select areas as needs arise and as funding allows.

2.1 Description of CDFs

CDFs are complicated landslide processes, typically associated with periods of heavy rainfall. For a general factsheet giving details on debris flow features, see Pierson (2005; https://pubs.usgs.gov/fs/2004/3142/pdf/fs2004-3142.pdf).

CDFs commonly start in three basic ways: 1) a shallow landslide entering a channel, 2) erosion of the slopes adjacent to the channel through rilling, or 3) erosion directly within a channel or in colluvium-filled hollows (Reid and others, 2016). As the debris flow continues down the channel, it erodes sediment in the channel, which commonly results in volume growth of the debris flow. Additional water and sediment can add to the debris flow along the channel path or additional debris flow pulses can form in adjacent channels and coalesce with the main flow. When the debris flow reaches the mouth of the channel, it tends to run out onto the flatter unconfined ground, forming a deposit with a consistency similar to wet cement (**Figure 2**).

Commonly, as CDFs transport down a channel, they grow in volume through erosion of sediments and debris on the channel bed and/or banks, rilling and surface erosion of slopes adjacent to a channel, or coalescence with neighboring channel debris flows, along with the addition of water (Reid and others, 2016). As they continue to down the channel, they can accelerate to speeds of tens of miles per hour, depending on material properties, confinement, and channel gradient. The transport process can reach relatively long distances, depending on the morphology of the channel. For example, some debris flows travel more than a mile down a channel before they stop.

When debris flows reach an unrestricted area, such as a canyon mouth, debris spreads out and slows down over the flatter, unconfined ground surface, commonly forming a fan-shaped run out deposit. (**Figure 2**). Debris flow fans can be made up of many events, stacking and accumulating over a long period of time.

CDFs tend to happen in the same channels repeatedly, because the factors leading to debris flows are all present. This can result in a fan deposit at the outlet of these drainages. A landslide inventory created by following DOGAMI Special Paper 42 (SP-42) contains these successive mapped debris flow fans (Burns and Madin, 2009). The Statewide Landslide Information Database for Oregon (SLIDO; Burns and others, 2008, and later releases) is a compilation of published landslide polygons from geologic maps in Oregon, updated with newly mapped SP-42 landslide inventory data where available (Franczyk and others, 2019). Another important dataset in the SP-42 landslide inventory is historic landslide starting points, which contain known CDF initiation locations (Franczyk and others, 2019).

Figure 2. Illustration displaying the three different types of CDF initiation, along with transport anddeposition. Note that the different types of CDF initiation do not commony occur together. If initiation starts in a channel or enters a channel, it can lead to transport). Transport can happen with or without erosion or volume increase. Most commonly, erosion happens during transport and the debris flow grows as it moves down channel. When the debris flow reaches the mouth of the channel, it tends to spread out in a fan-shapped deposit.

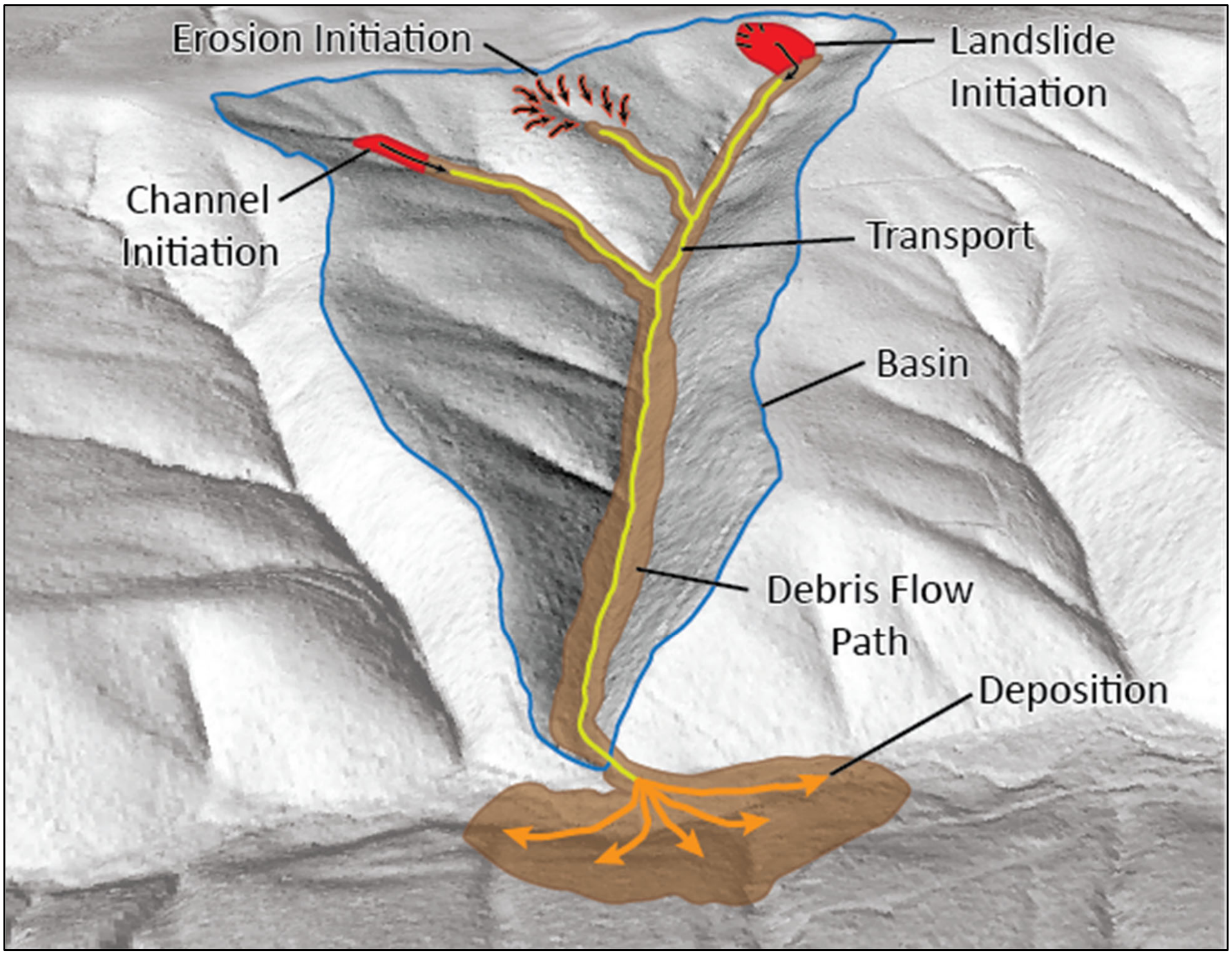

The protocol presented herein describes a new method to model areas susceptible to "typical," "intermediate," and "extreme" CDFs. The terms offer a range of CDF susceptibility zones from more frequent, smaller volume (typical) to least frequent, larger volume (extreme) events. This range is described in detail later in this paper. Note that some CDFs are very large and thus are anomalous and atypical. For example, if a large, deep landslide greater than >15 ft [4.6 m] deep) occurs within a basin—i.e., on the edifice of a volcano, or a from the sudden failure of mountain's flank—and transforms into a relatively very large catastrophic CDF that is so big it significantly changes the topography and morphology of the basin and the channels below, it is not a typical CDF (Burns and Madin, 2009).

The CDF process is part of a continuum of the mass movement to riverine processes that range from a CDF, to hyperconcentrated flow, to water flood. For context: CDFs generally have more than 50% sediment, hyperconcentrated flows have 20%-60% sediment, and water floods have less than 5%-10% sediment (Pierson, 2005). Because of this continuum, it is sometimes difficult to use field evidence to determine which process occurred. Sometimes, the process is a combination, changing back and forth from CDF to hyperconcentrated flow during the transport stage, for instance. The intent of this protocol is to help identify CDF susceptible areas and is not intended to identify the other processes of flooding or landsliding.

One important part of the CDF process is the increase in volume by channel bed erosion during transport, a process sometimes referred to as "entrainment" or "bulking." Volume growth along a channel can be expressed as a growth factor in map-view, along the horizontal channel length, or as a debris yield rate parallel to the channel (Reid and others, 2016). Debris flow events may exhaust sediment supply in a particular basin or initiation area. Between debris flow events, debris and/or colluvium can reaccumulate in the channel bed and banks. However, if colluvium does not reaccumulate in the channel between flow events, the CDF does not grow and may not continue to transport. In colluvium-poor conditions, the CDF may not even occur. Thus, the refilling process of the channel and bank debris affects the frequency (return period) and magnitude (size and volume) of CDFs.

Although the maps produced following this protocol are not intended to directly assess the frequency and magnitude of CDF hazards, they do identify areas susceptible to the CDF process in a nested hazard zone arrangement, which does imply generalized frequency and magnitude. Storm size and type (e.g., atmospheric river) can also affect the frequency and magnitude of CDFs. Future updates of this protocol should include frequency and/or magnitude data if available.

2.1.1 Confounding Factors

Wildfires can contribute to an increased frequency and magnitude of CDFs. This was evident in the 2018 post-fire debris flows in Montecito, California (Lukashova and others, 2019). The USGS Landslide Hazard Program has an active focus on post-fire debris flows through its Emergency Assessment of Post-Fire Debris Flow Hazards (https://www.usgs.gov/programs/landslide-hazards/science/post-fire-debris-flows).

Nonetheless, the research on post-fire CDFs has generally focused on more arid portions of the United States, such as southern California (De Graff and others, 2015). Research on post-fire CDFs is needed in western Oregon to understand the effects of wildfire better in a wetter and densely vegetated environment. Such research could then be integrated into future updates to CDF modeling. However, the protocol described here does not directly assess post-fire CDF hazards.

Forest management, such as road construction and removal of trees, can cause a loss of root strength and can change natural drainage patterns. This can increase susceptibility to CDF (Robison and others, 1999). Building roads, removing trees, changing drainage, and other factors involved with human-forest interaction can change over time, can change rapidly, and are site specific. Thus, unless the state creates some form of automated process, updating maps is nearly impossible. For example, clearcutting an area on private land can happen within weeks or months once a landowner makes that decision.

Thus, the maps produced following the protocol described in this report are not intended to assess forest management CDF hazards directly. However, they do identify areas already susceptible to CDF because of human actions; for example steep road fill embankments are visible in the lidar topography. Future updates of this protocol could include such factors if methods for tracking site-specific human-induced changes to landscapes can be established.

2.2 Model Calibration Data

Three large storms in 1996 and 1997 caused thousands of debris flows in Oregon (Hofmeister, 2000). These events caused several fatalities, and many Oregonians were impacted through property and infrastructural damage. Subsequently, many debris flows were mapped, cataloged into GIS, and analyzed. In addition, the potential for future debris flows in the same area were modeled.

An overview of mapping, cataloguing, analyzing, and modeling efforts is below:

- Robison and others (1999). Storm Impacts and Landslides of 1996.
- Hofmeister, R.J. (2000), Slope failures in Oregon, GIS inventory for three 1996/97 storm events.
- Hofmeister and others (2002), GIS overview map of potential RML hazards in western Oregon.

Several additional studies were performed years later including:

- Coe and others (2011a), Map of debris flows caused by rainfall during 1996 in parts of the Reedsport and Deer Head Point quadrangles, Douglas County, southern Coast Range, Oregon.
- Reid and others (2016), Forecasting inundation from debris flows that grow volumetrically during travel, with application to the Oregon Coast Range, USA.

The 1996 and 1997 landslide events triggered legislation geared at reducing future risk, the formation of a state task force, subsequent landslide mapping, and explanatory reports. Much of this is described in the recent publication by Burns and Franczyk (2021).

Many of the publications listed above form the basis for the CDF protocol presented here. To calibrate portions of this new model, we created a GIS dataset of initiation locations (points) and transport (lines). In this method, transport includes both erosion with volume increase and transport without erosion. We also used mapped CDF fan polygons from SLIDO 4.2 (Franczyk and others, 2019) to calibrate the model.

We initially attempted to use the historic CDF points in SLIDO 4.2, many of which are from the 1996-1997 events and include GPS locations. We realized that many point locations did not align with the lidar, likely due to the imprecision of GPS technology at the time (25 years ago) and of topographic base maps used during original mapping. An exception are the CDF locations mapped by Coe and others (2011a), which were initially located on orthophotos and then corrected to match the lidar topography (**Figure 3**, cluster near Reedsport).

A total of 680 historic CDF initiation sites were remapped by placing a new point in the central portion of the initiation area at each site. These 680 sites include those mapped by Coe and others (2011a). In this protocol, we define initiation as the CDF process that can occur as shallow landslide-adjacent or within a channel, erosion-adjacent or within a channel, rilling-adjacent to or in a channel, or by movement directly in a channel (**Figure 2**).

The 680 initiation points were located (not including Coe and others, 2011a) by examining 1) historic CDF data (SLIDO), 2) orthophotos collected as soon after the events as possible (less than 5 years in all cases), and 3) lidar hillshades (**Figure 4**). For many recorded debris flows in Oregon, lidar was collected after the events—such as the 1996-1997 debris flow events—and in many cases, the landslide scar or eroded area remains visible in the lidar hillshade. The 680 CDF initiation points were located as precisely as possible in the center of the initiation area using the lidar hillshades to ensure the best possible spatial statistics (slope, curvature, distance to channel).

After relocating initiation points, we buffered each point into a circular polygon with 36 ft (11 m) radius and area of 4,072 ft^2 (378 m^2) (**Figure 4**). Coe and others (2011a) found a mean CDF initiation size of 3,983 ft^2 (370 m^2) in the Oregon Coast Range.

Figure 3. Map of the 680 historic CDF initiation sites in western Oregon. Many of these historical records are newly updated with their locations corrected.

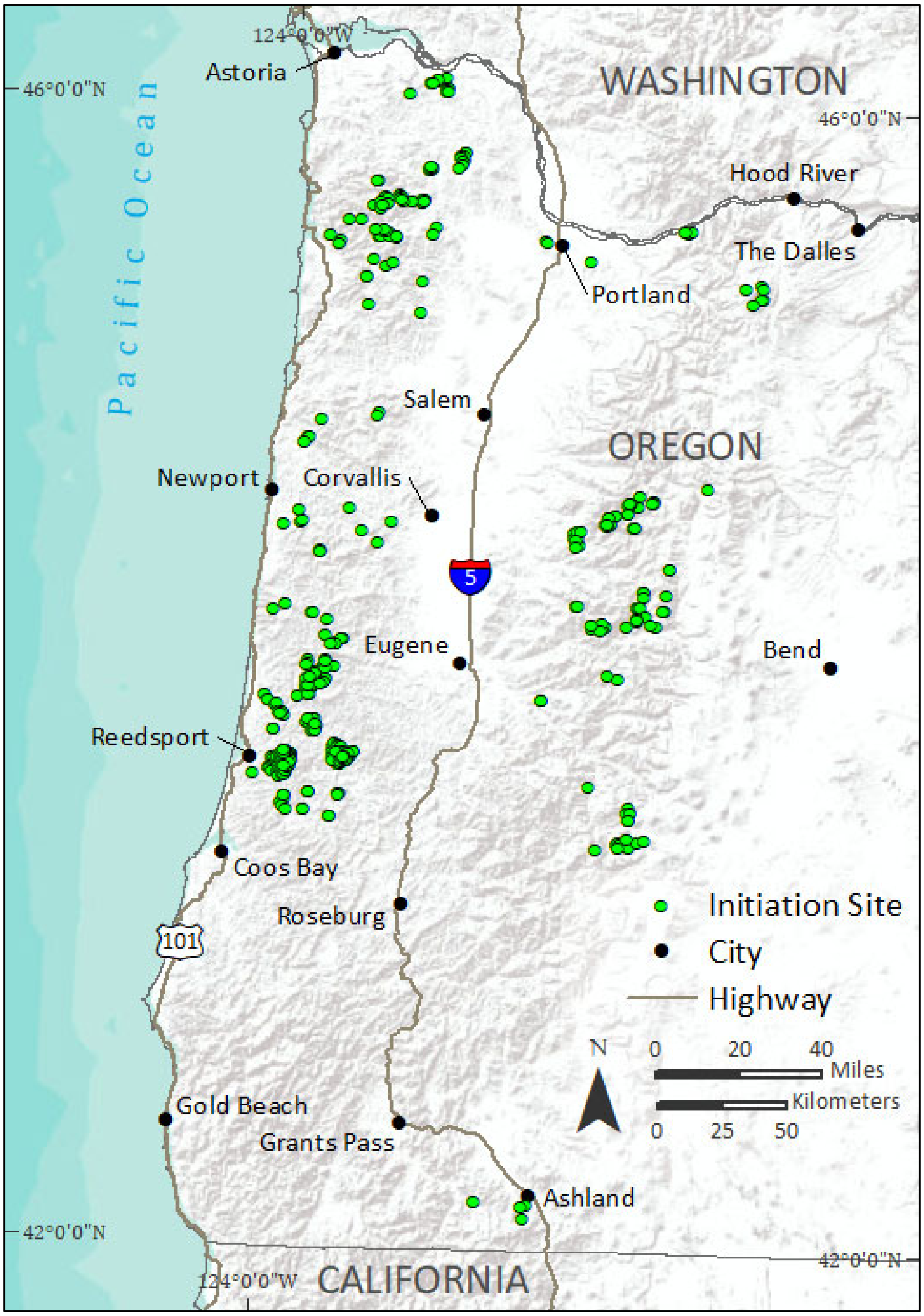

Figure 4. A) Example of a February 1996 CDF originally located in the field (2 black points) soon after the event. The base map is a 2000 orthophoto (NAIP) in which a single 1996 CDF event can be clearly seen. B) Same location and scale as inset A. Relocated CDF initiation centroid (green point) with visible scar in the lidar hillshade combined with the 2000 orthophoto (NAIP); includes originally located in the field (black points). C) Zoom view of the relocated point and 36-foot circular polygon (black outlined circle around the green point) used to perform the spatial statistics; includes originally located in the field (black point).

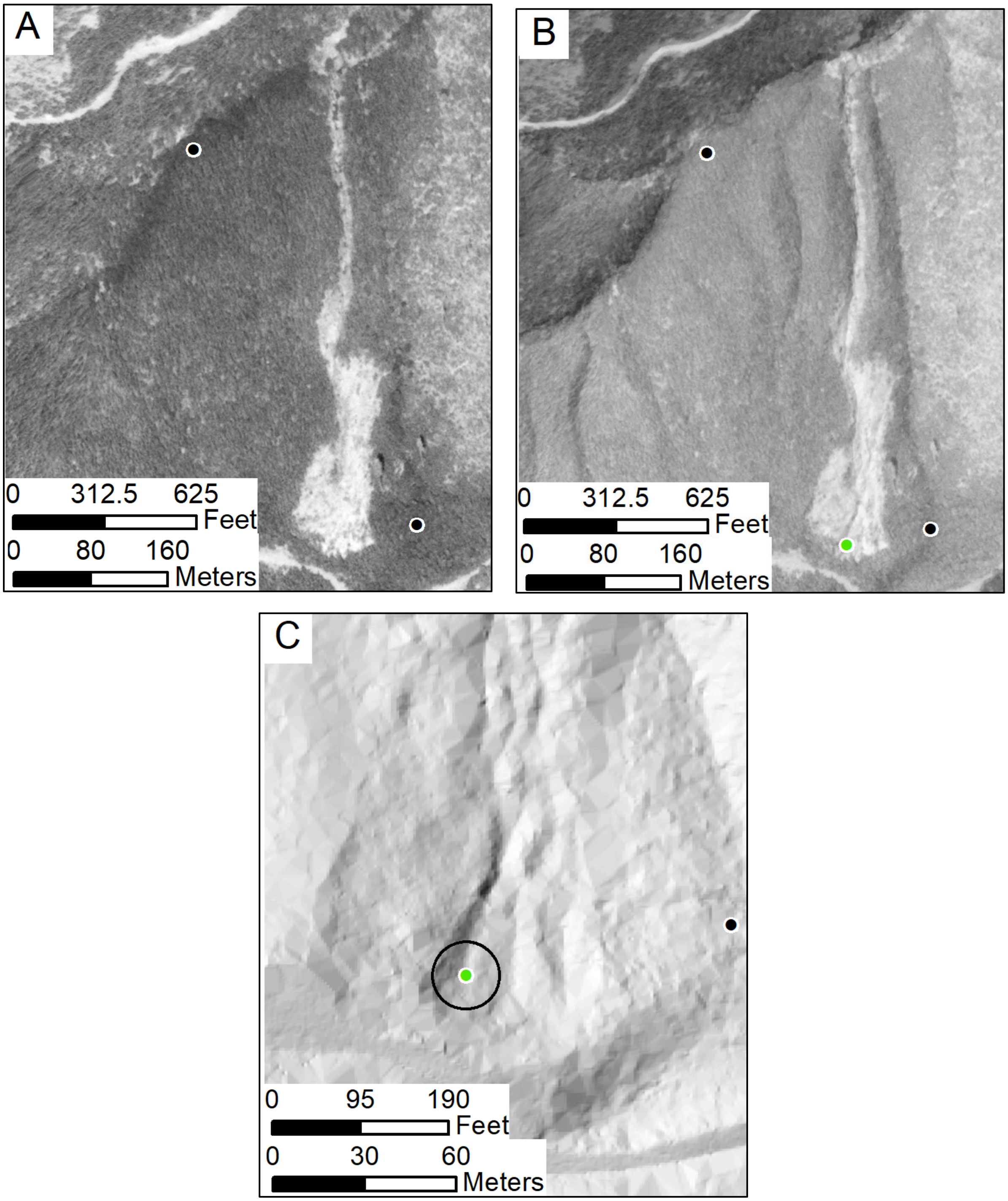

The 680 CDF initiation points, now aligned with lidar-based topography, were used as locations to select adjacent, downslope channel segments that experienced transport. All of the historic 680 events experienced transport in a channel. These channels were evaluated using spatial statistics to characterize the channel gradient and confinement, two factors that may affect debris flow behavior (**Figure 5**).

Channels mapped as having debris flow activity along them were divided into 100 ft (30.5 m) sections. Each of these segments were examined visually (using air photos and lidar-derived datasets such as slope and hillshade) and classified as segments experiencing transport and/or erosion or segments experiencing deposition. The dataset defining channel segments contains 11,787 total segments; 10,253 are segments of transport and/or erosion and 1,534 are segments that experienced deposition.

Figure 5. A. Example of a channel (green line) selected for spatial statistics. Initiation site (green dot) is the same locations in Figure 4B. Base map includes orthophoto from 2000 (NAIP) and lidar hillshade in which the 1996 CDF event can be clearly seen. In this example only the segements of transport and/or erosion are clearly identified. The depositon segements are likely off the map.

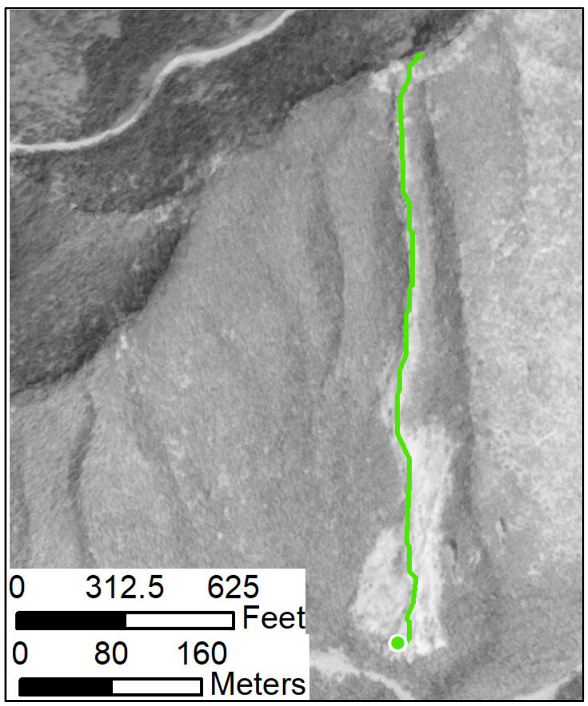

3.0 METHODS

3.1 Overview and Setup for Using Protocol

Channelized debris flows are typically divided into three major stages: initiation, transport (erosion), and deposition; these are the basis for the steps in this CDF protocol. The protocol consists of three primary sections: Section A - CDF Inventory; Section B – Initiation; Transport, and Basins; and Section C - Inundation. The inundation section uses a toolbox provided by Reid and others (2021: https://code.usgs.gov/ghsc/lhp/df_growth). The method has also been published as Reid and others, (2016). These three primary sections are divided into 11 steps, detailed below Table 1. This protocol includes two GIS toolboxes with the following parts:

DF_ArcPRO_Toolbox.tbx

Part 1_Base Maps

Part 2_Initiation and Transport

Part 3_Basins

Part 6_Inundation Zones Post-Processing

DF_Growth_ArcGIS_Toolbox.tbx

Part 4_Debris-Flow Growth Pre-Processor

Part 5_Multi-Point Laharz_py

Table 1. Graphical representation of the CDF susceptibility protocol discussed in this paper. A reduced-in-size version of this table is used throughout this paper as a flowchart, termed "methodology progress bar," to assist the user.

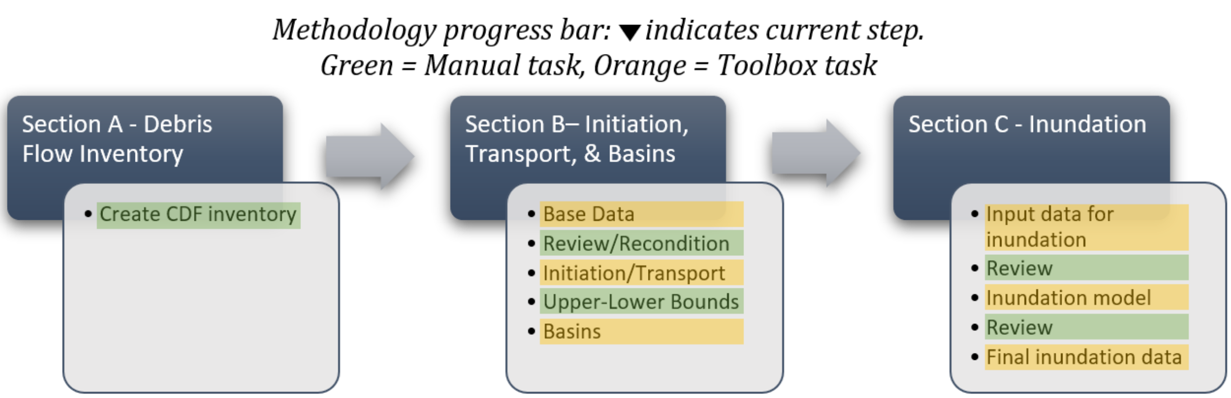

Section A: Debris Flow Inventory

Step 1 – Create an inventory dataset of historic and prehistoric channelized debris flow deposits (fans) and historic CDF events (initiation, transport, and deposition) in the proposed study area.

Section B: Initiation, Transport, and Basin Susceptibility

Step 2 - Create base datasets using DF_ArcPRO_Toolbox Part 1_Base Maps.

Step 3 - Review base datasets. Perform DEM reconditioning of erroneous channels. If reconditioning is needed, rerun Step 2 with reconditioned DEM.

Step 4 - Create initiation and transport susceptibility zones using DF_ArcPRO_Toolbox Part 2_Initiation and Transport.

Step 5 - Map upper-lower bounds. This will result in a polygon which crosses the channels, creating an intersection which becomes the pour points to define the basins.

Step 6 - Create the basins with overall susceptibility using DF_ArcPRO_Toolbox Part 3_ Basins.

Section C – Inundation Susceptibility

Step 7 - Create input data for inundation modeling using DF_Growth_ArcGIS_Toolbox Part 4_Debris-Flow Growth Pre-Processor.

Step 8 - Review and clean up pre-processor data.

Step 9 - Create inundation zones using DF_Growth_ArcGIS_Toolbox Part 5_Multi-Point Laharz_py.

Step 10 - Review typical inundation susceptibility zones and compare to CDF Inventory (Step 1). If zones are too small or too large, select new, more appropriate growth factor and rerun Steps 7 to 10.

Step 11 - Create final datasets for inundation zones using DF_ArcPRO_Toolbox Part 6_Inundation Zones Post-Processing.

We used the same four susceptibility classification schemes for all intermediate and final datasets (none-very low, low, moderate, and high), except for inundation which is classified as "typical," "intermediate," and "extreme." The susceptibility for the rest of the area not in these three zones is considered none-very low (**Figure 6**). Dividing susceptibility into more classes would exceed the level of detail in the available input datasets. The scores for each factor, for example slope, curvature, and distance to channel, are all equally weighted. In the future, determination of influence of each factor could lead to weighting the factors more appropriately than all equal.

We selected three pilot study areas on which to run the model: 1) the Dean Creek Watershed, which was previously estimated to have a high hazard throughout, 2) the Letz Creek Watershed, which was estimated to have a range of hazard levels, from none-very low to high, and 3) the Amazon Creek Watershed, which was estimated to have a none-very low CDF hazard (**Figure 7**). Following this protocol creates many intermediate and final datasets, as documented in **Figure 6**.

Figure 6. Diagram of various intermediate and final datasets and susceptibility classification schemes for the CDF protocol described in this report.

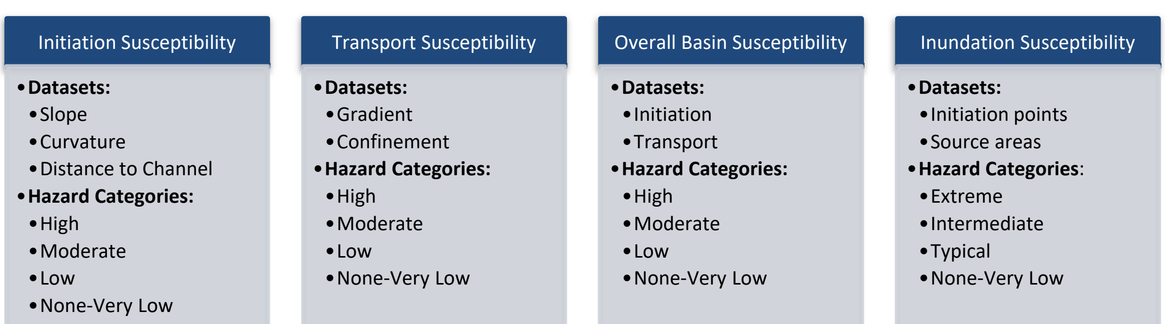

Figure 7. Locations of the three pilot study areas (orange outlines). (1) Dean Creek Watershed is estimated to have a high CDF susceptibility and has had many recorded CDF events. (2) Letz Creek Watershed is estimated to have a range of CDF susceptibility from none-very low to high and has had a few recorded CDF events. (3) Amazon Creek Watershed is estimated to have CDF susceptibilites of none-very low, and has no recorded CDF historic events.

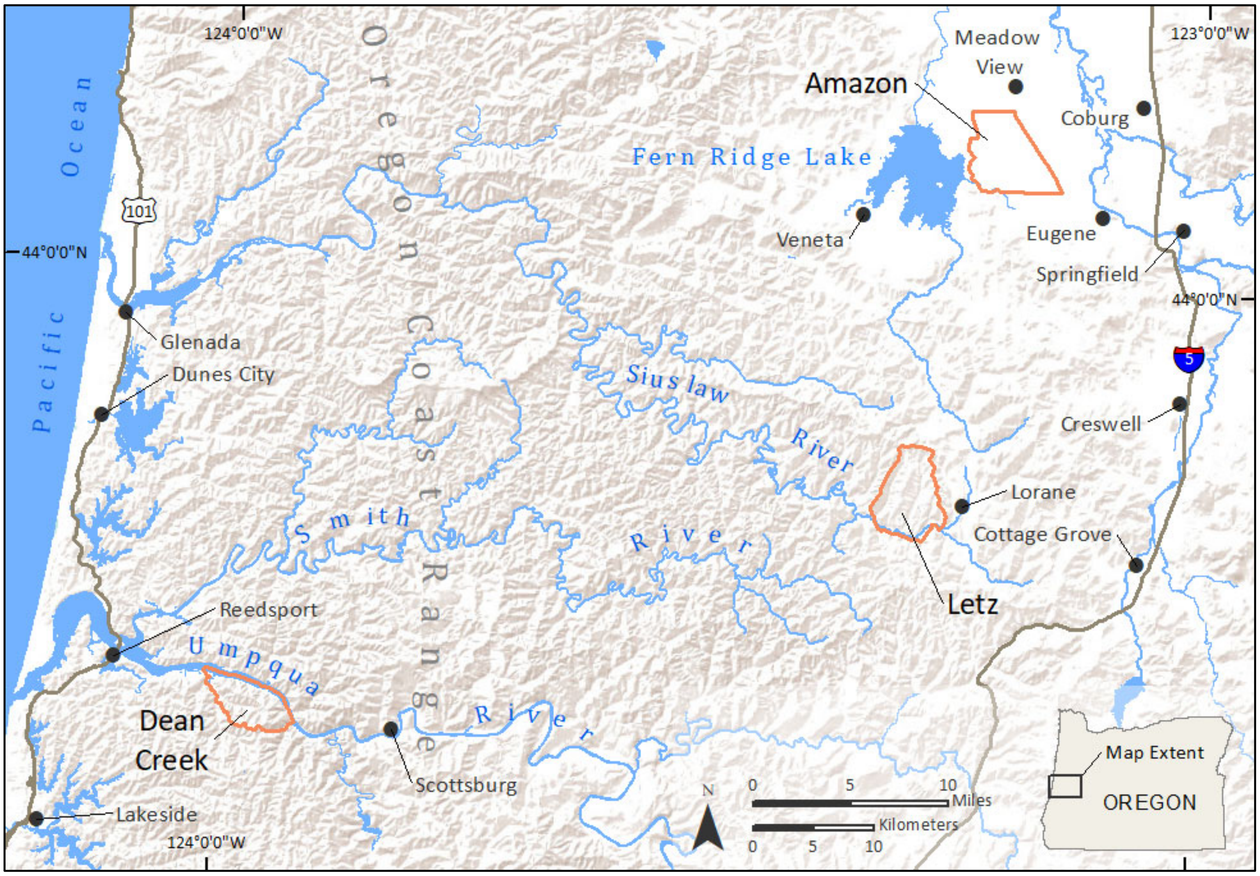

This protocol begins by defining a study area or areas with polygon(s) (**Figure 8**). We recommend using watershed boundaries to define study areas, as CDFs tend to follow natural channels and drainage systems. We recommend using National Hydrography Dataset Watershed Boundary Dataset sixth field or 12-digit hydrologic unit code polygons (HUC12) as a starting place to define the study area (https://www.usgs.gov/core-science-systems/ngp/national-hydrography). Depending on the area of interest or computing power, the user can reshape the HUC12 polygon to a smaller extent or combine with other HUC12 polygons.

Because some HUC watershed boundaries were created using the National Elevation Dataset which has a cell size of 10-m, make sure to extend slightly beyond the upper and lower boundaries of the watershed so the entire watershed is captured. Once the study area boundary is defined, use this extent to extract a lidar-derived bare earth DEM (**Figure 8**). In Oregon, most of the DEMs coming from the Oregon Lidar Consortium should have 3x3-ft (1x1-m) raster cells and be in the Oregon statewide projection (NAD1983HARN Oregon Statewide Lambert Ft Intl).

This DEM serves as the input dataset for Step 2 (DF_ArcPRO_Toolbox Part 1_Base Maps).

Figure 8. Example study area of the Letz Creek watershed, considered to have a range of CDF susceptibility levels. DEM displayed as a hillshade. The box is the location for many subsequent maps in this report, which also have a hillshade as the basemap.

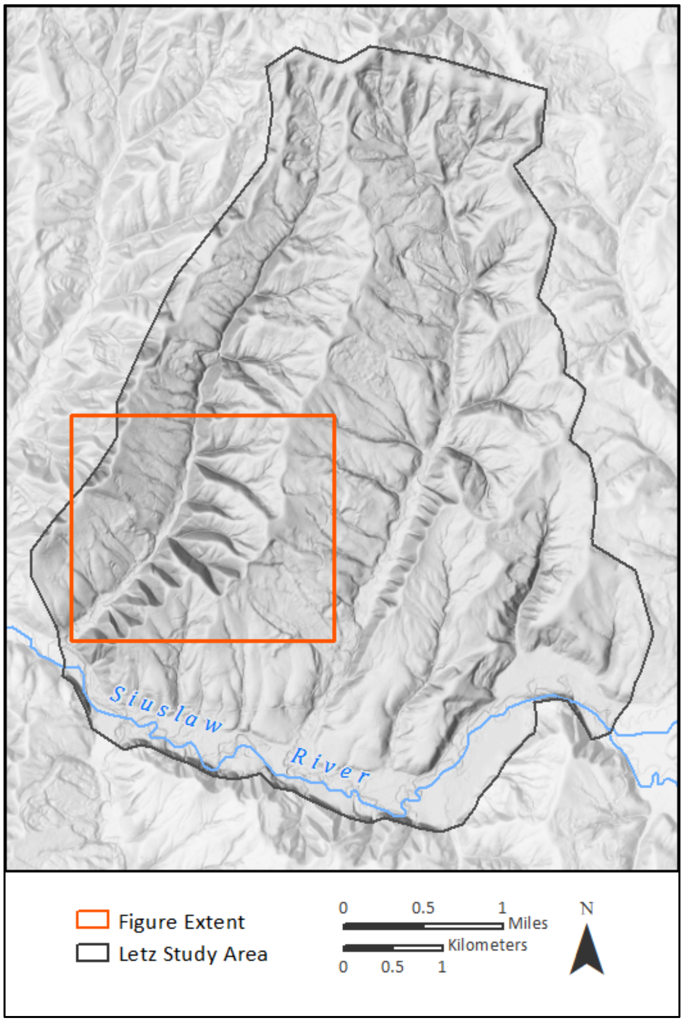

3.2 Step 1: Debris Flow Inventory

Methodology progress bar: ▼ indicates current step.
Green = Manual task, Orange = Toolbox task

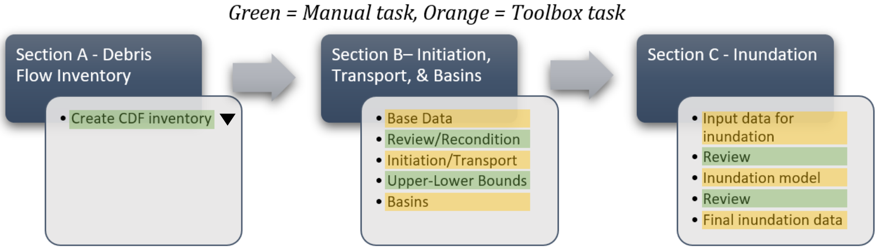

The first step is to document CDF activity in the study area. Start by creating an inventory dataset of historic and prehistoric CDF deposit areas or fans in the proposed study area (Burns and Madin, 2009). Next a historic landslide inventory should be created including any recorded CDF events, including delineation of initiation, transport, and deposition areas (**Figure 5**).

A geodatabase with the 680 CDF initiation sites is included with this publication as a template for future mapping efforts. In Oregon, statewide orthophotos from 1995 to 2022 (NAIP) are readily available, which should be used in combination with the lidar topography to create the historic events inventory. Additionally, all local data such as city and county records should be acquired and combined with data extracted from the most current release of SLIDO.

3.3 Step 2: Create Base Datasets

Methodology progress bar: ▼ indicates current step.
Green = Manual task, Orange = Toolbox task

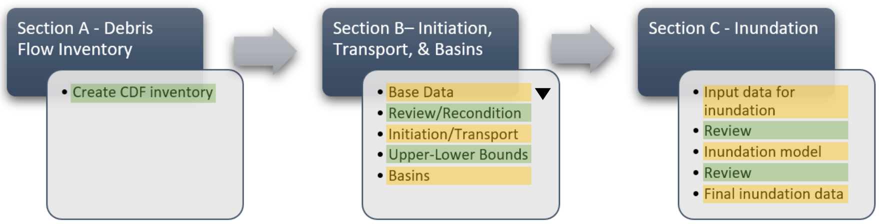

The second step is accomplished by running DF_ArcPRO_Toolbox Part 1_Base Maps. Because this is a regional evaluation and because it is a relatively automated method, the tool first changes the resolution of the bare earth lidar-derived DEM from the standard Oregon Lidar Consortium 3x3-ft (1x1-m) raster cells to 9x9-ft (2.7x2.7-m) raster cells. Hydrography tools such as flow direction and accumulation perform better at this resolution because it removes very small topographic changes, and can be processed faster without losing much topographic details. A series of base layers are created from the larger raster cells. The first is a "filled DEM," in which the closed depressions—where water may hypothetically pool and collect—are filled in. The hydrography toolset cannot interpret where, for example, culverts under roads exist, and open depressions may cause false "dams" in channels during analysis.

Using the filled DEM, the tool creates hillshade and slope layers. A flow direction grid is also created, followed by a flow accumulation grid (DF_ArcPRO_Toolbox Part 1_Base Maps.). The flow accumulation grid defines how many and which DEM cells flow into other cells over the entire study area. The flow accumulation grid is one of the datasets used to define the channels. Several studies have shown that defined minimal amounts of flow accumulation or drainage area are needed before enough area (and thus potential accumulated water) is concentrated for channels to initiate development (Montgomery and others, 1993). Coe and others (2011b) found the upslope contributing area for channel initiation in the Dean Creek watershed of Oregon to be 1,529 m^2 (16,458 ft^2) and Griswold and Iverson (2008) used 1,000 m^2 (10,764 ft^2).

Nonetheless, application of a single flow accumulation threshold over diverse geologic and geomorphic regions provided nonoptimal results across study areas, requiring usage of a curvature-based drainage network. Curvature-based drainage network delineation uses a method of identifying concave grid cells combined with a weighted drainage area computation (Tarboton and Ames, 2001). In conjunction with a flow accumulation grid, a curvature grid with a concavity threshold applied (below which channels are not delineated) is used as a weight so channels can be differentiated from nonchannelized overland flow (Brien, personal communication). The DEM is smoothed using a 32.8-ft (10-m) radius neighborhood before calculation of planform curvature. A concavity threshold of -2 in units of one hundredth (1/100) of a foot (1/30.5 of a meter) is used to create the curvature weight grid. Finally, the curvature weight grids, a minimum concavity size of 10 m^2 and contributing concave area of 200 m^2 (200 rasterized 9x9 m cells) are combined and a channel network is created.

The channel network is used to define stream orders using the Strahler method (Strahler, 1952), which defines a stream number based on hierarchy of tributaries. Finally, the channel network is converted to polylines (**Figure 9**). The lines are split into 100-ft (30.5-m) horizontal length segments (**Figure 10**). Because the channels are connected to each other, segments also occur where one channel meets another resulting in some segments less than 100-ft (30.5-m). Channels identified as first order (i.e., no contributing tributaries), with lengths less than two grid cells (or 18 ft [5.5 m] long), and on nearly flat ground are removed from the dataset, because they are unlikely to be susceptible to CDFs.

Figure 9. Map of a channel network (blue lines) defined by start locations of flow accumulation using a threshold of 16,000 ft^2 (1,500 m^2) or approximately 200 rasterized cells at 9x9 ft (2.7x2.7 m) each. The curvature weight grids, minimum concavity size of 10 m^2 and contributing concave area of 200 cells are combined and a channel network is created.

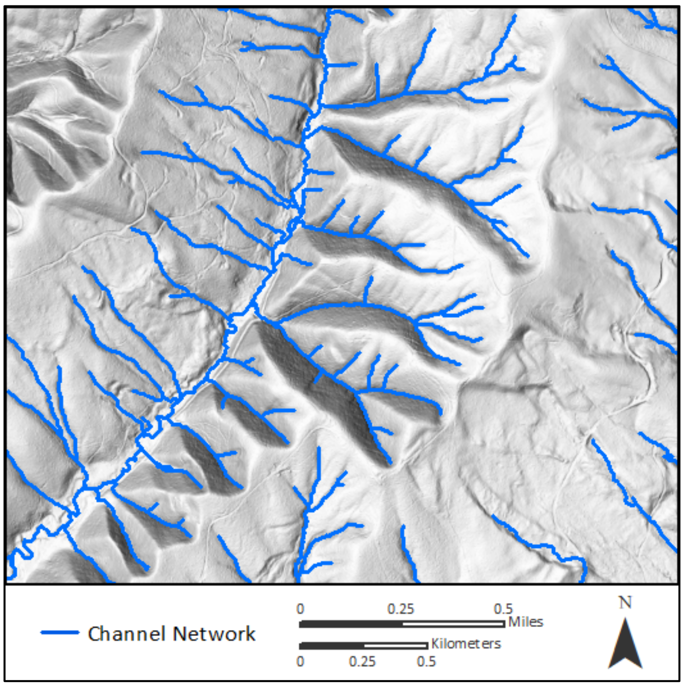

Figure 10. Example map of 100-ft (30-m) channel segments (blue lines are channels and red dots at 100-foot [30-m] segment intersections). Because the channels are connected to each other, segments also occur where one channel meets another resulting in some segments shorter than 100 ft (30 m).

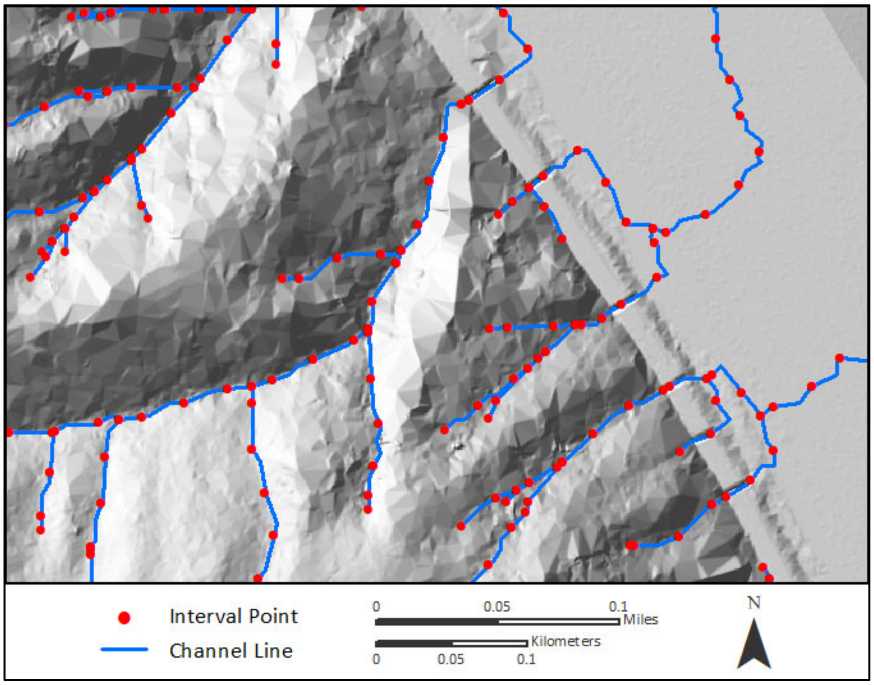

3.4 Step 3: Review, Reconditioning DEM, and Channel Cleanup

Methodology progress bar: ▼ indicates current step.
Green = Manual task, Orange = Toolbox task

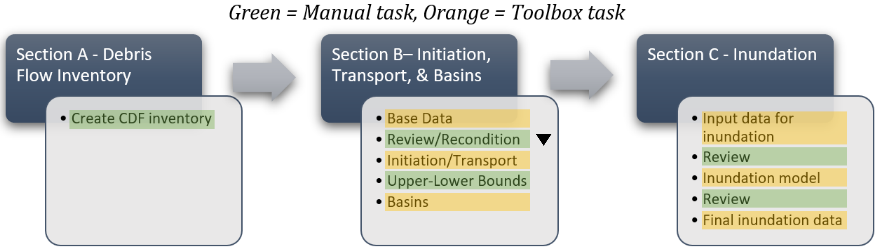

The results of Step 2 sometimes have erroneous channels even after the fill tool is implemented. This is primarily due to roads, large waterbodies, or very flat areas. For example, a channel intersects a road on a slope and turns 90° and follows the road ditch instead of continuing down channel below the road (likely through a culvert).

We recommend using the DEM Reconditioning tool to correct the channel paths, sometimes referred to as "burning in streamlines to the DEM." The DEM Reconditioning tool is part of the Esri Arc Hydro toolset, a free toolset downloadable from Esri website (**Figure 11**). The inputs are the original 3x3-ft (1x1-m) raster DEM and a set of generally short channel lines/segments that define where the DEM is reconditioned (**Figure 12C**). These reconditioning line segments should be as short as possible, for example from one edge of the relative flat road edge to the other, and not entirely up and down road fill embankments.

Note, each reconditioned channel line needs a unique identification for the tool to run correctly. We recommend using minimal values in the tool, so the final DEM has minimal differences (**Figure 11**). For example, a stream buffer of three cells (wide) and depth or smooth drop/raise of 1–5 ft (0.31-1.5 m) works in most cases.

Figure 11. DEM Reconditioning tool interface window. Each reconditioned channel line needs a unique identification for the tool to run correctly.

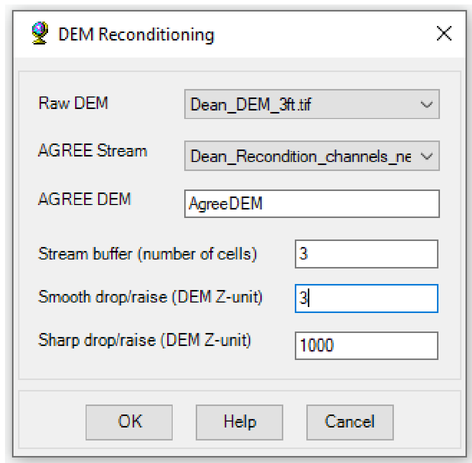

The amount of artificial filling performed by the ArcGIS Fill tool can be extreme (greater than several feet). These areas should be examined, and judgment used to decide when to recondition (e.g., manually inserting a channel across a road embankment) or to leave the channel to end behind the impediment. This is because the sink or closed basin (if deep enough) can act as a natural debris flow catch basin. These areas can be noted and later in the process, the inundation flow volumes can be compared to the closed basin volumes.

This part of the process can be extremely difficult; extreme caution should be used when deciding whether or not to undo the DEM Fill in a particular drainage. Undoing DEM Fill requires modeling the inundation only into the closed basin and not continuing past the closed basin; keeping the DEM Fill requires modeling the inundation as it continues down the channel, past the intentionally filled closed basin. Most cases should not require this decision, but some might, so this potential process is discussed below. This portion of the process occurs during the multi-point laharz inundation modeling step.

To recondition the DEM, start by identifying the locations of channels that do not continue down the natural slope (for example, channels following a road ditch at an angle to the natural hillside). If channel lines do not continue in a realistic location, use the DEM Reconditioning tool to align or “burn” new channels in the DEM through the road prism and/or into a waterbody (**Figure 12**).

Figure 12. "Burning in stream lines" technique. (A) Map showing the location and size of the Umpqua River (large waterbody) and Highway 38 (along the southwestern side of the Umpqua River). (B) Example of initial channel network output (blue lines). The channels intersect Highway 38 road prism along the southern bank of the Umpqua River and incorrectly follow the ditch on the upslope side of the road. The map also includes locations of proposed DEM reconditioning channels (red lines). The lines are drawn so that the channels will continue downslope over or through the road prism. (C) Reconditioned DEM. The new channels are "burned" into the DEM so flow paths will continue down the natural slope. (D) Output of reconditioned DEM channel lines, after the reconditioned DEM was used as input data for rerunning DF_ArcPRO_Toolbox Part 1_Base Maps. Note: The channels within the Umpqua River are examples of false channels.

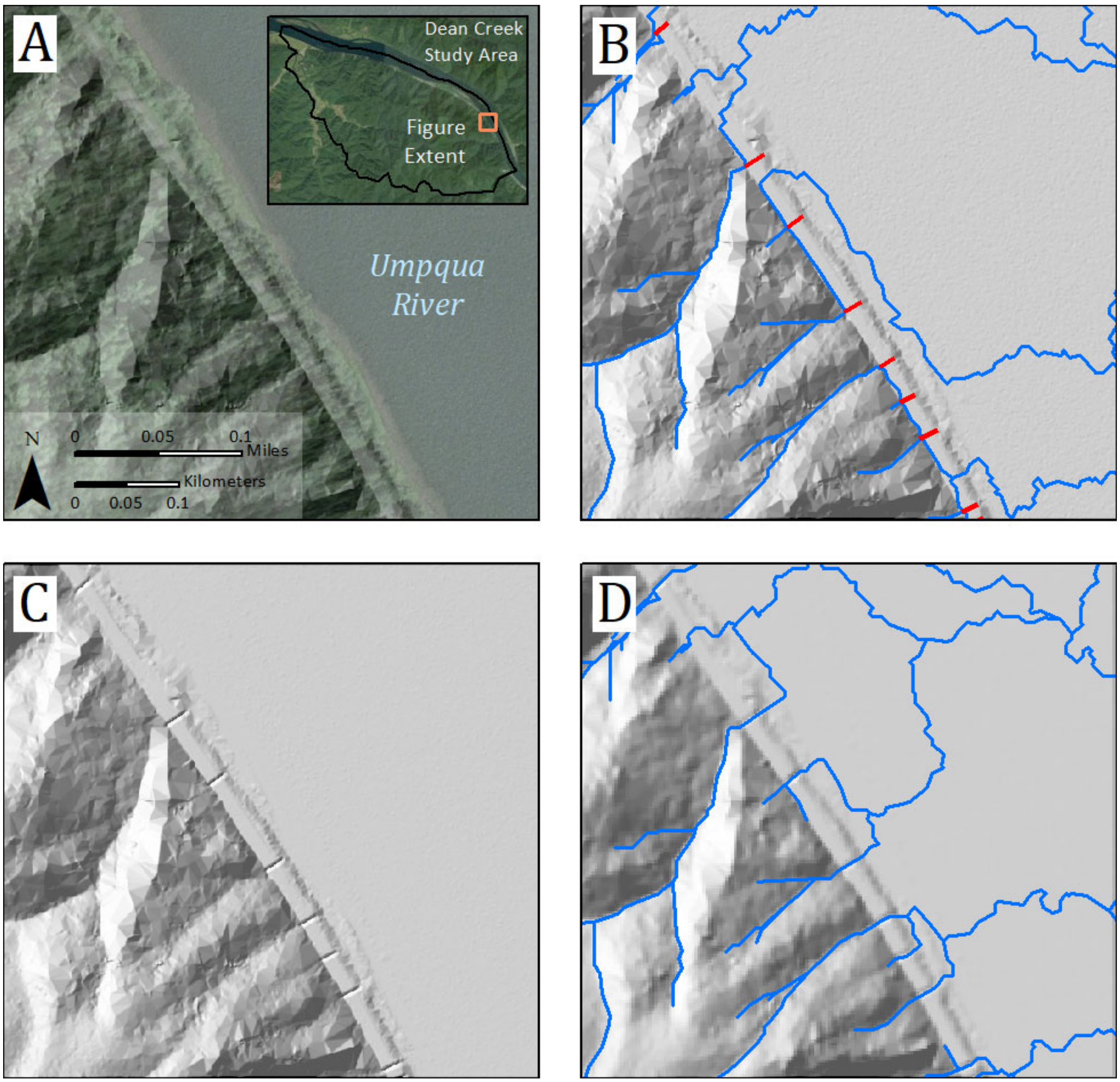

The hydrography tools have limitations in waterbodies and/or very flat areas. The hydrography tools do not recognize waterbodies as different materials than terrestrial land in the DEM and can create false channels (**Figure 12**). These tools treat the top of the water as a flat ground surface. Most channel lines within large waterbodies should be deleted during the channel cleanup process. However, we recommend keeping or reconditioning the DEM so that the channels continue into the waterbodies, so the inundation portion of this protocol can predict CDF inundation past the contact of land and water (**Figure 12**).

Once the channels traverse the waterbody for a reasonable distance, the remaining channels in the waterbody can be deleted. Later in the method, the inundation mapping within the waterbodies should be removed for the final susceptibility maps (DF_ArcPRO_Toolbox Part 6_Inundation Zones Post-Processing). This is because the LAHARZ model is only appropriately used on land. Some other more advanced channel-specific models are developed and appropriately model the interactions between a debris flow and a water body (George and others, 2017).

3.5 Step 4: Initiation and Transport

Methodology progress bar: ▼ indicates current step.
Green = Manual task, Orange = Toolbox task

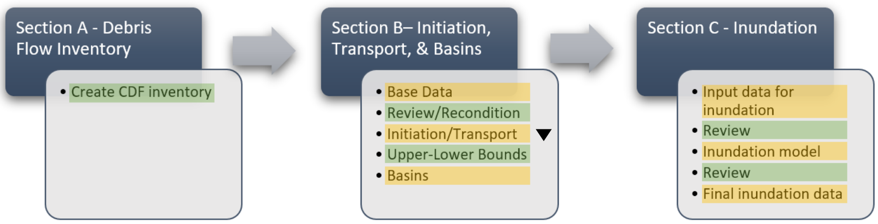

There are many ways a CDF can start. In Oregon, there are three primary ways debris flows initiate: 1) a landslide occurs on a slope, then material enters a channel and continues as a CDF, 2) erosion/rilling of material adjacent to a channel occurs; the material enters a channel and continues as a CDF, 3) erosion/initiation occurs within a channel and continues as a CDF.

Many criteria affect initiation of debris flows including geology, slope, curvature, concentration of water, minimal contributing area, distance to the channel, and human activities such as cuts and fills along a road prism and/or changes to hydrography. Some CDF initiation factors are easier to map than others. Also, as previously discussed, these factors can change over time, either slowly or rapidly. There are further details within these criteria for CDF initiation; for example, geologic information could include unit or formation level information, with details about the rate that each geologic unit produces colluvium into channels, and/or details about the specific geotechnical properties of each geologic unit.

Many studies have shown that steep slopes (most studies conclude 20°–30° or greater) are required to initiate CDFs and, inversely, CDFs will not continue in low gradient channels (Hungr and others, 1984; Benda and Cundy, 1990; Fannin and Rollerson, 1993; Fannin and others, 1997; Robinson and others, 1999; Washington Department of Natural Resources, 2004; Griswold and Iverson, 2008; Coe and others, 2011a; Blais-Stevens and Behnia, 2016; Reid and others, 2016).

We evaluated the mean slope angle, mean planform curvature, and distance to channels at the 680 historic CDF initiation sites throughout western Oregon to define this protocol's criteria for evaluation of initiation (**Figure 3**). DF_ArcPRO_Toolbox Part 2_Initiation and Transport is implemented next. The next sections of this paper describe the details used to create DF_ArcPRO_Toolbox Part 2_Initiation and Transport.

3.5.1 Steep Slopes

Spatial statistics were performed between the 680 initiation site polygons and the 9-ft^2 (~3-m^2) cell slope raster. We selected the mean slope within each initiation site polygon as the representative slope for each site. The results show an exponential increase of initiation frequency with increased mean slope (**Figure 13**).

The mean of all initiation sites slope angles is 39° with a standard deviation of 4.6° (**Figure 13**). No initiation sites had a mean slope of less than 15° or greater than 55°. As previously mentioned, many other researchers have found a slope of greater than 20°–30° is necessary to initiate CDFs. The 680 CDF initiation sites mapped in western Oregon support this conclusion through a sharp increase in frequency above 30° (**Figure 13**). The absence of CDF initiation sites on slopes steeper than 55° is likely due to minimal soil/colluvium development on slopes this steep.

Figure 13. Histogram and cumulative percent chart of 680 CDF initiation sites in western Oregon. No sites had a slope less than 15° or greater than 55°.

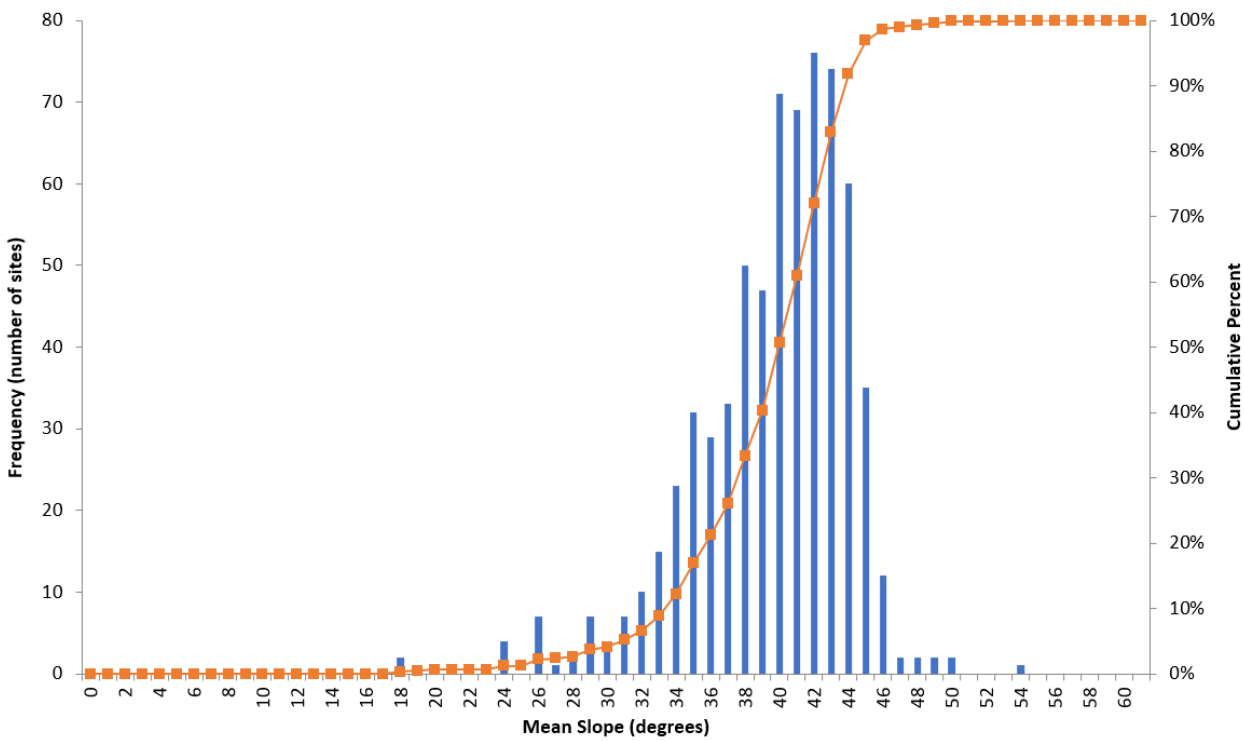

Robison and others (1999) examined hundreds of CDFs from the 1996 events throughout Western Oregon and found average slopes at initiation sites of 83% (40°), 92% (42.5°), and 55.5% (29°) for sites up slope of the channels, adjacent to the channels, and within the channels, respectively. Reid and others (2016) and Coe and others (2011a) examined approximately 155 CDF initiations in the Dean Creek watershed (Central Oregon Coast Range) and found nearly all CDFs initiated on slopes or in channels with a slope angle/gradient greater than 10° and up to approximately 60°. The new results found in this paper examining 680 CDF initiation sites were very similar to many past studies (**Table 2**).

Based on statistical results from the 680 sites and other studies, we selected a slope threshold for the high slope initiation class of 35° or greater, which is the mean (39°) minus one standard deviation (4.6°). We also selected a none-very low slope initiation class of 15° or less. Because the none-very low threshold of 15° and the high threshold of 35° are well supported, we selected 25° as the division between moderate and low, which is halfway between the high and the none-very low classifications (**Table 2**).

Once the slope thresholds are selected, the slope raster was classified into four classes and given a corresponding score (1 to 4):

- None-Very Low (1)
- Low (2)
- Moderate (3)
- High (4)

This process of establishing thresholds and converting to four classes and corresponding scores is used consistently throughout this protocol. Scores for slope, curvature, distance to channel, and other factors are then added together to determine overall initiation, transport, and basin susceptibility to CDFs. The number and percent of sites in each slope initiation class are shown in **Table 2**. **Figure 14** shows the spatial distribution of these four slope classes in the Letz Creek Watershed pilot area.

Table 2. Slope angle, number of sites, percent of sites, and slope initiation susceptibility classification and score of the 680 CDF sites in western Oregon.

Slope (degrees)	Number of Sites	Percent of Sites	Slope Initiation Class & Score
35+	597	88%	High (4)
25–35	75	11%	Moderate (3)
15–25	8	1%	Low (2)
0–15	0	0%	None-very low (1)
Total	680	100%	

Figure 14. Map of a portion of Letz Creek Watershed with preliminary slope initiation classes (Table 2).

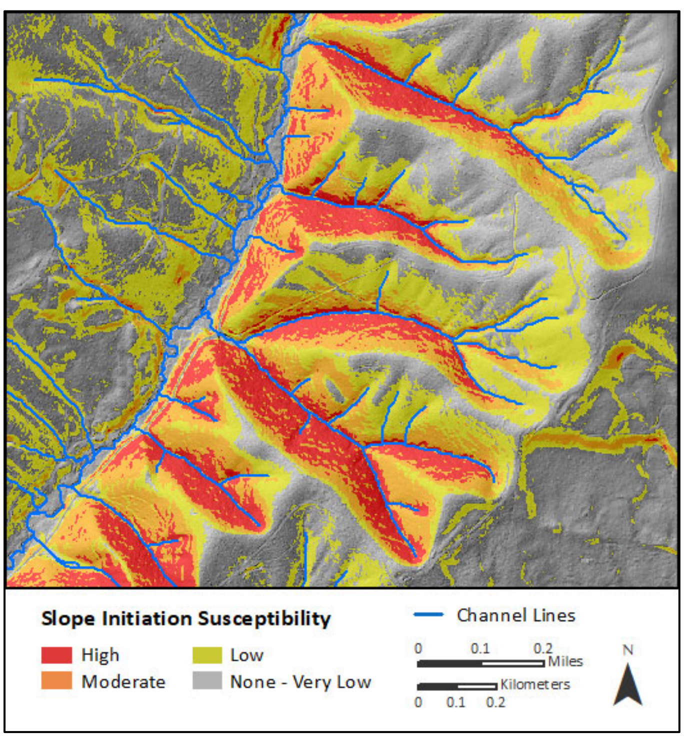

3.5.2 Slope Curvature

Most CDFs in Oregon consist of a mixture of soil, rock, woody debris, and water that turns into a liquefied slurry or flow. To obtain the necessary high percent of water, CDFs typically initiate in areas where water concentration occurs naturally. High intensity, long duration rainfall events, or combined rain-on-snow events tend to trigger CDFs; therefore, the water for CDF initiation comes from the surface or near surface versus deeper groundwater sources. The water at the surface and near surface tends to follow the surface topography, concentrating in areas where the topography converges and dispersing in areas of divergent slope planform.

Curvature is an initiation factor as it reflects areas where colluvium can accumulate (Blais-Stevens and Behnia, 2016). To include this criterion, slope curvature is used (**Figure 15**). The curvature is calculated directly from the 9x9 ft (2.7x2.7 m) cell DEM. The planform curvature identifies topography that is convergent or divergent and thus where water might be concentrated or dispersed and where colluvium is more likely to accumulate. All values less than zero are areas with convergent topography. A value of zero is a planar slope, and values greater than zero are divergent.

Figure 15. Block diagrams illustrating the three different possible planform curvature results. Planform values are positive, negative, and 0 (left to right). Positive values have convergent topography; negative values have divergent topography. (Source: https://desktop.arcgis.com/en/arcmap/10.3/manage-data/raster-and-images/curvature-function.htm)

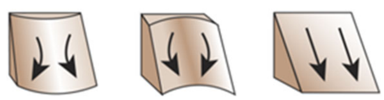

Spatial statistics were performed between the 680 initiation site polygons and the 9x9-ft (2.7x2.7-m) cell cell planform curvature raster. The units of curvature are one hundredth (1/100) of a foot (z-unit) (https://desktop.arcgis.com/en/arcmap/10.3/manage-data/raster-and-images/curvature-function.htm). The results show a relatively bell-shaped distribution around the mean of −1.0 (**Figure 16).** This indicates most CDF initiation sites are located where the slope curvature is convergent or less than zero. Above a value of zero (divergent slopes) the distribution has an exponential decrease in frequency (**Figure 16**) indicating fewer CDF initiation sites are located where slope curvature is divergent. The standard deviation is 0.7, and there are no sites above a value of 1.2.

As previously mentioned, other researchers have found that CDF initiation is more likely in convergent topography (Blais-Stevens and Behnia, 2016). The 680 CDF initiation sites support this conclusion through a sharp decrease in frequency between −0.5 and 0.5 (**Figure 16**). Furthermore, approximately 90% of the initiation sites have a planform curvature of less than zero.

Figure 16. Histogram and cumulative percent of 680 CDF initiation sites with planform curvature. Zero or planar is identified with a black vertical line. Convergent slopes are negative values and divergent slopes are postitive values.

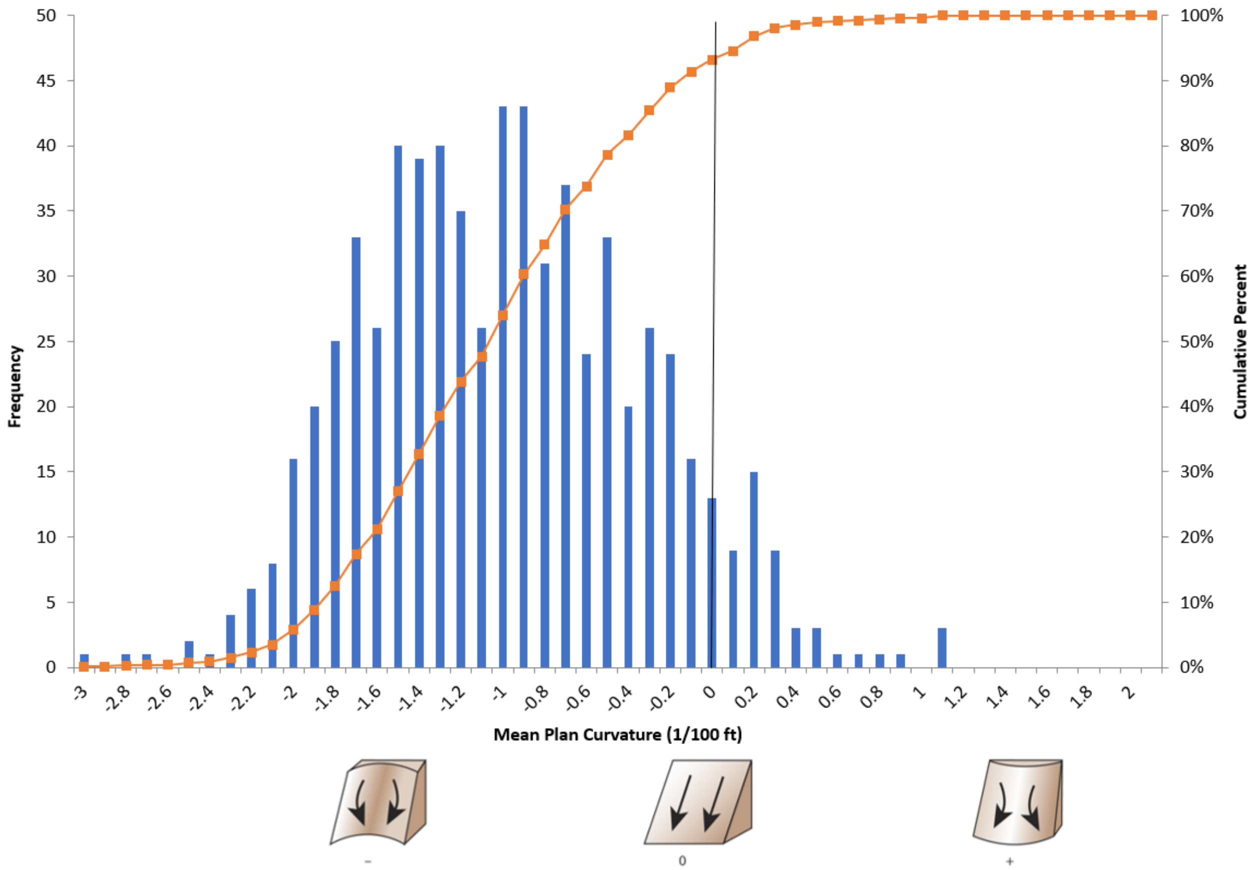

Curvature thresholds between the proposed none-very low, low, moderate, and high classes were evaluated by examining the mean, standard deviation, and cumulative capture. The new results found in western Oregon with 680 CDF initiation sites are displayed in **Table 3**. Because the none-very low threshold of 1.1 and the high threshold of −0.4 are well supported by percent of sites (82% and 0%), we selected a division between the low and moderate threshold of 0.3, which is approximately halfway between the high and the none-very low categories with respect to percent capture. **Figure 17** shows an example of mapped curvature classes.

Table 3. Curvature, number of sites, percent of sites, and curvature initiation class and score of the 680 CDF sites in western Oregon.

Curvature (1/100 ft [0.0035 m])	Number of Sites	Percent of Sites	Curvature Initiation Class & Score
≤ −0.4	555	82%	High (4)
−0.4 to 0.3	112	16%	Moderate (3)
0.3 to 1.1	13	2%	Low (2)
1.1+	0	0%	None-very low (1)
Total	680	100%	

Figure 17. Map of a portion of the Letz Creek watershed areas with curvature initiation susceptibility. Convergent slopes are where water is more likely to concentrate and colluvium is more likely to accumulate.

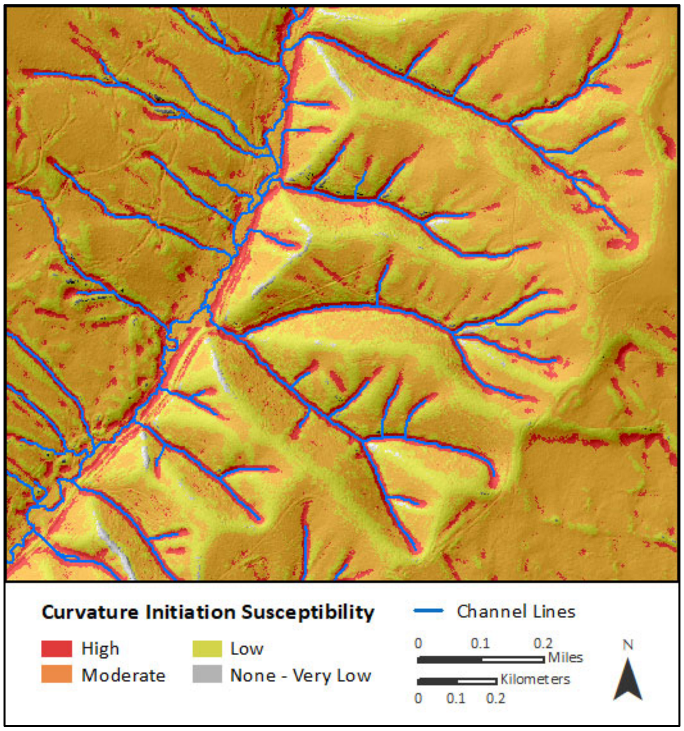

3.5.3 Distance to Channel

To continue downslope with the least impediments (i.e., in a channel), debris flows typically initiate close to or in a channel. If initiation is too far from the channel, the landslide can stop on the slope and thus not reach the channel. Blais-Stevens and Behnia (2016) considered distance to channel important and used values of 0–50, 50–100, 100–150, and 200+ meters to rank the landscape for CDF initiation susceptibility.

To include this criterion, distance to channels was examined using the channels created earlier in the method (**Figure 9**). The distance to channels was calculated with the Esri ArcGIS Near tool, which calculates the closest distance, regardless of topography, between the initiation sites and the channels. In this case we used the 680 site initiation points instead of the polygons. This was done because using the polygons results in a zero distance from channels for all sites within the radius (36 ft [11 m]) of the polygon. Using the points provides more detail at all distances.

The results show a log normal type of distribution with a mean of 48 ft (15 m) (**Figure 18**). This indicates the majority of CDF initiation sites are located within 100 ft (30.5 m) from their channels. The standard deviation is 56. Above a distance of 100 ft (31 m), the frequency drops and stays below 10%. Ten sites sit above a distance of 200 ft (61 m), and only three sites above 300 ft (91 m) (approximately 320 ft, 400 ft, and 500 ft [98 m, 122 m, and 152 m respectively). These 10 appear to be outliers of the dataset (**Figure 18**).

Figure 18. Histogram and cumulative percent of 680 CDF initiation site points distance to channels.

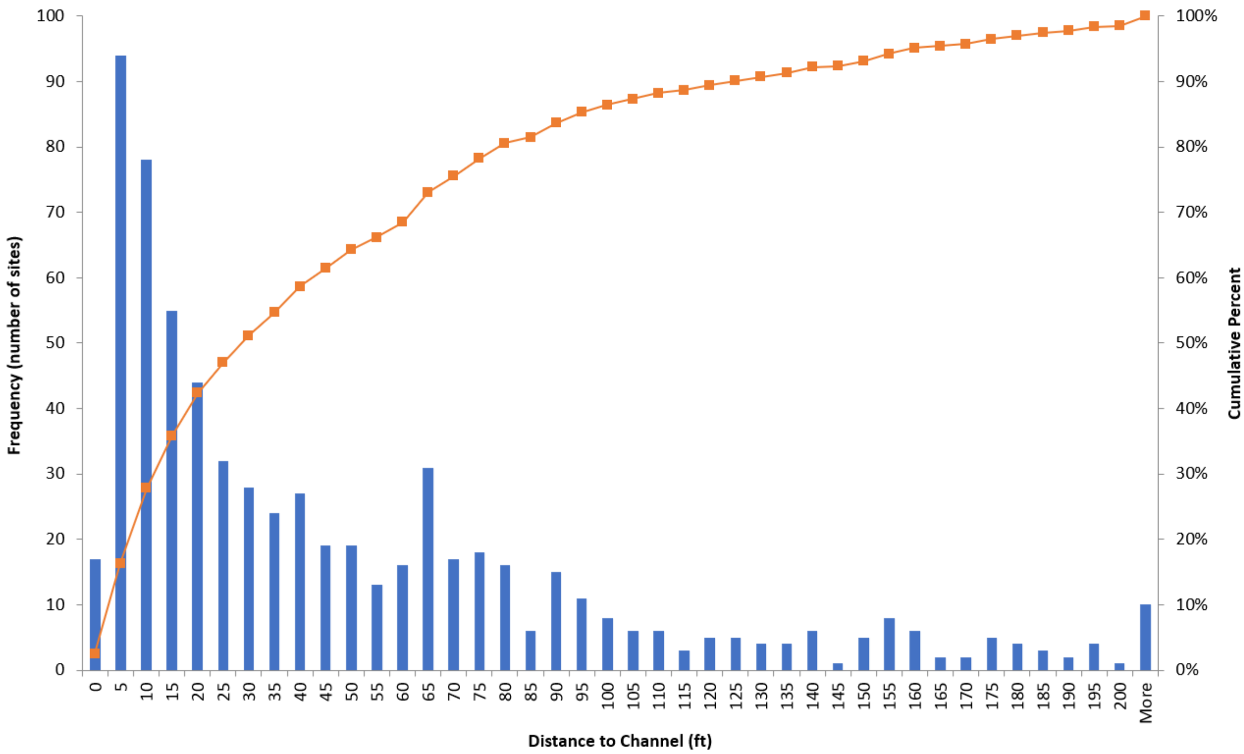

Distance to channels thresholds between the proposed very low-none, low, moderate, and high classes were evaluated through examining the mean, standard deviation, and cumulative capture, as well as results by others. The new preliminary results found in western Oregon with 680 CDF initiation sites are displayed in **Table 4**. Because the none-very low threshold of 300+ ft (91 m) and the high threshold of 100 ft (30.5 m) are well supported, we selected a moderate to low threshold of 200 ft (61 m), which is half way between the distances of the high and the none-very low categories (**Table 4**, example mapped in **Figure 19**).

Table 4. Distance to channel, number of sites, percent of sites, and distance initiation class and score of the 680 CDF sites in western Oregon.

Distance to Channel (feet)	Number of Sites	Percent of Sites	Distance Initiation Class & Score
≤ 100 (30.5 m)	588	86.5%	High (4)
100–200 (30.5-61 m)	82	12.1%	Moderate (3)
200–300 (61-91 m)	7	1%	Low (2)
300+ (91+ m)	3	0.4%	None-very low (1)
Total	680	100%	

Figure 19. Map of a portion of Letz Creek Watershed showing distance to channels. High is <100 ft (30.5m), Moderate is 100-200 ft (30.5-61 m), low is 200-300 ft (61-91 m), and none-very low is 300+ ft (91 m).

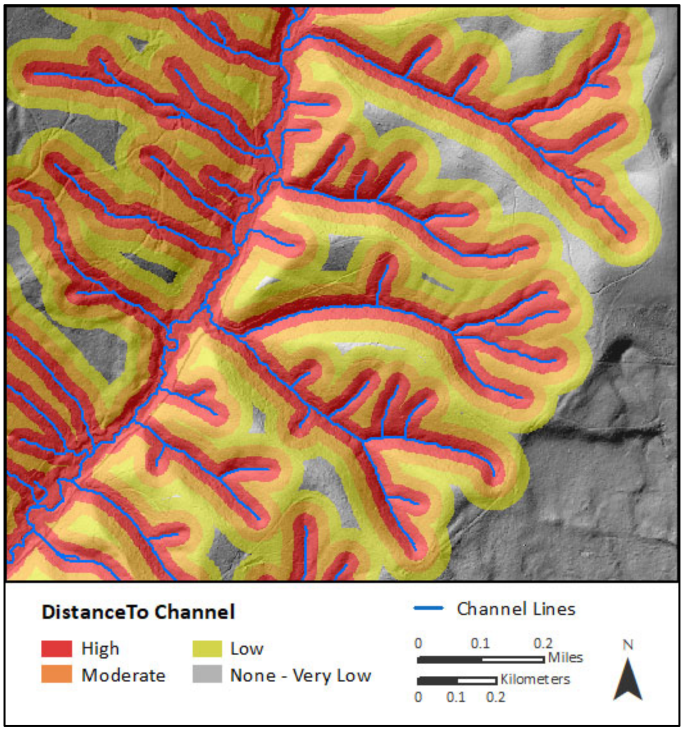

3.5.4 Initiation Susceptibility

The final CDF initiation susceptibility dataset is created by combining the slope, curvature, and distance to channel datasets (**Table 5**). Each of these three datasets (slope, curvature, and distance) have four classes and each class has a score of 1 through 4, corresponding with none-very low, low, moderate, and high. Therefore, the total score at any location on the map can vary from 3 to 12.

Table 5. Summary of slope, curvature, and distance to channel.

Curvature (1/100 of a foot)	Slope (degrees)	Distance (ft)	Category
≤ −0.4	≤ 35	100 (30.5 m)	High
−0.4 to 0.3	35 to 25	200 (61 m)	Moderate
0.3 to 1.1	25 to 15	300 (91 m)	Low
> 1.1	< 15	>300 (>91 m)	None-very low

The final initiation susceptibility layer is created by adding the scores for each of these three datasets, which results in the final initiation susceptibility scores displayed in **Table 6** and **Figure 20.**

Table 6. Final initiation susceptibility scores.

Final Possible Scores	Susceptibility	Sites	Percent Sites
3	none-very low	0	0%
4		0	
5		0	
6	low	0	0.10%
7		0	
8		1	
9	moderate	6	29%
10		28	
11		163	
12	high	482	71%

Figure 20. Map of a portion of Letz Creek Watershed showing final initiation susceptibility.

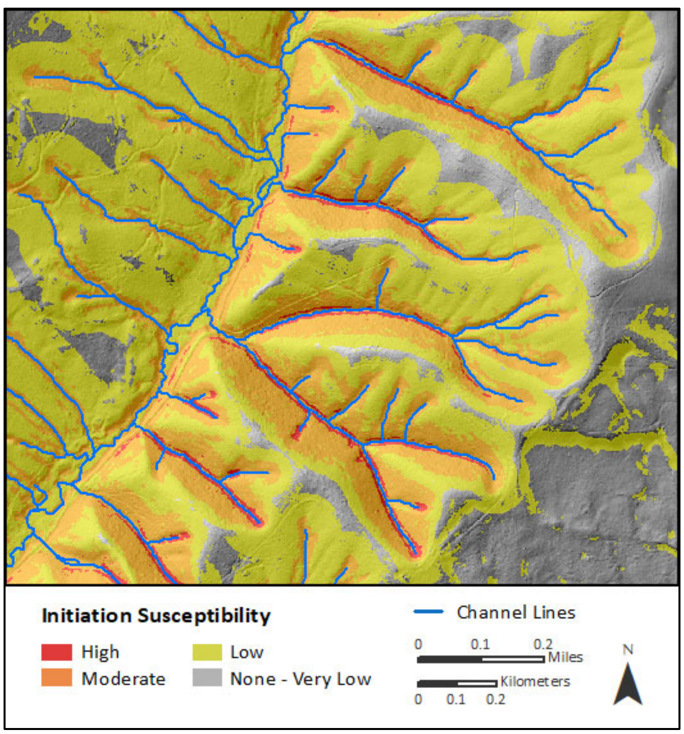

An additional figure is provided here (**Figure 21**) which includes the historic initiation sites and the initiation susceptibility.

Figure 21. Map of a portion of the Dean Creek Watershed showing the initiation susceptibility and spatial correlation of historic CDF initiation sites.

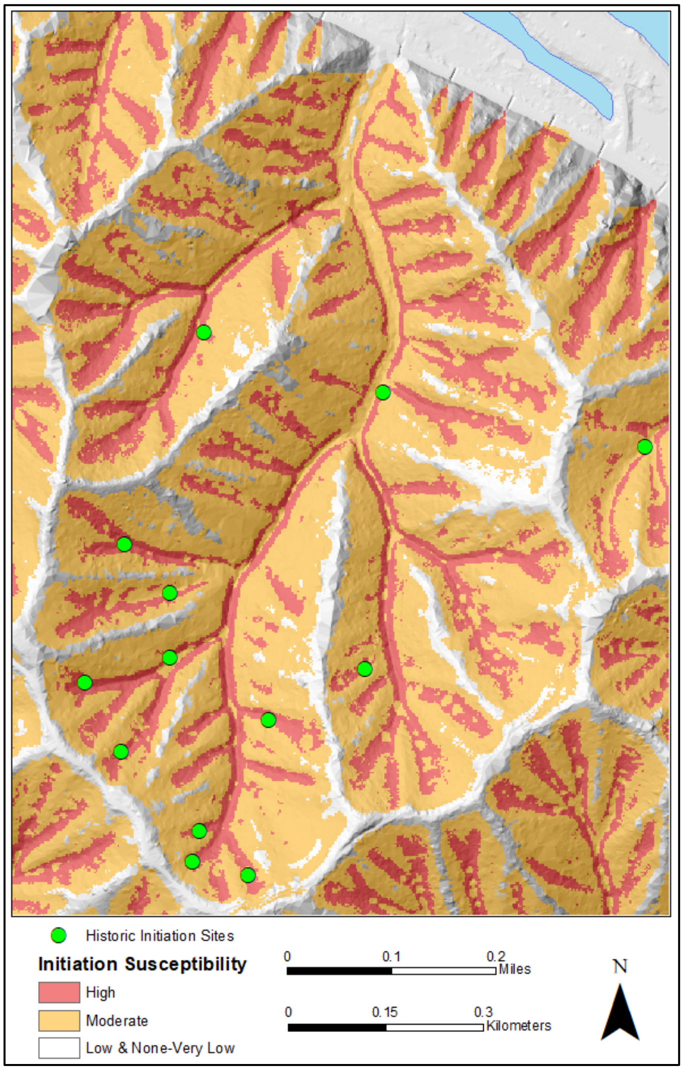

3.5.5 Transport

After a CDF begins moving down a channel, certain conditions must remain to promote progress down channel. Several criteria widely recognized and applied in evaluating the potential of transport and/or erosion and volume growth of CDFs are channel gradient, potential energy (elevation change along length of channel), channel junction angle, and channel confinement (Hungr and other, 1984; Benda and Cundy, 1990; Washington Department of Natural Resources, 2004). Junction angles are not considered in this analysis but could be considered in future updates. Another factor to consider is that sometimes a CDF can transition from erosion to deposition or vice versa along channels of similar gradient (Coe and others, 2011a).

We have selected channel gradient and confinement as the two primary criteria to define the transportation potential or susceptibility of channel segments to through flowing CDFs because these criteria are more easily evaluated. To evaluate channel gradient and confinement, the channel segments created earlier in this method were used. This divided channels into 100-ft (30.5-m) increments. Again, of the total 11,787 segments, 10,253 segments were classified as having transport, and 1,534 were classified as experiencing deposition (**Section 2.2**

3.5.6 Channel Gradient

Previous research has concluded that steeper channel gradients transport CDFs more readily. Most research has been focused on channel gradient where the CDFs start (initiate) or stop and deposit (Hungr and others, 1984; Benda and Cundy, 1990; Fannin and Rollerson, 1993; Fannin and others, 1997; Washington Department of Natural Resources, 2004;). Some reported depositional channel gradients are 3°, 3.5°, 5–13°, 8–12°, 9–15°, and 10–15°. Reid and others (2016) found channels with gradients below 5° were more likely to promote deposition. They also found that transport with erosion was likely to dominate in channels with gradients greater than 10° (Reid and others, 2016).

Mapping of CDF fan deposits following the protocol by Burns and Madin (2009) results in an estimated channel gradient in the fan deposit area, measured directly from the lidar-derived bare earth DEM. SLIDO-4.2 contains 6,893 mapped fan deposits. A histogram displays the distribution of channel gradients (**Figure 22**). The mean is 12.7°, with a standard deviation of 6.7°.

Figure 22. Histogram and cumulative percent of channel gradient across 6,893 debris flow fan deposits from SLIDO 4.2.

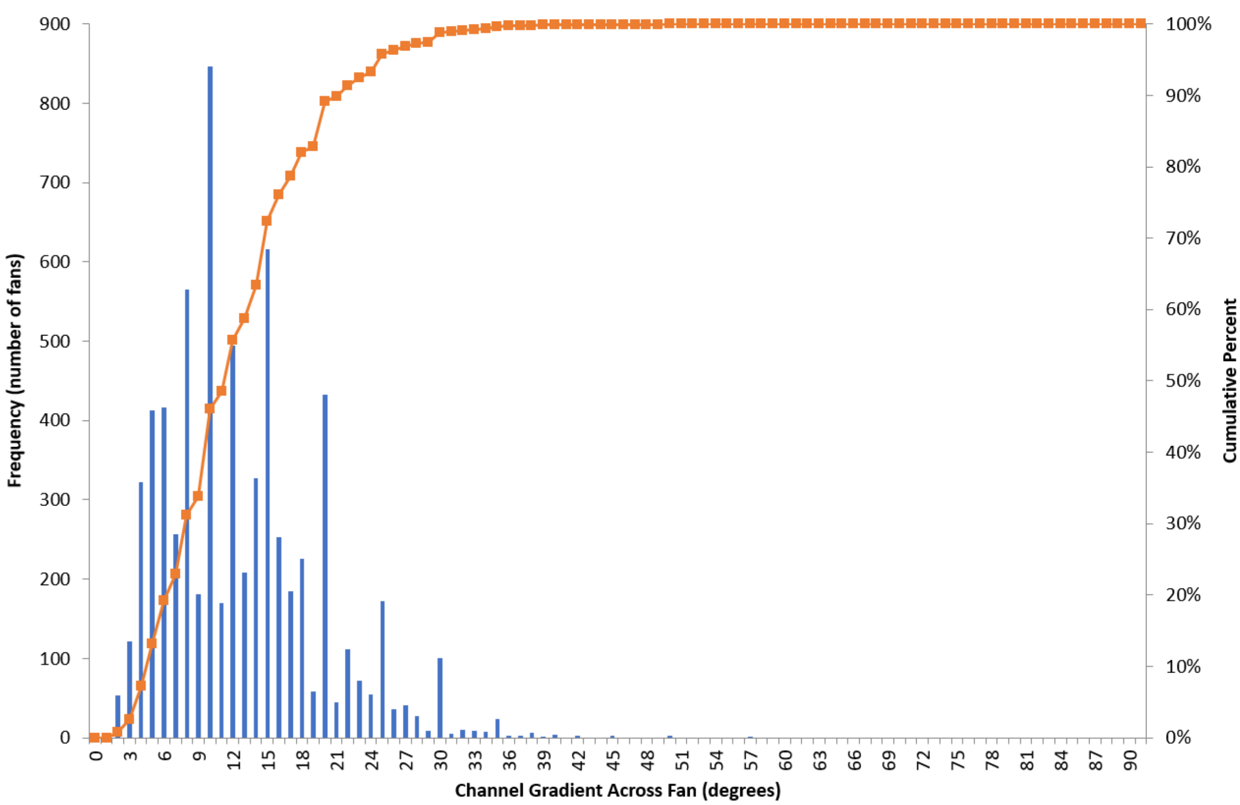

Geologists use slope angle to assist in determining the classification of deposits at the mouth of channels; previously, most deposits located were lumped into either alluvial fan deposits or deposits dominated by fluvial processes. Wiley and others (2014) used a slope angle of greater than 6% (3.5°) and in some cases greater than 25% (14°) to define debris flow deposits.

To further evaluate where transport or deposition occurs along the channel, spatial statistics were performed on the 11,787 transport segments. Of the spatial statistical results, we selected the mean slope along each 100-ft (30.5-m) segment as the best to represent the overall channel gradient of that segment. The results from the 10,253 segments with CDF transport classification show a steep increase of frequency above approximately 5° (**Figure 23**). The mean of the channel segments that displayed transport of CDFs is 20°, with a standard deviation of 10°.

Figure 23. Histogram and cumulative percent of the mean gradient from 10,253 CDF channel segments classified as having transport.

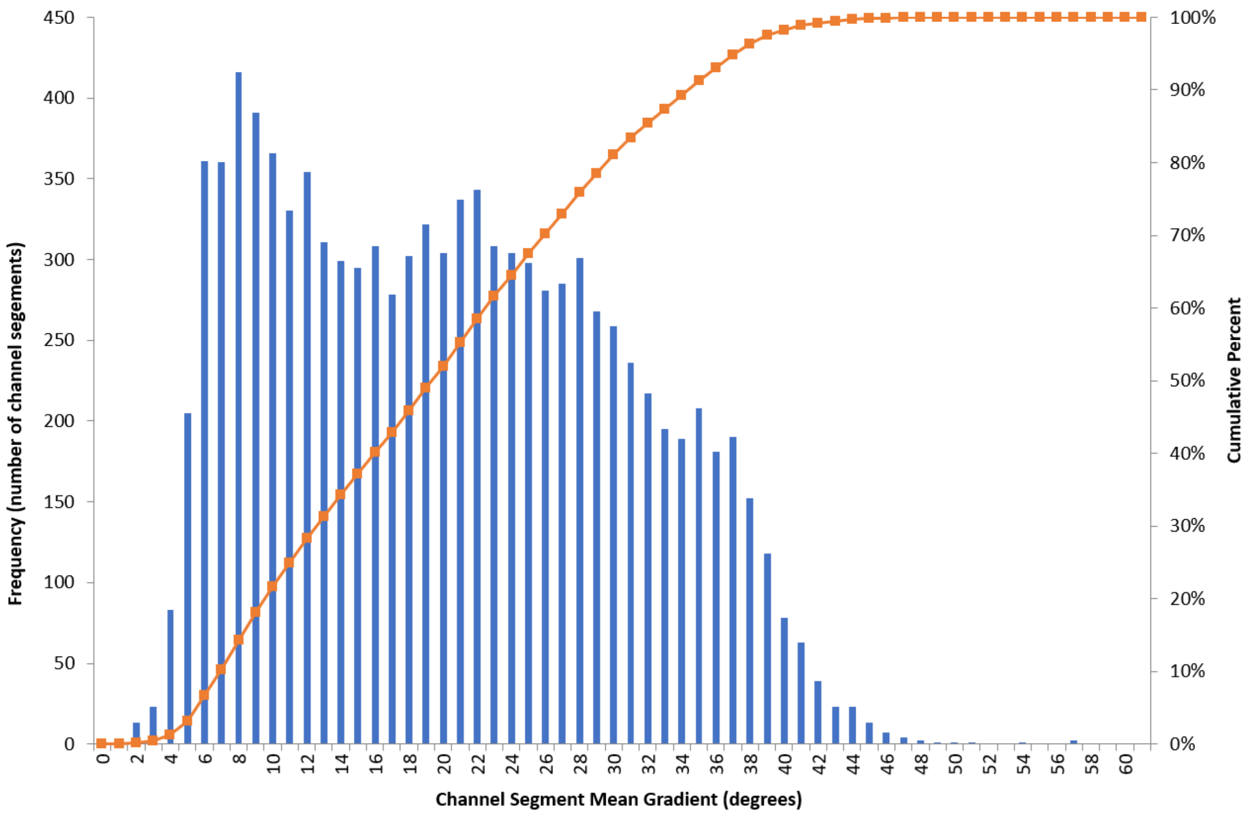

The statistic results from the 1,534 channel segments classified as having CDF deposition was a mean of 9°, and the greatest frequency was 6° (**Figure 24**).

Figure 24. Histogram and cumulative percent of mean gradient from 1,534 CDF channel segements classified as deposition.

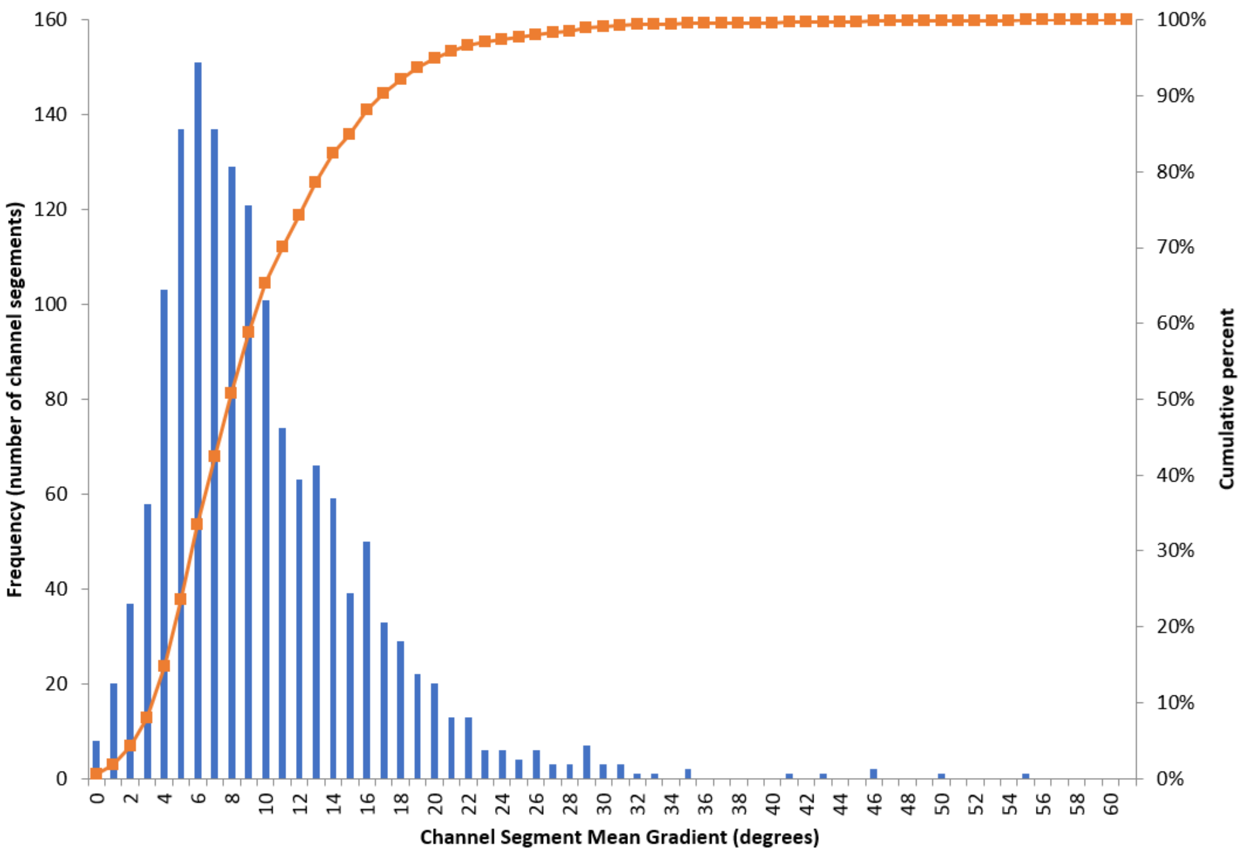

Channel gradient transport thresholds between the none-very low, low, moderate, and high classes were evaluated by examining the spatial statistics from this study and results by others (Hungr and others, 1984; Benda and Cundy, 1990; Fannin and Rollerson, 1993; Fannin and others, 1997; Washington Department of Natural Resources, 2004; and Reid and others, 2016; see **Table 7**). The new results found in western Oregon are displayed in **Table 8**. Because the none-very low threshold of 5° and the high threshold of 15° are well supported by the percentage of segments within these values, as well as being in agreement with results from other studies in Oregon, we selected a moderate threshold of 10°, which is half way between the high and the none-very low categories with respect to percent of channel segments (**Table 8**). The transport gradient class results are displayed in **Figure 25**.

Table 7. Summary of transport and depostion channel gradient values developed in this study and by Fannin and others, 1997; Washington Department of Natural Resources, 2004; Hungr and others, 1984; Benda and Cundy, 1990; Fannin and Rollerson, 1993; and Reid and others, 2016.

	Reported Numbers or Ranges	Average, Range
Transport	20°, > 10°	~15° > 10°–20°
Deposition	3°, 3.5°, 5°, 5–13°, 6°, 8–12°, 9°, 9–15°, 10–15°, < 3.5°–14°	~7.5° 3°–15°

Table 8. Channel gradient and percent of the 11,897 CDF channel segments in western Oregon.

Channel Gradient (degrees)	Percent of Channel Segments	Transport Class & Score
15+	56.9%	High (4)
10–15	20.6%	Moderate (3)
5–10	22.4%	Low (2)
< 5	0.01%	None-very low (1)

Figure 25. Map of a portion of Letz Creek Watershed showing channel gradient based transport potential.

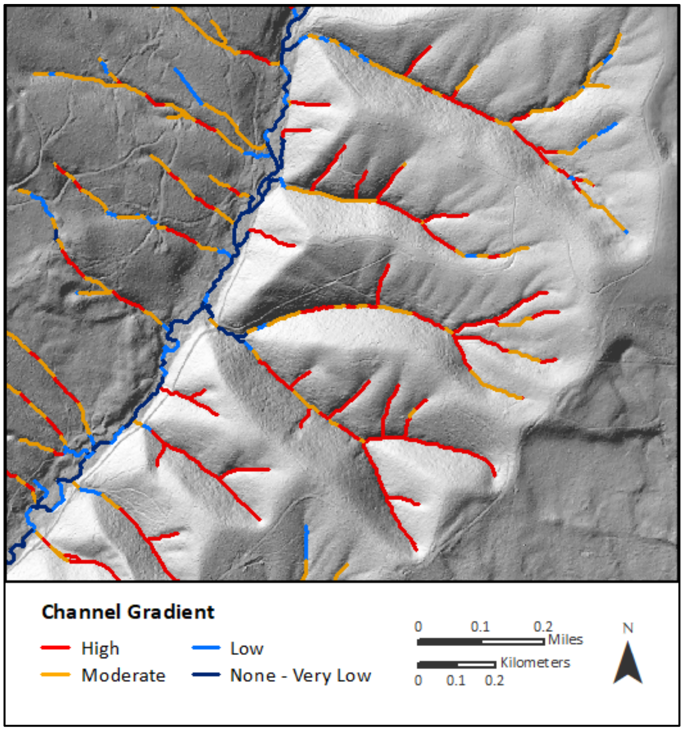

3.5.7 Channel Confinement

Previous research has shown that channel confinement also contributes to transport potential (Iverson and others, 1998; Cannon and others, 2003; Hungr and others, 2008). However, most research has been focused on channel gradient, so very few values or methods to calculate confinement are readily available. The Oregon Department of Forestry (ODF) measures the width of the confining valley walls at a height of 10 feet (3 m) above the channel bed. If the horizontal distance as measured from a point approximately 10 feet (3 m) above the channel bed is greater than 200 ft (61 m), the channel is considered to be unconfined. They note the 200-foot (61-m) criterion is likely conservative https://www.oregon.gov/odf/Documents/workingforests/LandslideImpactRatingTechNote6.pdf

We developed a method in GIS to calculate confinement. We placed perpendicular transects at intervals of 25 ft (8 m) along all the channel segments, as well as transects at the beginning and end of each segment, which results in approximately five transects per segment (**Figure 26**). The transect lines extend 100 feet (30.5m) in both directions from the channel line, creating a transect with a width of 200 ft (61 m), which is the same horizontal distance ODF uses. Next, points were placed at 9-ft (3-m) intervals along the transects; elevation data from each point were extracted from the DEM (**Figure 26**). The maximum elevation difference was examined along each transect, and the average maximum range (from the five transects) was applied to the channel segment.

The average maximum elevation difference was then used directly to define the amount of confinement for that segment (**Figure 26**). For example, if the maximum elevation difference is 10 ft (3 m), we assume this is above the 100-ft (30.5- m) length of the channel segment. This is the lower threshold of confinement and is in agreement with the rule of thumb used by ODF. However, if the maximum elevation difference is 75 ft (23 m) per 100 ft (30.5 m), this indicates high confinement.

Local topographic conditions along segment transects may result in confinement values which are inconsistent with those generated from the 100-foot (30.5-m) transect lengths. However, addressing these fine scale variations are beyond the scope of this protocol, and may be appropriate to address in future updates of this protocol.

Figure 26. Perspective view map example of two sections (confined and unconfined) of transects along a channel (top). Diagram of the two sections of transects and equations used in calculation.

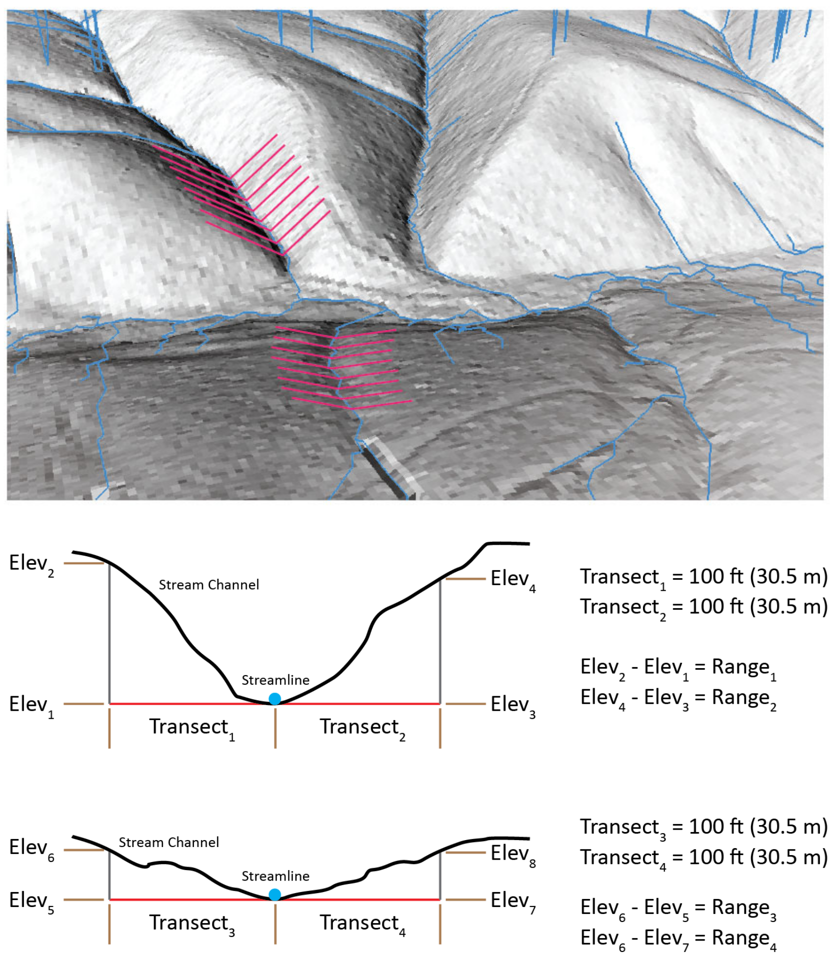

To determine where confinement occurs, spatial statistics were performed on the 11,787 total transport segments. As discussed, each channel segment has about five transects, which are averaged to find the mean maximum elevation difference for each channel segment. The mean of the channel segment confinements is 60 ft (18 m) per 100 ft (61 m), and the standard deviation is 20 ft (6 m) (**Figure 27**). Very few channels had values above 100 ft (61 m) (100 ft [61 m]/100 ft [61 m]).

Figure 27. Histogram and cumulative percent of confinement (vertical feet per 100-foot [30.5 m] horizontal) from 10,253 CDF channel segments classified as having transport.

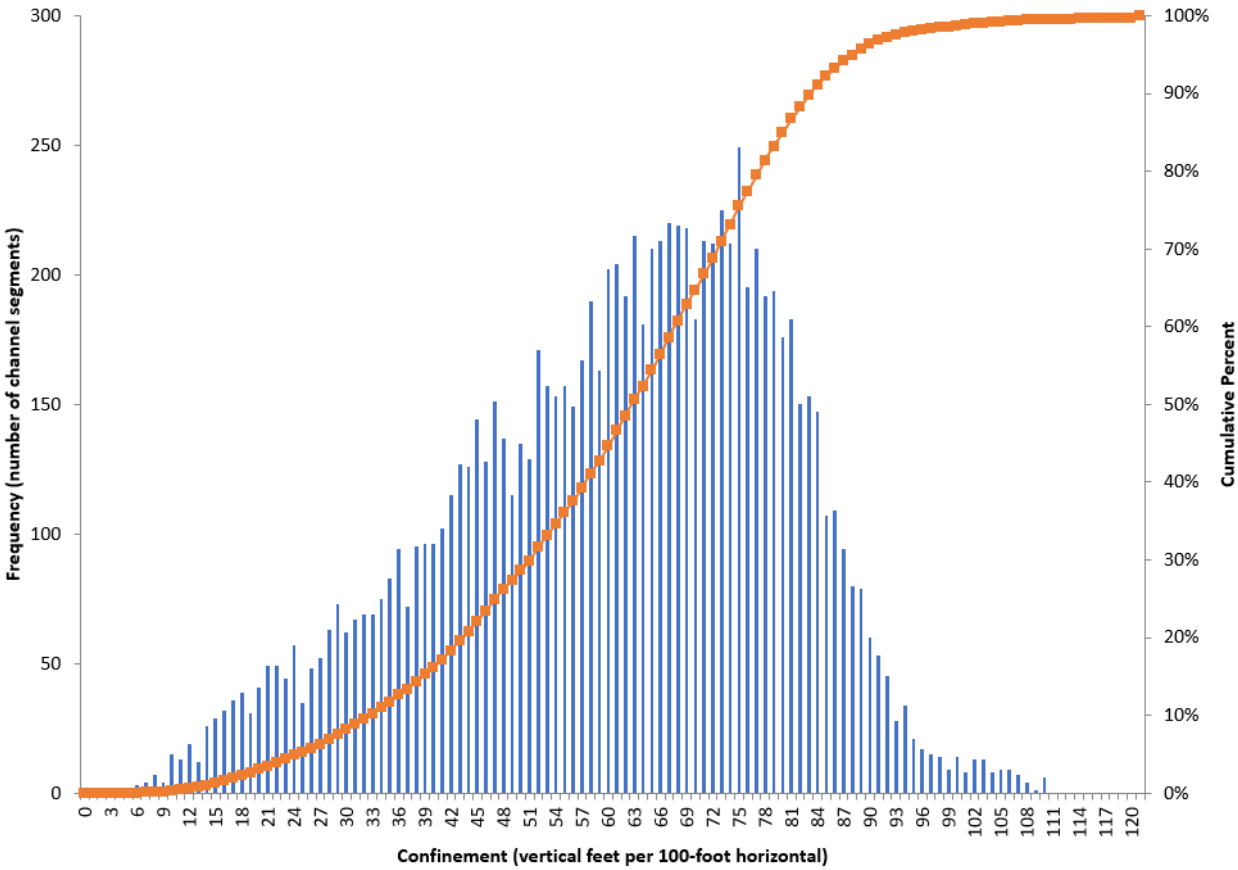

Channel confinement transport thresholds between the proposed none-very low, low, moderate, and high classes, were evaluated by examining the spatial statistics from this study. These new, preliminary results from western Oregon are displayed in **Table 9**. We selected a value of 40 ft (12 m) or greater for the high class, which is the mean minus one standard deviation and captures approximately 85% of transport segments. We selected a moderate threshold of 20 ft (6 m), which is the mean minus two standard deviations and captures 12.6% of the transport segments. We selected the none-very low threshold of 10 ft (3 m), which is what ODF uses. Together, the moderate and high classes capture 97% of channel segments (**Table 9**). These transport confinement classes are illustrated in **Figure 28**).

Table 9. Channel confinement and percent of channel segments in each transport confinement class.

Channel Confinement (feet)	Percent of Channel Segments	Transport Confinement Class & Score
40+	84.7%	High (4)
20–40	12.6%	Moderate (3)
10–20	2.5%	Low (2)
< 10	0.2%	None-very low (1)

Figure 28. Map of a portion of Letz Creek Watershed showing channel confinement classification. Note the high confinement in the steep valleys (middle of the map) and the low to moderate confinement in the wider, main valley.

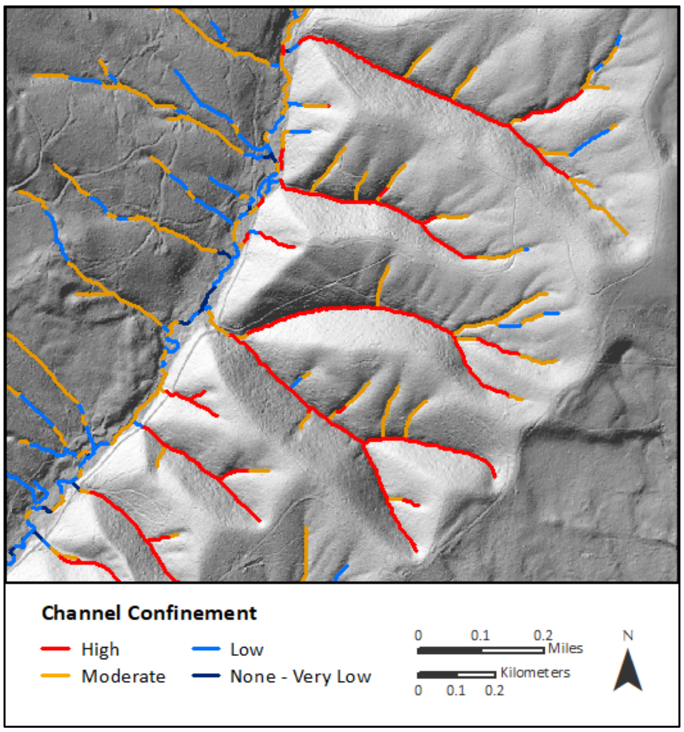

3.5.8 Transport Susceptibility

The final CDF transport susceptibility dataset was created by combining the channel gradient and confinement datasets. The graph of the combined gradient and confinement results indicates the strong influence of confinement in channels with lower gradients (**Figure 29**). At higher channel gradients, above ~7.5°, confinement does not increase much with increasing gradient. The increase in confinement from 0 ft (0 m) to 60 ft (18 m) at low gradients, followed by a rapid increase in gradient (10°–45°) without much increase in confinement, indicates the importance of confinement at lower gradients and lack of necessary confinement at high gradients. To reduce the number of channels with transport in the none-very low category, we reduced the previously selected gradient for the moderate category from 10° (**Table 8**) to 7.5° (**Table 10**).

Figure 29. Chart of channel segement mean gradient and mean confinement, with thresholds (red lines) and percent of 11,787 transport channel segments that experienced transport in each zone (black dots). Channel segments classified as deposition are shown as blue dots. An expert-judgment-based estimated trend line is shown as an orange line.

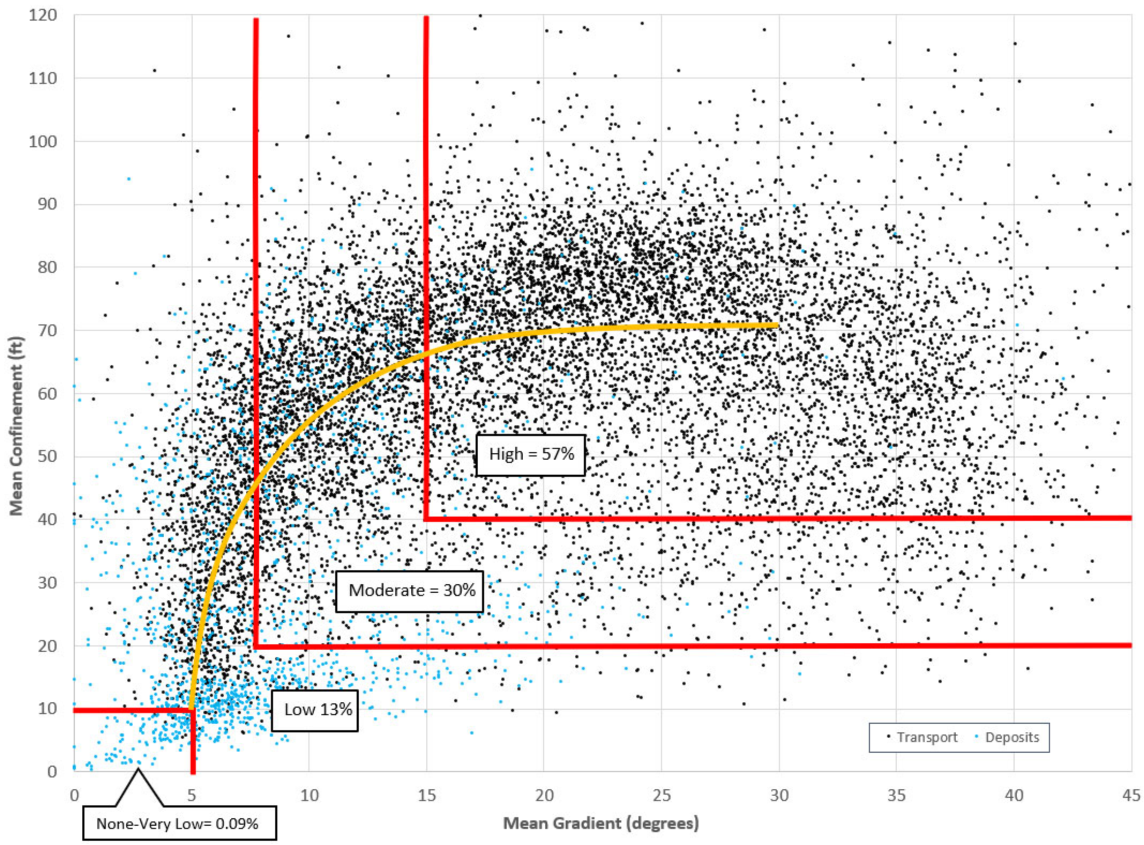

Table 10. Final transport susceptibility values. The transport susceptibility class is applied when both conditions conditions of confinement and gradient area met.

Confinement (Vertical feet per 100-foot horizontal)	Gradient (degrees)	Percent of Channel Segments	Transport Susceptibility Class & Score
40+	15+	57%	High (4)
20–40	7.5–15	30%	Moderate (3)
10–20	5–7.5	13%	Low (2)
< 10	< 5	0.098%	None-very low (1)

The final channel transport susceptibility dataset is created by adding the confinement score (1–4) of each segment to the channel gradient score (1–4), equaling a final score and classification (**Table 11**; **Figure** 30). The none-very low transport susceptibility class, which has 0.09% of the 11,787 channel segments, contains channels not considered likely to promote transport of CDFs and therefore do not have volume increases. These channel segments are used in a later step to define where an increase in inundation volume stops and thus where the primarily deposition portion of the inundation is modeled.

Table 11. Final transport susceptibility scores, classes, and percent of total channels captured.

Final Scores	Transport Susceptibility Class	Percent of Channel Segments
2 3	none-very low	0.09%
4 5	low	13%
6 7	moderate	30%
8	high	57%

Figure 30. Map of a portion of Letz Creek Watershed showing final transport susceptibility. The underlying geology consists of bedding sloped toward the east, which creates gentler, less confined channels on the west side and steep, confined channels on the east side.

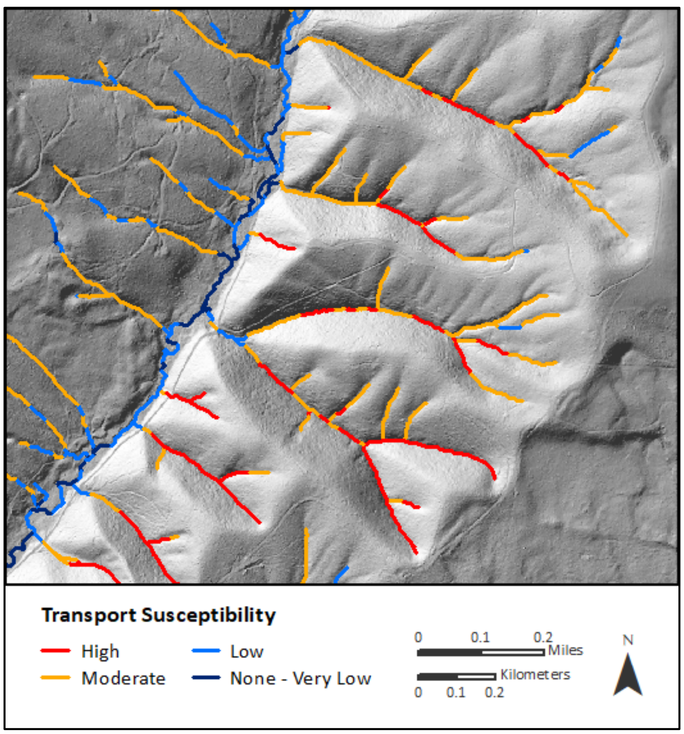

3.6 Step 5: Upper-Lower Bounds

Methodology progress bar: ▼ indicates current step.
Green = Manual task, Orange = Toolbox task

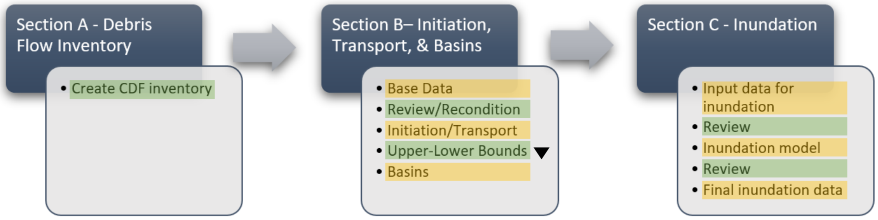

To evaluate the overall basin susceptibility to CDFs, the basins must first be delineated. To delineate a basin, a point must be placed to define the outlet of the basin; this is known as a “pour point” in ArcGIS. This pour point is used to delineate basin polygons (or watersheds) using standard hydrography tools in ArcGIS. Initiation and transport data are joined with the basin polygons to classify each basin with overall CDF susceptibility. The basins should generally not include the main portions of the primary depositional areas (defined by the transport channel susceptibility, inventory mapping of CDF fan areas, and other datasets). Basin areas are defined to categorize susceptibility of the whole basin or overall, based on the transport and initiation susceptibility within the basin area.

We use a manual ArcMAP technique to create the basin pour points. A professional who is familiar with both the study area and debris flow processes creates a polygon referred to as an “upper-lower bounds” polygon. This polygon encapsulates the upper and lower elevation limits of the basins being delineated.

We selected a polygon so the professional creating the upper-lower bounds cannot make overlapping basins, which can happen if a line or point types of feature class datasets are used to establish the pour points. The upper-lower bounds polygon should cross each selected channel, thus creating a point at that intersection. The upper-lower bounds polygon should be drawn first at 1:12,000 scale, then refined at 1:4,000, and again at 1:2,000 so the intersection of the upper-lower bounds and the channels creates the pour point in the correct location. This point is then used as the basin pour point, through which CDF transport must occur.

The following is a list of layers and symbol settings that should be used to assist in drawing the upper-lower bounds polygon (**Figure 31**).

- **The transport susceptibility layer** (
- **Figure** 30) should be used with the following symbology:
  - dark blue (none-very low), light blue (low), orange (moderate), and red (high).
  - For lower bounds (i.e., pour point locations), avoid or do not cross channel lines of consistent none-very low (dark blue) transport and areas of low (light blue). interspersed with none-very low values. **Figure 31** has examples of this situation.
  - Avoid crossing channels with negligible contributing areas; this results in micro basins that do not have initiation areas along them or above them.
- **Slope map layer** should be used with the following symbology: less than 5° (blue), otherwise transparent. Avoid mapping areas with consistent slopes less than 5°.
- **The landslide inventory mapped fans layer** should be used and symbolized with blue. Attempt to intersect the channels with the upper-lower bounds in the fan areas. Commonly, the transport layer will change from high/moderate to low/very low-none in the fan areas.

- **The CDF initiation susceptibility layer** (**Figure 20**) should be used and symbolized with red for its high classification. The upper-lower bounds polygon should intersect channels connected to potentially high initiation areas up stream to ensure those basins are delineated.

There are some specific spots to take extra care when creating the upper-lower bounds. Where the upper-lower bounds and the channels intersect, a pour point will be created (DF_ArcPRO_Toolbox Part 3_ Basins). That point is then snapped to the highest flow accumulation within a 9-ft (3-m) radius. Therefore, avoid intersecting the upper-lower bounds polygon with the channel lines within several cells of an adjacent channel or a channel intersection. This will avoid the pour point snapping to the wrong channel. Again, attempt to intersect within the fan polygons, because the fans are joined to the basins using the pour points.

Figure 31. Map of a portion of Letz Creek Watershed showing delineated upper-lower bounds polygon (black lines). Pour points are only created where the upper-lower bounds polygon and the channel lines intersect, therefore the upper-lower bounds polygon in between the intersections of the channels is just a method to get to the next channel intersect.

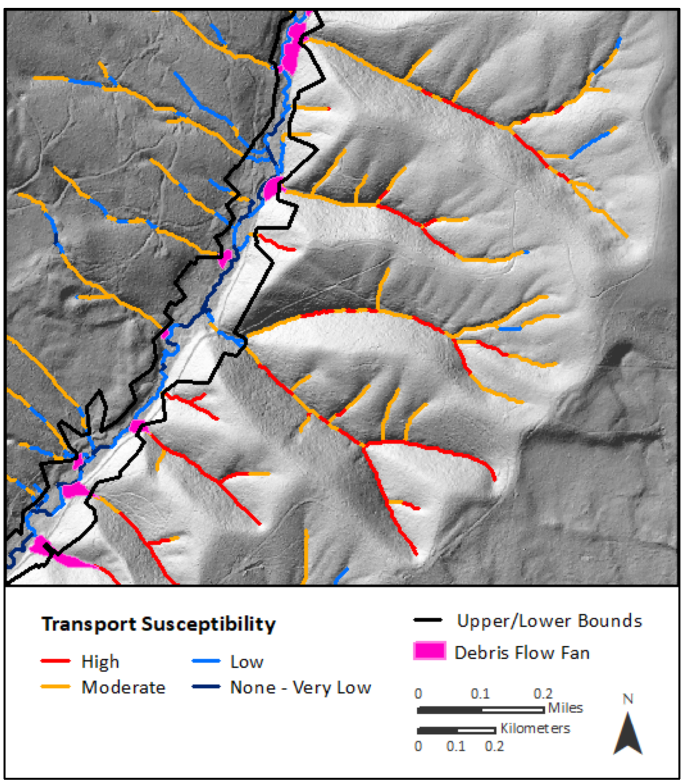

3.7 Step 6: Basin Delineation

Methodology progress bar: ▼ indicates current step.
Green = Manual task, Orange = Toolbox task

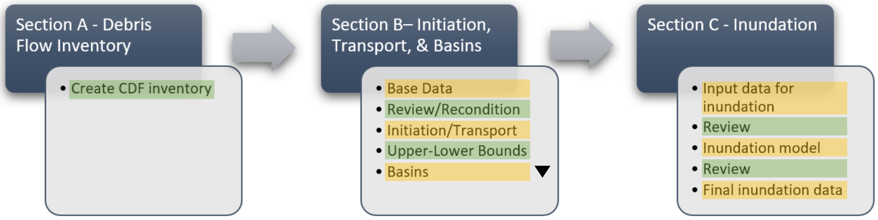

Once the upper-lower bounds polygon is finalized, the DF_ArcPRO_Toolbox Part 3_ Basins can be implemented. This toolbox uses two datasets (upper-lower bounds and transport lines) to intersect and create pour points for each basin. These points are then used by the tool to delineate the basins (**Figure 32**). After the basins are created, any that are less than 16,146 ft^2 (1,500 m^2) are automatically removed from the dataset.

Figure 32. Map of a portion of Letz Creek Watershed showing intersection points (pour points, red dots) and delineated basins (black outlines).

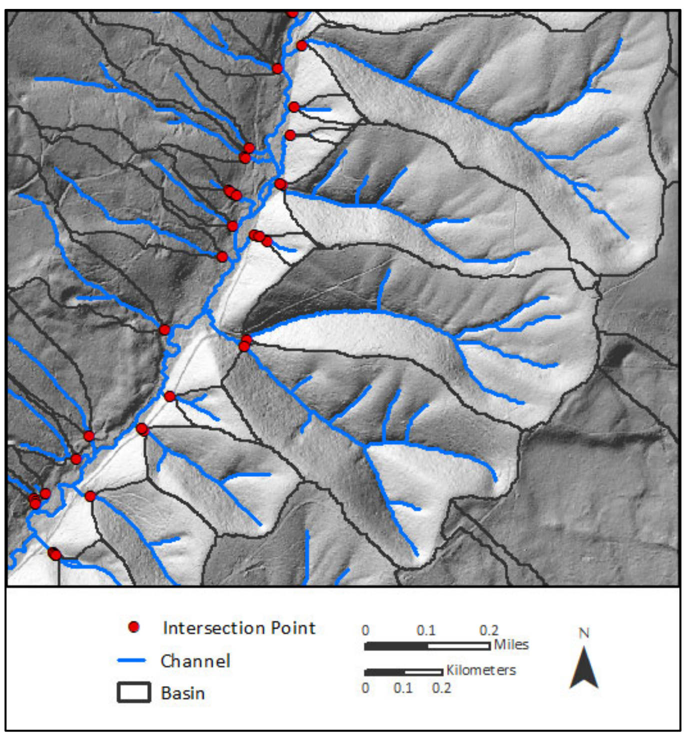

3.7.1 Initiation Susceptibility Per Basins

Once the basins are delineated, initiation susceptibility results are joined to each basin. Tabulation of the areas of none-very low, low, moderate, and high are performed by the toolbox part 6 and the results joined to the basins.

Because area of initiation classes is difficult to compare between basins, we also estimate the number of potential initiation sites per basin using the area. In other words, we normalize the initiation area using the number of square feet and the number of estimated future initiation sites. This results in a single unitless number which is easier to comprehend and compare across basins. More important, it helps decipher which basins have less than one estimated future initiation site, which implies it is very unlikely for even one CDF to initiate within the basin.

The size of CDF initiation areas varies with each event. However, several studies have estimated average initiation areas for different locations throughout Oregon. Coe and others (2011a) found a mean CDF initiation size of 3,983 ft^2 (370 m^2) in the central portion of the Oregon Coast Range. Benda and Cundy (1990) found average initiation volumes in the midnorthern portion of the Oregon Coast Range to be 15,892 ft^3 (450 m^3) and estimated thickness of 3 m (9.8 ft), which is an area of 1,615 ft^2 (150 m^2). Robison and others (1999) found an average CDF initiation volume of approximately 100 yards^3 (2,700 ft^3, 76 m^3) throughout western Oregon. Here we selected 1,000 ft^2 (93 m^2) because it results in the most conservative (or greatest number) of estimated potential future initiation sites based on area only. Using an area to define the initiation sites also allows for the various types of initiation (shallow landslide, erosion, or in-channel) to be represented.

We use the selected CDF initiation size of 1,000 ft^2 (93 m^2) to divide the high initiation susceptibility area per basin into an estimated number of high potential future initiation sites (**Table 12**). For example, if a basin has 10,000 ft^2 (929 m^2) of high initiation susceptibility area, this will result in 10 potential initiation sites (10,000 ft^2 [929 m^2] / 1000 ft^2 [93 m^2]) for that basin. Some basins in Dean Creek, which has had hundreds of historic CDFs, have hundreds of estimated potential initiation sites, and thus will have a high potential to start a CDF in the future (**Table 12**). On the other hand, some basins in Letz Creek have zero potential initiation sites and these basins will be classified as none-very low (**Figure 33**). Because we found ~70% of the historic events start in the high initiation susceptibility class, we selected the high initiation class area to calculate the number of potential initiation sites.

Table 12. Number of estimated potential intiation sites per basin and relationship to initiation susceptibility per basin.

Number of Estimated Potential Initiation Sites/Basin	Initiation Susceptibility/Basin	Score	Reasoning
0–0.5	None-very low	1	basin has almost no potential initiation sites
0.5–1	Low	2	basin has potentially only one initiation site
1–5	Moderate	3	basin has multiple initiation sites
5+	High	4	basin has many potential initiation sites

After a CDF event occurs, it can take decades to thousands of years to refill the evacuated initiation site with debris, depending on the geology, location of the basin, and many other factors. If a basin has zero or one potential initiation sites, this implies there could be a significant amount of time between events. The initiation susceptibility of the basin is limited to the time it takes to refill the sites with debris (Parker and others, 2016). This increased time between potential initiations implies a reduced frequency and thus reduced overall susceptibility to CDFs in the particular basin (May and Gresswell, 2004).

Figure 33. Map of Letz Creek basins with initiation susceptibility per basin. In this area, the bedrock is dipping toward the east-southeast. This results in generally steeper slopes in basins facing west-northwest.

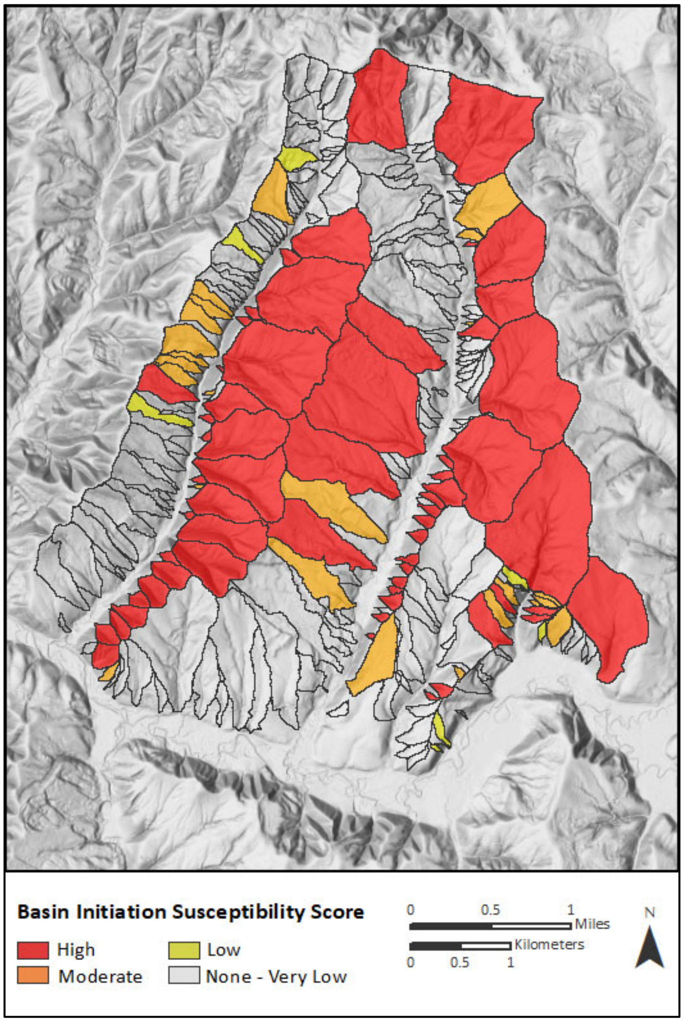

3.7.2 Transport Susceptibility Per Basin

Data from the transport susceptibility layer are joined to each basin so that a relative overall level of transport susceptibility per basin can be quantified. The tool tabulates the total length of channels with transport susceptibility of none-very low, low, moderate, and high inside each basin first. Because approximately 87% of the CDF transport takes place in the moderate and high ranked channel segments (**Figure 29**), we select the percent of moderate and high channels to evaluate the overall potential for CDF transport per basin (**Table 13**; **Figure 34**).

Table 13. **Basin transport susceptibility classification by percent of total transport channels high and moderate.**

Percent of High and Moderate Channels in the Basin	Transport Susceptibility/Basin	Score	Reasoning
0–10%	None-very low	1	basin lacks overall transport potential
10–25%	Low	2	basin has limited transport potential
25–50%	Moderate	3	basin has reasonable transport potential
50%+	High	4	majority of channels in basin have moderate and high transport potential

Figure 34. Map of Letz Creek Watershed with basin transport susceptibility scores.

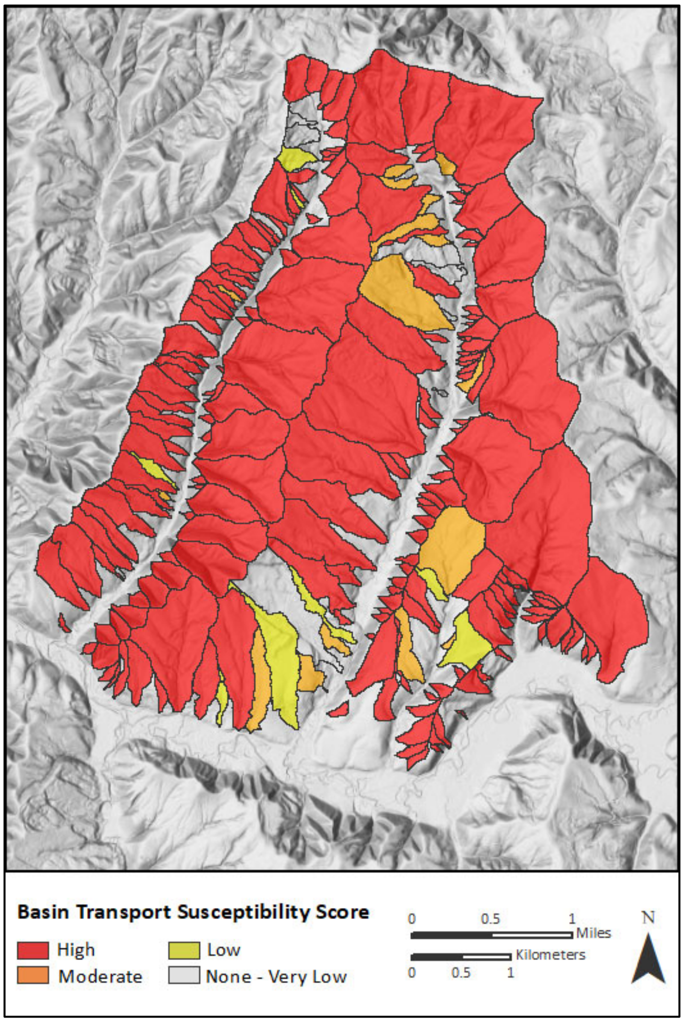

3.7.3 Overall CDF Susceptibility Per Basin

The overall susceptibility to CDFs per basin is determined with the following datasets:

- Initiation susceptibility/basin: scores 1 to 4
- Transport susceptibility/basin: scores 1 to 4

Initiation and transport susceptibility per basin are added together to make the basin overall CDF score which has a range from 2 to 8 (**Table 14**).

Table 14. Final overall CDF susceptibility and score per basin.

Final Possible Scores	Susceptibility
2	Very low-none
3	
4	low
5	
6	moderate
7	
8	high

Figure 35 Map of Letz Creek Watershed with overall basin susceptibility to CDFs.

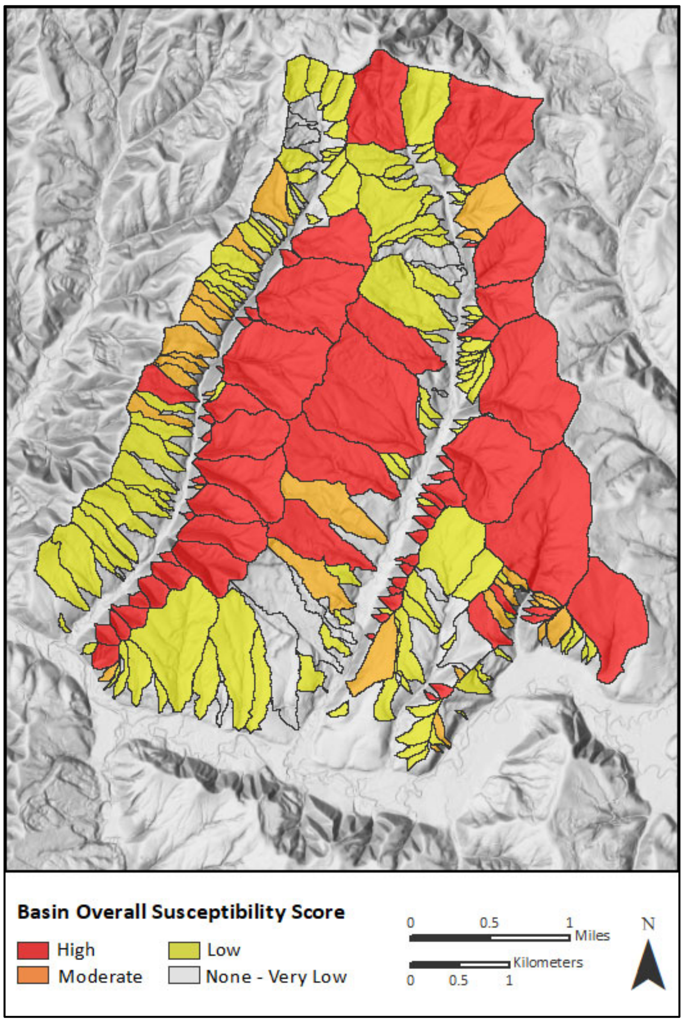

3.8 Step 7 and Step 8: Inundation Input Data and Review

Methodology progress bar: ▼ indicates current step.
Green = Manual task, Orange = Toolbox task

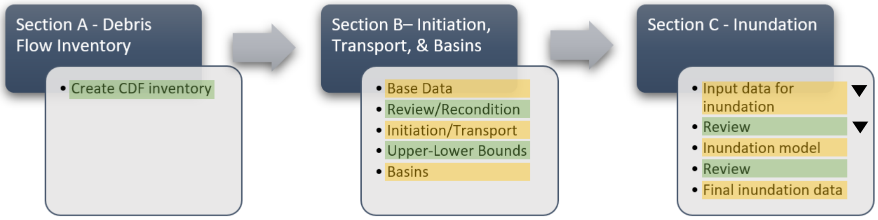

The next step is to model inundation areas, sometimes referred to as runout, for basins with low, moderate, or high susceptibility to CDFs. Basins with non-very low susceptibility to CDFs have no need for inundation modeling.

Iverson and others (1998) created a method called "Objective delineation of lahar-inundation hazard zones," also known as LAHARZ. The method delineates hazard zones with objective and reproducible results. The method relies on semiempirical equations that predict cross-sectional areas of an inundated valley and planimetric areas as functions of lahar volume (Iverson and others, 1998). LAHARZ, originally developed to delineate volcanic lahar hazards, was modified to include CDFs (Griswold and Iverson, 2008; Schilling, 2014). Both previous methods have volumes fixed throughout the CDF process (e.g., volumes are equal at initiation, channel transport, and deposition sectors).

Reid and others (2016) added the ability for volumes to grow down channel using LAHARZ, resulting in more realistic hazard zones (e.g., smaller volume at initiation, growth in volume down the channel during transport, and the largest volume in the deposition area). The new method accommodates growth not just by erosion in the channel or channel entrainment (sometimes referred to as bulking), but by any sources that increase volume which could include coalescence of multiple CDFs, channel bank failures, and hillslope rilling (Reid and others, 2016).

The method by Reid and others (2016) was developed for general use and tested in Oregon. It is the method selected for the inundation modeling portion of this protocol. Because inundation modeling for debris flows that accommodate volumetric growth is a current and rapidly advancing science, we note that this section of the CDF protocol could soon be updated by the latest version provided by the USGS.

The inundation portion has two parts: DF_Growth_ArcGIS_Toolbox Part 4_Debris-Flow Growth Pre-Processor (creates the input data for the inundation model) and DF_Growth_ArcGIS_Toolbox Part 5_Multi-Point Laharz_py (inundation modeling; https://code.usgs.gov/ghsc/lhp/df_growth). The pre-processor calculates the volumes at set intervals along the channel (growth points) based on the upslope contributing source area and the growth factor. The multi-point LAHARZ part takes the growth points with volumes and delineates the inundation area on the landscape.

There are several necessary input datasets for the pre-processor. Output datasets of the pre-processor are input datasets for the multi-point laharz. Below, we provide recommendations for the input datasets and settings for the pre-processor. The paper written by Reid and others (2016) should be consulted for more details on how their model was developed.

We have selected to model three CDF inundation susceptibility zones in each pilot area and intend to do the same in future study areas (**Table 15**). Areas not modeled in these three zones should be considered to have none-very low susceptibility to CDF activity.

Table 15. Three CDF inundation susceptibility zones for each pilot area and future study areas. All of the terms in this table are qualitative.

CDF Inundation Susceptibility Zones	Relative Frequency	Estimated Return Frequency (years)	Magnitude or Spatial Impact
Typical	high	tens to hundreds	small-medium
Intermediate	moderate	hundreds to thousands	medium-large
Extreme	low	thousands	large-extreme

3.8.1 Debris Flow Growth Pre-Processor

The first step is to prepare the pre-processor input data. Three datasets are needed:

1. 9 ft^2 (3 m^2), filled and reconditioned DEM (output dataset from DF_ArcPRO_Toolbox Part 1_Base Maps).
2. Initiation and growth points for typical, intermediate, and extreme (intermediate and extreme use the same set of growth points; output datasets from DF_ArcPRO_Toolbox Part 3_ Basins).
3. Upslope contributing source area raster for typical, intermediate, extreme (intermediate and extreme use the same source raster; output datasets from DF_ArcPRO_Toolbox Part 3_ Basins). This dataset is slightly different than the initiation susceptibility data previously created as part of this method.

To create the initiation and growth points dataset for the typical CDF inundation susceptibility zone, toolbox part 4 completes the follow steps:

- Selects basins with low, moderate, high overall CDF susceptibility.
- Selects basins that have at least one high initiation site potential, which means a minimum of 1,000 ft^2 [93 m^2]) of high initiation area (**Table 12**).
- Selects and exports transport line segments with low, moderate, and high transport potential. None-very low segments are removed.
- Finally, new points are added at the beginning, end, and in 25 ft (7.6 m) intervals along the set of exported transport lines (output dataset from DF_ArcPRO_Toolbox Part 3_ Basins). This is the initiation and growth points dataset for the typical zone.

To create the initiation and growth points dataset for the intermediate and extreme CDF inundation susceptibility zones, DF_Growth_ArcGIS_Toolbox Part 4_Debris-Flow Growth Pre-Processor completes the follow steps:

- Selects basins with low, moderate, high overall CDF susceptibility.
- Selects and exports transport line segments with low, moderate, and high transport potential. None-very low segments are removed.
- New points are added at the beginning, end, and in 25-ft (7.6-m) intervals along the set of exported transport lines (output dataset from DF_ArcPRO_Toolbox Part 3_ Basins). This is the initiation and growth point dataset for the intermediate and extreme zones.

The remaining preprocessor input datasets to prepare are raster datasets on upslope source areas for typical and intermediate/extreme zones. This is all accomplished by DF_ArcPRO_Toolbox Part 3_ Basins. Starting with the high zone of the initiation susceptibility raster, the confinement transects are used to measure the horizontal distance from the channel to the furthest cell with high initiation susceptibility (width of the typical source area). This is done along the high and moderate transport channel segments. We define typical source areas as the areas along the moderate and high transport channel segments with a width defined by the high initiation zone. This estimated width of the high source area generally includes the channel inner gorge where colluvium and debris are routinely deposited by slope colluvial processes and then carried away by CDFs (**Figure 36**).

Figure 36. Block diagrams of inner gorges (left, modified from WA DNR, 2004 and right, from Benda and others, 1998).

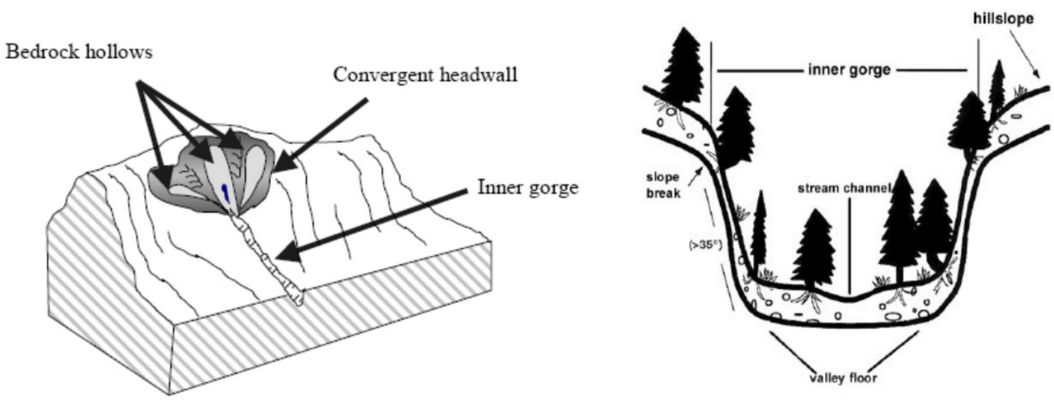

The mean width for each transport susceptibility class (both high and moderate) within each basin is calculated using the intersection of the transects and the high initiation zone **Figure 37 A**. The channel lines are then buffered by the mean widths for each basin and the high initiation zone is added to create the typical source area (**Figure 37 B**). Next, the intermediate/extreme source area are created by combining the new high source area with the moderate initiation raster (**Figure 37 C**).

Figure 37. A. Moderate (orange) and high (red) CDF initiation susceptibiltiy zones. B. Typical source area (purple) with typical CDF initiation and growth points. C. Intermediate/extreme source area (green) with intermediate/extreme CDF initiation and growth points.

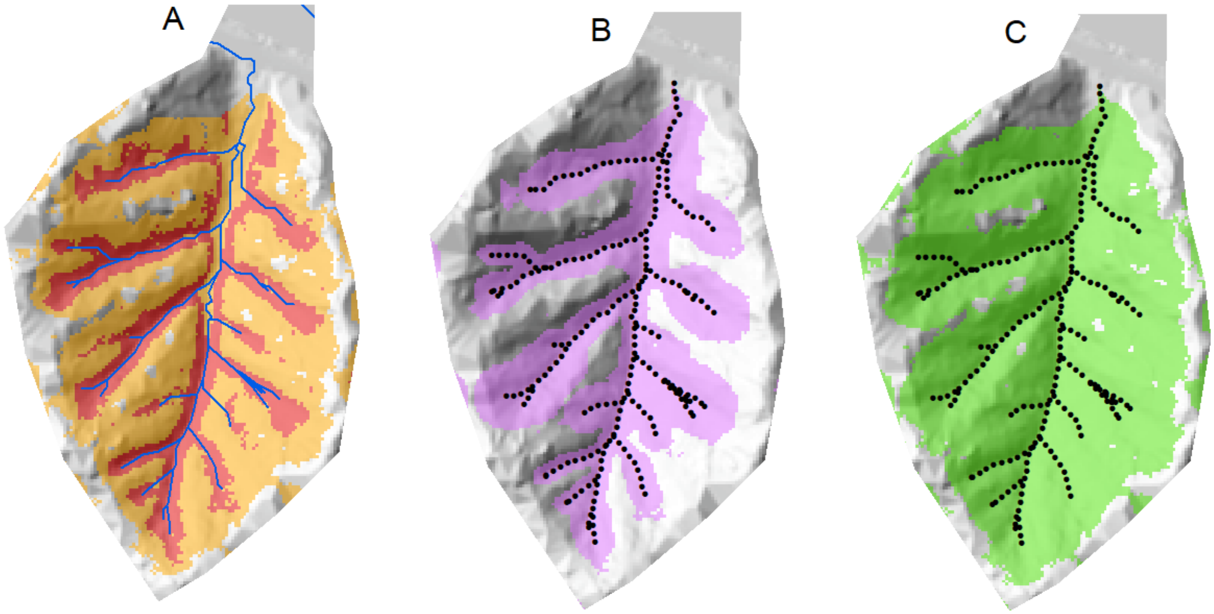

An additional value required by the preprocessor are the maximum possible volumes. We recommend using one-quarter order of magnitude increases of maximum possible volumes (**Table 16**). These recommended maximum volumes are based on the following published datasets: Robison and others (1999) found a maximum volume of 864,000 ft^3 (24,000 m^3) in the 1996 events; Griswold and Iverson (2008) suggested a range of up to 1,116,756 ft^3 (32,000 m^3); SLIDO 4.2 has 6,882 mapped debris flow fans deposits with a mean volume of 1,605,539 ft^3 (4,5463 m^3); and Gallaino and Pierson (1984) found a CDF volume of which they report as 100,000 $yards^3$, which is 2,699,000 ft^3 (76,455 m^3).

Another required input for the pre-processor is the growth factor. The growth factor has units of volume per unit area m^3/m^2, where the source area is defined spatially as typical or intermediate/extreme source area (**Table 16**). Reid and others (2016) estimated growth factors from post-event mapping of the 1996-97 CDF events in Dean Creek of the Oregon Coast Range, which represents a typical to intermediate event in the region. Their results indicated growth factors ranging from 0.12 to 0.20 m^3/m^2 (0.39 to 0.66 ft^3/ft^2) are appropriate for the 1996-97 events. From Reid and others (2016) and testing we performed, we have selected the following growth factors for CDF inundation susceptibility zones in the Dean Creek pilot study area.

- Typical growth factor: 0.105 ft^3/ft^2 (0.032 m^3/m^2); $10^{-1.5}$
- Intermediate growth factor: 0.328 ft^3/ft^2 (0.10 m^3/m^2); $10^{-1.0}$
- Extreme growth factor: 1.05 ft^3/ft^2 (0.32 m^3/m^2); $10^{-0.5}$

The above list is expressed as: CDF inundation susceptibility zone: growth factor; growth factor by half-order of magnitude.

Table 16. Recommended starting values for typical, intermediate, and extreme CDF inundation susceptibility zones, depending on results of channelized debris flow inventory mapping. Metric values are presented first, because metric units are required as inputs into the pre-processor.

General Inundation Susceptibility Zones	Initiation Growth Points & Source Area	Growth Factors by Half Orders of Magnitude	Growth Factor m^3/m^2 (ft^3/ft^2)	Proportion & Depth of Source Area Raster	Maximum Volume by One-Quarter Order of Magnitude Increase	Maximum Volume m^3 (ft^3)
typical small	typical	$10^{-2.0}$	0.01 (0.03)	1% × 1 m deep	$10^{4.25}$	18,000 (635,664)
typical medium or intermediate small	typical	$10^{-1.5}$	0.032 (0.1)	3% × 1 m deep	$10^{4.5}$	35,000 (1,116,756)
typical large, intermediate medium, or extreme small	typical or intermediate/ extreme	$10^{-1.0}$	0.10 (0.3)	1/10 × 1 m deep	$10^{4.75}$	56,000 (1,985,885)
typical extra-large, intermediate large, or extreme medium	intermediate/ extreme	$10^{-0.5}$	0.32 (1.1)	1/3 × 1 m deep	10^{5}	100,000 (3,531,467)
intermediate extra-large or extreme large	intermediate/ extreme	10^{0}	1.0 (3.3)	1 × 1 m deep	$10^{5.25}$	178,000 (?)
extreme extra-large	intermediate/ extreme	$10^{0.5}$	3.2 (10.5)	1 × 3.2 m deep	$10^{5.5}$	316,000 (?)
Extreme-extreme	extreme	$10^{1.0}$	10 (32.8)	1 × 10 m deep	$10^{5.75}$	562,000 (?)

The concept is to first use the CDF inventory data to select which typical zone to use. Once the typical zone is established, the two rows below the selected typical zone in **Table 16** are used for the intermediate and extreme zones. For example, in Dean Creek, the typical medium was selected and thus the intermediate medium and extreme medium rows were used for the intermediate and extreme zones.

Growth factors accommodate the erosion and entrainment of debris, which add to the volume of a CDF during movement down channel. One way to think of the growth factor is the overall depth of the source area expected to be eroded in each of the three CDF inundation susceptibility zones (i.e., typical, intermediate, and extreme). For example, in **Figure 38A**, the typical source area of the basin is 1,095,201 ft^2 (101,748 m^2). When the typical medium growth factor is applied (0.105 ft^3/ft^2 [0.032 m^3/m^2]; **Table 16**), the result is an inundation volume of 120,472 ft^3 (3,411 m^3) beyond the basin outlet (red zone below mouth of basin **Figure 38B**). The same volume and inundation area beyond the basin outlet are achieved if approximately 5% of the typical source area (54,856 ft^2 [5,096 m^2]) is eroded and entrained, as it was in an actual February 1996 debris flow event (**Figure 38B**, black outline). The reduced source area (black outline) requires a proportional increase in the growth factor from 0.105 ft^3/ft^2 to 2.2 ft^3/ft^2 to achieve the same inundation volume of 120,472 ft^3 (3,411 m^3) beyond the basin outlet.

Robison and others (1999) found average CDF landslide initiation depths of 1.9 ft (0.58 m), 2.1 ft (0.64 m), and 3.3 ft (1.01 m) in three of their study areas closest to or within the area that Coe and others (2011a) mapped the 1996 event (**Figure 38B**). In this way, the use of growth factors and source areas covers many possible situations, all of which can be represented by the inundation beyond the basin outlet.

Figure 38. A. Map of typical source area (purple) and actual source area (black outline; the upper part was classified as growth and the lower part [foot shape at mouth of basin] as deposition) from a CDF event in 1996 (Coe and others, 2011a). B. Results after modeling typical CDF inundation susceptibility zone (coral is primarily transport and growth and red is primarily deposition).

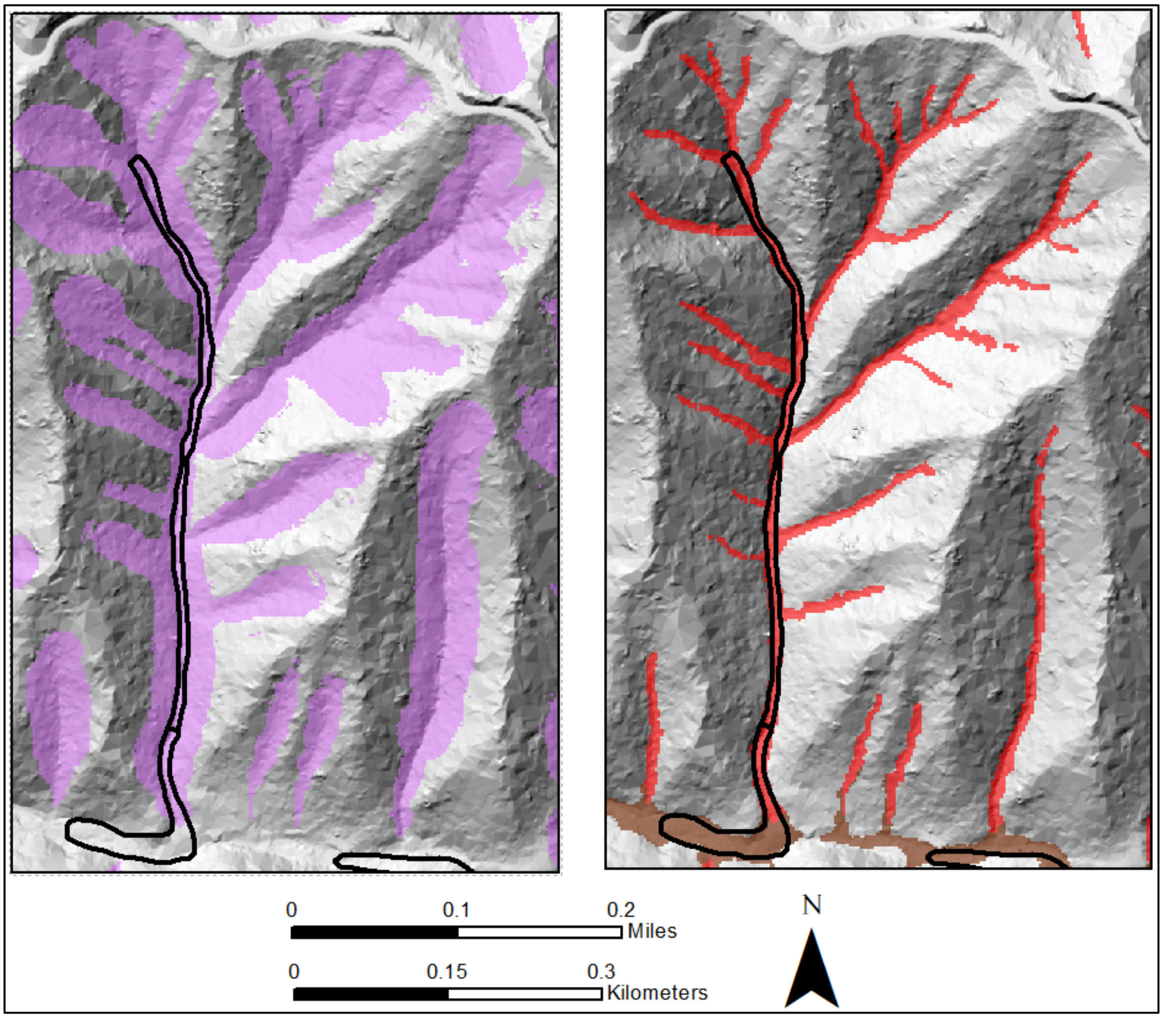

In current and future study areas evaluated following this protocol, the results will include three final CDF inundation susceptibility zones: typical, intermediate, and extreme (**Table 14**). The CDF inventory should be examined first, and regions of the study area should be defined that have relatively similar-sized historic initiation, transport, deposits, mapped CDF fans, and general runout distance. Start with the region with the smallest events and model the small or medium typical inundation susceptibility zone (see next section in this report). The results of the modeling should then be compared to the CDF inventory data and a determination of relative match should be evaluated.

For example, if none of the modeled inundation area overlaps the historic debris flow deposits or debris flow fans, it is an indication that a larger class of typical zone should be used. The most important part of this process is to establish the closest correlation of typical CDF events (past events) to the typical CDF inundation susceptibility zone (modeled future susceptibility zones). Once the typical CDF inundation susceptibility zone is established for a region, the intermediate and extreme zones should be modeled using the next two larger growth factors (**Table 16**).

From experience mapping in Oregon, we found the “typical medium” (**Table 16**) worked well as the CDF inundation susceptibility zone in the Oregon Coast Range. The volumes of some historic events on Mount Hood are in the range of maximum volumes for typical large and typical extra-large. Within a single study area, there could be several regions with different sized typical zones. For example, the western half of a study area within the Cascades might have typical small historic CDFs and the eastern half might be within the high Cascades and have typical large historic CDFs. These regions should be separated, and inundation modeled appropriately for each region within the study area.

Once the initial typical value is selected, the next step is to use the debris flow growth pre-processor (Reid and others, 2016; **Figure 39**).

Figure 39. Debris flow growth pre-processor tool (https://code.usgs.gov/ghsc/lhp/df_growth)

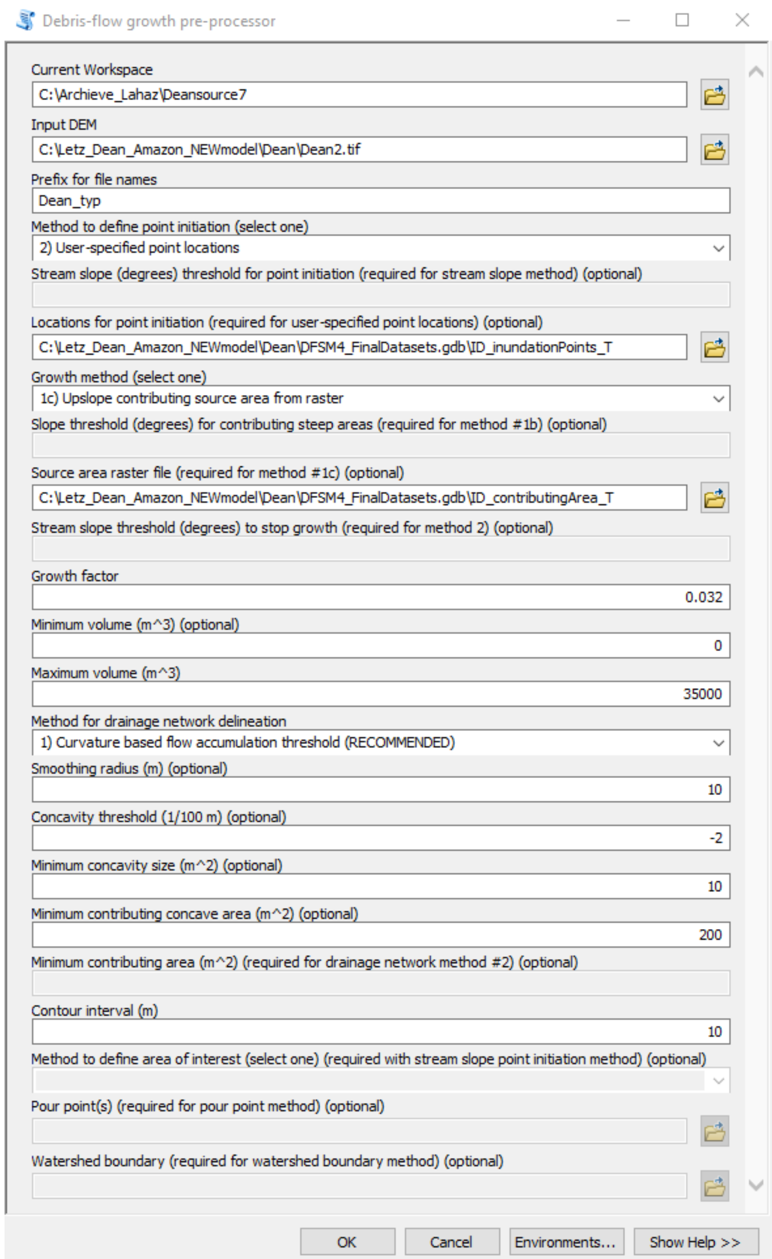

Tips for some debris flow growth pre-processor tool fields:

- **Current Workspace** – Create three folders for the typical, intermediate, and extreme inundation datasets. For example: Letz1, Letz2, Letz3. Select the appropriate folder for the current workspace.
- **Input DEM** – This file is the 9x9-ft (2.7x2.7-m) cell, filled, and reconditioned DEM created in the toolbox part 1.
- **Prefix for file names** – Use a shorted version of the folder names above. For example: L1, L2, and L3.
- **Method to define point initiation or stream slope threshold for point initiation**– Select option *2) User-specific point locations*.
- **Locations for point initiation** – Because we have selected user-specific point locations, a point dataset is required here. This dataset is the initiation point file for typical, intermediate, extreme previously described and created by DF_ArcPRO_Toolbox Part 3_ Basins.
- **Growth method** – Select option *1c) Upslope contributing source area from raster*. This option invokes a method that represents overall effects of potential debris flow growth (i.e., landslides on hillslopes, erosion on hillslopes, and erosion in the channel). This method calculates a volume as a function of the upslope contributing source area susceptible to debris flows, thereby allowing flexible spatial variations. Over this area, all debris flow growth processes are integrated in a single growth factor.
- **Source area raster file** – Because we have selected option *1c) Upslope contributing source area from raster*, a source area raster dataset is required. These datasets are the two source area datasets: typical or intermediate and extreme created by DF_ArcPRO_Toolbox Part 3_ Basins.
- **Growth factor** – Because we are selecting the growth method of contributing source area from a raster, a growth factor value is required. The growth factors recommended are in **Table 16**.
- **Minimum volume** – 0–2,825 ft^3 (0–80 m^3). Generally, a minimum volume is not necessary when using the upslope source area method. However, if the upper initiation/volume growth points result in separated inundation areas, a minimum volume can be used. We recommend using 80 m^3 (2,825 ft^3). Robinson and others (1999) found average initial volumes of ~100 cubic yards, which is 77 m^3 = 2,700 ft^3 (~31 ft × 31 ft × 2.7 ft deep).
- **Maximum volume** – The recommended maximum volumes are in **Table 16**.

Note: all other input parameters can be left as is. Run the debris flow growth pre-processor (toolbox part 4) for all three CDF inundation susceptibility zones. If the study area is divided into more than one region with different growth factors, the debris flow growth pre-processor should be run separately on each region.

After the pre-processor tool is completed, review all datasets and remove volume growth points that exhibit zero volume from the .csv file (produced by the DF_Growth_ArcGIS_Toolbox Part 4_Debris-Flow Growth Pre-Processor).

3.9 Step 9 and Step 10: Inundation Modeling (Multi-Point LAHARZ) and Review

Methodology progress bar: ▼indicates current step.
Green = Manual task, Orange = Toolbox task

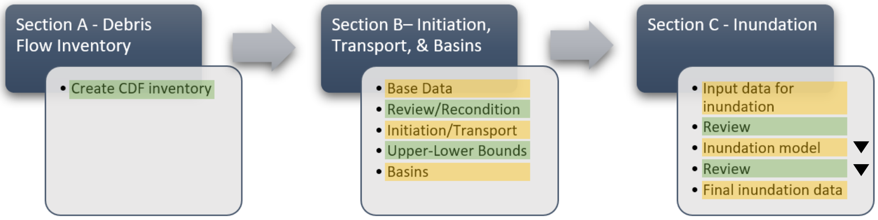

The next step is to delineate the inundation zones using DF_Growth_ArcGIS_Toolbox Part 5_Multi-Point Laharz_py. Enter the paths to the input datasets in DF_Growth_ArcGIS_Toolbox Part 5_Multi-Point Laharz_py and set the type of flow to *debris flow*. Execute the DF_Growth_ArcGIS_Toolbox Part 5_Multi-Point Laharz_py starting with the zone selected (typical small, typical medium, or typical large). Once the typical CDF inundation susceptibility zone is created, it needs to be visually inspected and compared to the datasets created in Step 1, CDF fan inventory and historic CDF initiation, transport, and inundation.

The typical CDF inundation susceptibility zone should approximately overlay with the inventory data. If they do not have similar spatial overlap, try to increase or decrease the typical growth factor and rerun steps 8 to 11. Once the typical zone is established, the intermediate and extreme zones can be created using the next two increased growth factors.

3.10 Step 11: Post Model Cleanup and Reclassification

Methodology progress bar: ▼indicates current step.
Green = Manual task, Orange = Toolbox task

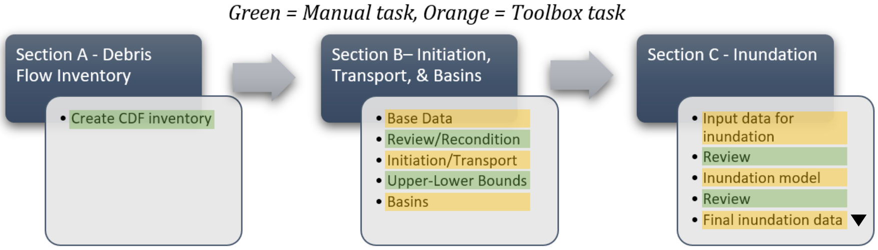

Once the final typical, intermediate, and extreme inundation zones are created for the study area or region of a study area, DF_ArcPRO_Toolbox Part 6_Inundation Zones Post-Processing should be run. The Part 5_Multi-Point Laharz_py output files include many different values. All values greater than 0 will be reclassed to 1; 0 and no data values will be reclassed to 0.

After the reclassification, these datasets will be cleaned up to remove anomalies and add in missing single cells (**Figure 40**). Part 6_Inundation Zones Post-Processing starts by using the ArcGIS Neighborhood tool (Focal Statistics) with three cells rectangular and sum. The output values are reclassed with values equal or greater to 4 to a value of 1. In other words, remove cells that have value 3 or less in the neighborhood. This process is repeated for each inundation zone (typical, intermediate, and extreme).

Figure 40. Typical inundation zone raw output. The single blue cells that appear as "stringers" extending from the main inundation zone and the single red cells that appear as holes within the main inundation zone are the two targets for cleanup. The final post cleanup inundation zone is the purple plus red.

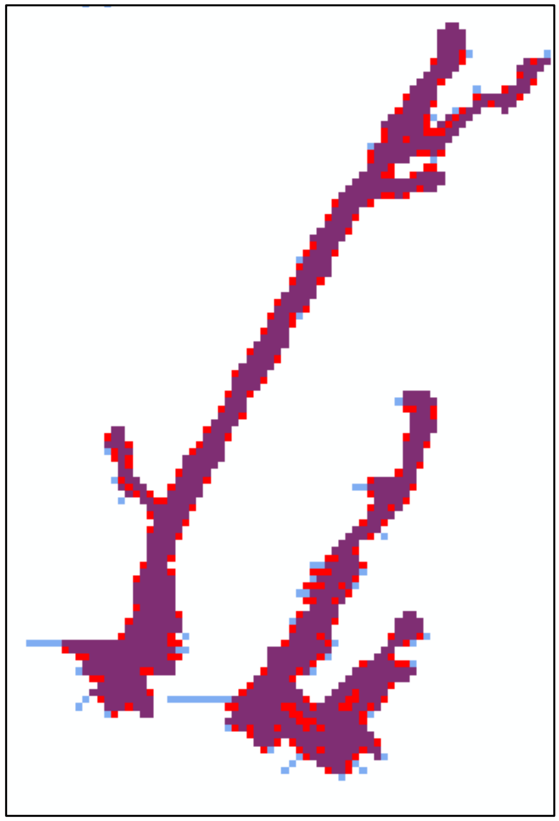

If the inundation zones go into a waterbody, Part 6_Inundation Zones Post-Processing has an input location for a waterbody shapefile and will use that file to clip the final inundation zones. The final step performed by Part 6_Inundation Zones Post-Processing is to classify the datasets into portions that are primarily transport/erosion and those that are primarily deposition. The basin polygons are used to divide the inundation datasets. Inside the basin polygons, values primarily show transport/erosion. Outside the basins, values primarily show deposition. The toolbox uses the file name to capture the zone (typical, intermediate, and extreme) for example "Letz_typical." The toolbox uses the values in the raster to differentiate between the primarily transport/erosion (1), primarily deposition (2), and none (0). Once this is complete, there should be the following three final inundation zone datasets (**Figure 41**):

- Typical, Primarily Transport/Erosion, Primarily Deposition
- Intermediate, Primarily Transport/Erosion, Primarily Deposition
- Extreme, Primarily Transport/Erosion, Primarily Deposition

Figure 41. Letz pilot study area with post model cleanup and reclassified into primarily transport/erosion and primarily deposition for typical (A), intermediate (B), and extreme (C) CDF inundation zones.

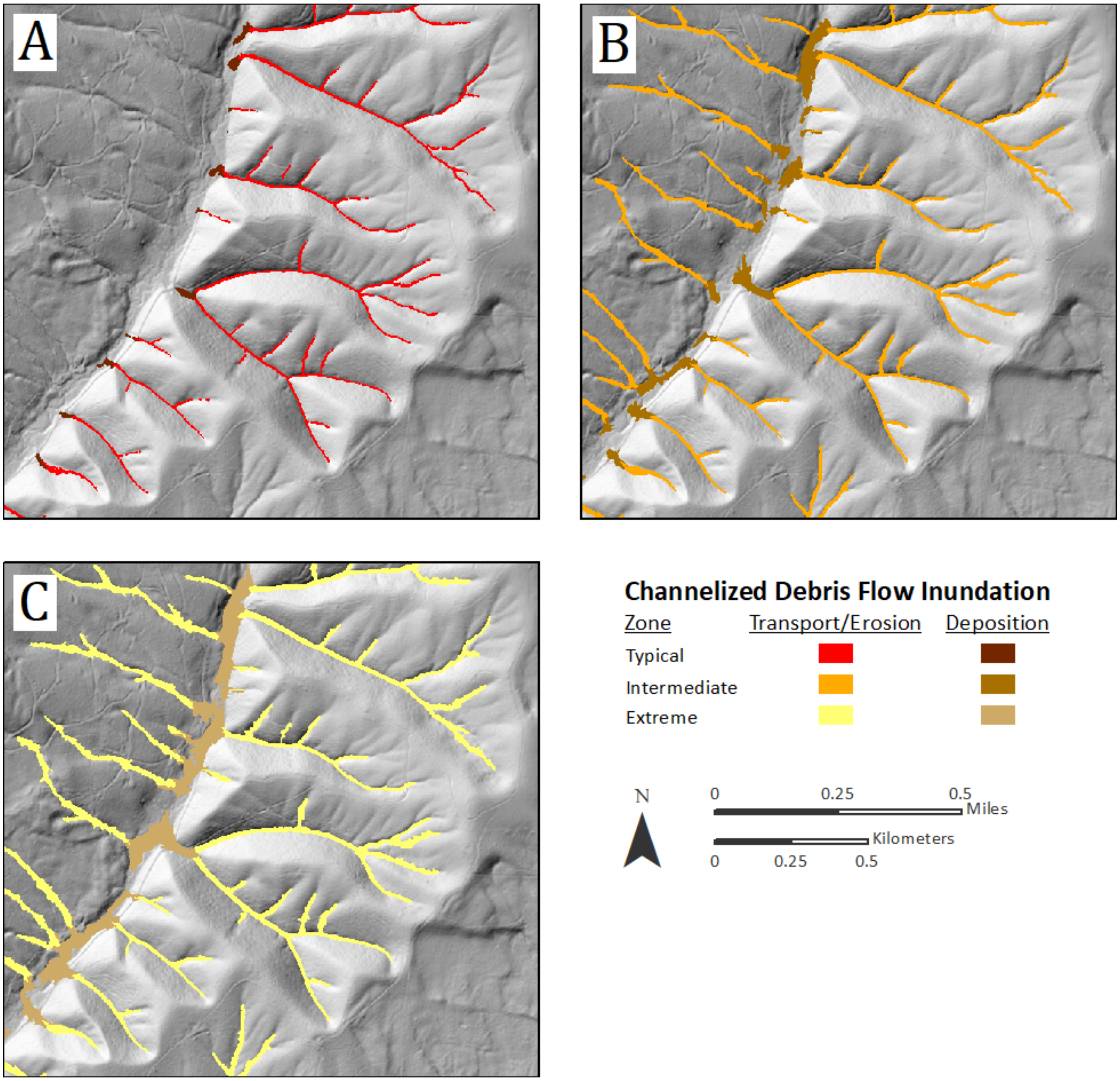

3.10.1 Final Datasets

When the entire process is complete, the following datasets are compiled into two geodatabases for distribution:

CDF Inventory

- Historic CDF Initiation Sites (points)
- Historic CDF Transport Paths (lines)
- Historic CDF Deposition Areas (polygons)
- CDF Fan Deposition Areas (polygons)

CDF Susceptibility

- CDF Initiation Susceptibility
    - None-Very Low, Low, Moderate, High
- CDF Transport Susceptibility
    - None-Very Low, Low, Moderate, High
- Overall CDF Basin Susceptibility
    - None-Very Low, Low, Moderate, High
- CDF Inundation Susceptibility
    - Typical, Primarily Transport/Erosion, Primarily Deposition
    - Intermediate, Primarily Transport/Erosion, Primarily Deposition
    - Extreme, Primarily Transport/Erosion, Primarily Deposition

Hillshade of the 9x9-ft (2.7x2.7-m) cell DEM

4.0 CDF SUSCEPTIBILITY HAZARD MAP EFFECTIVENESS

The objective of a CDF susceptibility dataset is to minimize the extent of the moderate and high susceptibility hazard zones but at the same time encompass all future CDFs (Godt and others, 2008). For example, a susceptibility map that captures 100% of the historic CDFs in a particular area but also maps the entire area as high hazard zone is potentially overly conservative. While this conservative approach accomplishes one hazard mapping goal—predicting areas of future landslide occurrence—the approach almost completely fails at a second goal—predicting which areas are not expected to have future landslides. Our objective is to maximize both goals.

As previously noted, we selected three pilot study areas with a range of relative levels of CDF hazards, from very low to none (Amazon Creek watershed), mixed (Letz Creek Watershed), and mostly high (Dean Creek watershed). To test the effectiveness of both of our goals, we performed testing on the three pilot areas and six more areas (Scottsburg, Tillamook, Clatskanie, Dodson, Mount Hood, and Ashland; **Figure 42**). The additional six areas were selected based on availability of 1) lidar-based DEM (3-ft resolution), 2) SP-42 landslide inventory, 3) historic initiation points of past CDFs, and 4) few to none of the 680 historic CDF initiation sites used to develop this method.

We performed two tests in each of the nine areas (three pilot and six additional test areas). In the first test, we evaluated the ability of the datasets to identify areas of moderate and high hazard through the spatial intersection of known historic CDF events and through the basins identified as having high susceptibility to future CDFs. In the second test, we evaluated the ability of the datasets to identify areas of none-very low to low CDF susceptibility through the spatial intersection of areas previously modeled to have no potential for future rapidly moving landslides/debris flows by Hofmeister and others (2002) in DOGAMI Interpretive Map 22 (IMS-22), which is a GIS overview map of potential RML hazards in western Oregon (from here on referred to as IMS-22-No Potential). IMS-22 has two zones: One identifies areas that have the potential for future debris flows and the other is the areas which were identified as no potential for future debris flows. Thus, the IMS-22-No Potential refers to the second zone. This second test was also aimed at understanding the potential overprediction of model outputs. In addition to these two tests, we performed another test in the three pilot study areas (specifically in places where we performed the DF_Growth_ArcGIS_Toolbox Part 5_Multi-Point Laharz_py) to examine the ability of the datasets to predict the inundation areas.

Figure 42. The six additional testing areas (red fill), located throughout western Oregon, selected to test the effectiveness of the protocol for CDF susceptibility mapping .

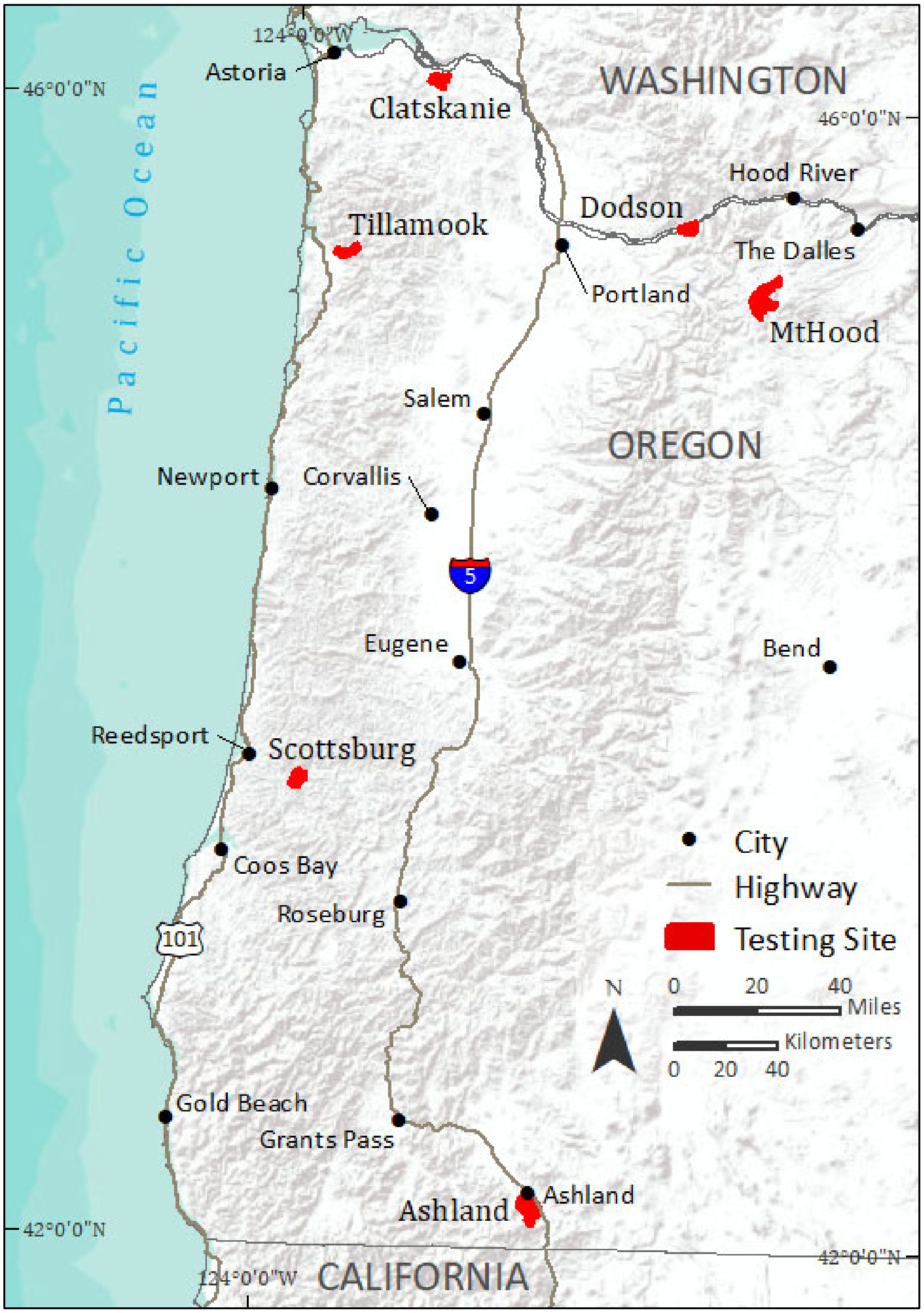

4.1 Ability to Map High Susceptibility

We examined the model output scores of the basins by comparing the overall basin scores (none-very low to high) with historic CDF initiation points in the nine test areas. There were 612 historic CDF initiation points in the test areas. We found that 97% of these historic CDF events were in basins with an overall basin score of 8 (high). Of the 3% (9 points) not in basins with a high score, seven points (2%) were in basins with a score of 7 (moderate), and two points (1%) were in basins with a score of 5 (low). These results indicate the model does a very good job of identifying basins as moderate or high hazard.

Each basin also has an estimated number of potential future CDF initiation sites, found by taking the initiation high zone and dividing by 1,000 ft^2 [93 m^2]) as previously discussed in the basin initiation susceptibility section. We compared the number of actual historic initiation sites to the estimated number of potential sites and found a general trend that places with more historic initiation sites tended to have more potential future initiation sites. Although not a strong correlation, the general trend indicates that more potential initiation sites (or an area of high initiation in a basin) could result in a greater frequency of CDF in that basin. We did not consider frequency in this paper; frequency could be a component to consider in future updates to this protocol.

4.2 Ability to Map None-Very Low Susceptibility

To see if the model results are correctly predicting areas not expected to have CDFs, we tested nine areas with overall CDF susceptibility scores of 2-3 (none-very low) (**Table 14**). We examined the percent area of each basin covered with IMS-22-No potential mapping (Hofmeister and others, 2002). In other words, we compared the very low-none and no potential hazard zones of the two models in the same basins.

Within the nine areas, 285 basins with overall basin classification of none-very low were examined. We found 74% of the basins were covered by IMS-22-No potential or, in other words, the two models had a high agreement that CDF were not likely in the same basins. The remaining 26% of basins had a range of coverage by IMS-22; however, all had relatively low coverage percentage.

These results indicate the model has a moderate to high degree of agreement with IMS-22. It is also an indication that the new modeled susceptibility dataset minimizes over-coverage by moderate and high susceptibility hazard zones.

4.3 Ability to Map Primarily Deposition Inundation Susceptibility

We examined the spatial overlap of CDF inundation zones with the mapped fans in the three pilot study areas to determine the ability of the model to identify areas of known past deposition. There were 46 mapped CDF fans in the Dean Creek pilot area and 85 fans in the Letz Creek pilot area. These mapped CDF fans are very likely the result of several-to-many past CDF events, and therefore we expect the typical inundation zones to cover only a portion of these fans.

Burns and Lindsey (2017) mapped fans and historic deposits on the Oregon side of the Columbia River Gorge and found the 1996 historic CDF events covered the fans in a range from approximately 10% to 25%. The 1996 events examined in Coe and others (2011a) in the Dean Creek area cover an average of approximately 45% of the fans in Dean Creek, with a range of nearly 0% to almost 100%. Depending on the size and longevity of the CDF fan and the local CDF frequency and magnitude, we would expect the typical CDF inundation zones in Oregon to generally cover 10% to 50% of the fans but the percentage could range higher. We found the following spatial overlap of fans and the three CDF inundation zones (**Table 17**).

Table 17. Percent of spatial overlap of CDF inundation zones with mapped fans.

Pilot Study Areas	CDF Inundation Zones	Percent of Inundation Zones Covering Mapped Fans
Dean Creek	typical	69%
Dean Creek	intermediate	92%
Dean Creek	extreme	97%
Letz Creek	typical	20%
Letz Creek	intermediate	49%
Letz Creek	extreme	66%

These percent of the modeled inundation zones covering mapped fans indicate results are sensible when identifying primary inundation deposition areas. We also looked at the spatial overlap of CDF inundation zones with the 1996 CDF event polygons mapped by Coe and others (2011a) in Dean Creek. We found 76%, 91%, and 97% for typical, intermediate, and extreme inundation zones, respectively.

There were 91 historic CDF events in Dean Creek and three in Letz Creek (over a ~25-year time period). When these events are annualized, there are approximately 3.3 events per year in Dean Creek and 0.1 events per year in Letz Creek. This relatively large difference in estimated annualized frequency is likely one of the reasons why the percentages are lower in Letz Creek than in Dean Creek (**Table 17**). The Dean Creek pilot area is located partially within the flood zones of the Umpqua River, which is extensive in this region, and thus CDF fans were likely eroded during flooding much more often than in Letz Creek pilot area, which has no large river near the fans. This continuous erosion of the fan deposits results in relatively smaller CDF fans and likely is another reason why the percentages are higher in Dean Creek than in Letz Creek (**Table 17**).

4.4 Comparison to IMS-22

The method Hofmeister and others (2002) used to create IMS-22 after the 1996-97 CDF events is unclear as it was not extensively documented, but they did use a 10 m DEM (lidar-derived DEMs were not available at the time). They used a yes/no potential for future debris flows classification for hazard, not zones of none-very low, low, moderate, and high and typical, intermediate, and extreme as the present study does. We visually examined the spatial difference (**Figure 43**). It is hard to compare hazard maps when the input datasets and the methods are different; however, based on visual overlap, it appears the new method provides a more refined way to identify CDF hazard zones.

Figure 43. Comparison of IMS-22 (Hofmeister and others, 2002; purple outline) with results from this CDF protocol (moderate [orange] and high [red] initiation susceptibility and typical, intermediate, and extreme channelized debris flow inundation zones [brown] are plotted). Black outlines are mapped CDF fans. The area is a portion of Letz Creek Watershed.

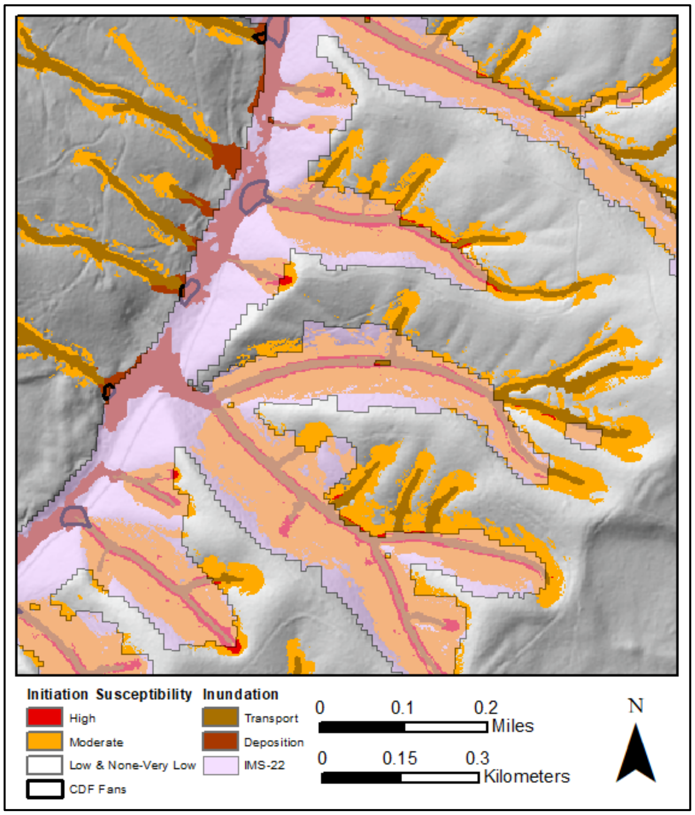

5.0 ARCGIS TOOLBOX, LIMITATIONS, AND POTENTIAL DATA USE

To expedite the protocol and reduce errors, we created GIS toolboxes. The described protocol was scripted into ArcPRO and AcrMAP Toolboxes (see appendix). The model consists of six parts and is described in general below. Details of the model are outlined in the GIS Procedure and Data Dictionary (appendix).

- DF_ArcPRO_Toolbox.tbx
    - Part 1_Base Maps
    - Part 2_Initiation and Transport
    - Part 3_ Basins
    - Part 6_Inundation Zones Post-Processing
- DF_Growth_ArcGIS_Toolbox.tbx*
    - Part 4_Debris-Flow Growth Pre-Processor*
    - Part 5_Multi-Point Laharz_py*
- *DF_Growth software repository: https://code.usgs.gov/ghsc/lhp/df_growth

Executing the model is straightforward, but to help clarify data processing and model design we have provided documentation to assist user (see appendix). A "read me" document outlines the steps to run the model and gives an overview of model outputs. A GIS procedure document explains the GIS tools and parameters used for the tools. The toolbox itself also contains explanations and directions.

5.1 Limitations

The limitations of the CDF susceptibility mapping/modeling protocol are listed below. Because of these limitations, the resulting hazard maps are useful for regional applications but should not be used as alternatives to site-specific studies in critical areas.

1. Every effort has been made to ensure the accuracy of the GIS and tabular components of the debris flow inventory database, but it is not feasible to completely verify all original input data.
2. As previously discussed, the protocol is based on the debris flow inventory. The quality and completeness of this dataset, which have inherent uncertainty, can affect the level of detail and accuracy of the final debris flow susceptibility map.
3. The landslide inventory data have limitations that are discussed Burns and Madin (2009).
4. The GIS database is a “snapshot” view of current data; new information regarding landslides can be found, or new landsliding may occur that could change the map.
5. Because the lidar-based bare earth DEM is only a model of the ground elevation, it does not distinguish elevation changes from human structures like buildings and retaining walls. Furthermore, it does not include other items found on the surface such as trees. For a protocol and map intended to be used at the regional scale, it is not possible to conduct the extensive fieldwork required to locate and evaluate existing structures, trees, etc., and the changes to them that can occur throughout time. Therefore, these must be examined on a site-specific basis.
6. Some landslide areas in the inventory may have been mitigated, thereby reducing their level of susceptibility. Because it is not feasible to collect detailed site-specific information on every landslide, existing mitigation measures are not taken into account.
7. There are many debris flow models in use. Most are appropriate for site-specific applications. This model can help identify basins and outlets in need of site-specific investigations; this model does not perform the same task as existing site-specific models, which for example examine flow speeds, hydrographs of flow height, clast sizes, and impact forces.
8. This debris flow model is intended for CDF processes and does not accommodate shallow landsliding, earth flows, or riverine flooding processes.
9. This CDF protocol does not include rain intensity, drought, or climate change.

5.2 Potential Uses

The main purpose of this protocol is to provide a detailed explanation of the CDF susceptibility mapping process. Following the protocol ensures consistency in future maps produced by DOGAMI, or by other practitioners, and provides a technical reference for those maps. We intend these maps to provide useful information to guide site-specific investigations for future developments, to support regional planning, and to assist mitigation of existing landslides and slopes.

CDF susceptibility maps can serve as useful tools for differentiating areas of higher and lower hazards. This information is foundational to emergency and land use applications. The maps can be used to aid the development and refinement of emergency response plans. They can also help with estimations of resource impacts from future landslide movement. Common applications of landslide susceptibility data in land-use planning include inclusion in comprehensive planning and the development of hazard ordinances with attached zoning and regulations. While the data and resultant maps are not appropriate for site-specific evaluations, they are valuable for regional screening for landslides and the selection of appropriate areas on which to focus further site-specific studies. The data and maps are particularly suitable for incorporation into state, county, and city hillside development ordinances (Sears and others, 2019).

6.0 ACKNOWLEDGMENTS

Funding for this project was initially provided by the U.S. Geological Survey Landslide Program. We would also like to thank the U.S. Geological Survey Landslide Program for generous technical support, including assistance by Richard Iverson, Julie Griswold, and Steve Schilling with Laharz training. We are very grateful to Mark Reid, Dianne Brien, and Jeff Coe for their research over more than a decade on CDF hazards in Oregon, which is the foundation of this protocol. Reid and Brien also provided reviews and guidance during the development of this protocol, which fundamentally improved the result.

Additional funding for this project was provided by FEMA through the Hazard Mitigation Grant Program, routed through Oregon Emergency Management (DR-4258-8-F). We thank Amie Bashant for her support.

We thank DOGAMI staff who helped work on this project through technical assistance, review, and general assistance, especially Yumei Wang, Sean Pickner, Kaleena Hughes, Ian Madin, and Deb Schueller. We thank Jason McClaughry for his DOGAMI Technical Review Committee review. Finally, we thank the staff at Gneiss Editing for performing final copyediting.

7.0 REFERENCES

Benda, L.; Veldhuisen, C.; Miller, D.; and Miller, L.R., 1997/8, Slope Instability and Forest Land Managers: a Primer and Field Guide, Earth Systems Institute, 98 p.

Benda, L. E., and Cundy, T. W., 1990, Predicting deposition of debris flows in mountain channels: Canadian Geotechnical Journal, v. 27, no. 4, p. 409–417. https://doi.org/10.1139/t90-057

Blais-Stevens, A., and Behnia, P., 2016, Debris flow susceptibility mapping using a qualitative heuristic method and Flow-R along the Yukon Alaska Highway Corridor, Canada: Nat. Hazards Earth Syst. Sci., v. 16, no. 2, p. 449-462. https://doi.org/10.5194/nhess-16-449-2016

Burns, W. J., 2007, Comparison of remote sensing datasets for the establishment of a landslide mapping protocol *in* Schaefer, V. R., Schuster, R. L., and Turner, A. K., (eds.), Conference Presentations, 1st North American Landslide Conference, Vail, Colorado: Association of Environmental & Engineering Geologists, AEG Special Publication 23, CD-ROM, 1895 p. + index.

Burns, W. J., Madin, I. P., and Ma, L., 2008, Statewide landslide information database for Oregon (SLIDO), release 1. [Release 1 database superseded by later releases: http://www.oregongeology.org/slido/]

Burns, W. J., and Madin, I. P., 2009, Landslide protocol for inventory mapping of landslide deposits from light detection and ranging (lidar) imagery: Oregon Department of Geology and Mineral Industries Special Paper 42, 30 p. https://www.oregongeology.org/pubs/sp/p-SP-42.htm

Burns, W. J., Madin, I. P., and Mickelson, K. A., 2012, Protocol for shallow-landslide susceptibility mapping: Oregon Department of Geology and Mineral Industries Special Paper 45. http://www.oregongeology.org/pubs/sp/p-SP-45.htm

Burns, W. J., and Mickelson, K. A., 2016, Protocol for deep landslide susceptibility mapping: Oregon Department of Geology and Mineral Industries Special Paper 48. http://www.oregongeology.org/pubs/sp/p-SP-48.htm

Burns, W. J., and Lindsey, K. O., 2017, Landslide inventory of eastern Multnomah County, Oregon: Oregon Department of Geology and Mineral Industries Open-File Report O-17-03. http://www.oregongeology.org/pubs/ofr/p-O-17-03.htm

Burns, W. J., and Franczyk, J. J., 2021, History of the Oregon Landslide Warning System 1997–2018 and recommendations for improvement: Oregon Department of Geology and Mineral Industries Open-File Report O-21-01. https://www.oregongeology.org/pubs/ofr/p-O-21-01.htm

Cannon, S. H., Gartner, J. E., Parrett, C., and Parise, M., 2003, Wildfire-related debris-flow generation through episodic progressive sediment-bulking processes, western USA, *in* Rickenmann, D., and Chen, C. L. (eds.), Proceedings of the Third International Conference on Debris-Flow Hazards Mitigation, Davos, Switzerland, September 10-12, 2003: Rotterdam, Millpress, p. 71–82. https://pubs.er.usgs.gov/publication/70025321 [available at https://www.researchgate.net/profile/Susan_Cannon/publication/34532125_Debris-flow_response_of_watersheds_recently_burned_by_wildfire/links/543d414c0cf25d6b1ad73d9c.pdf]

Coe, J. A., Michael, J. A., and Burgos, M. M., 2011a, Map of debris flows caused by rainfall during 1996 in parts of the Reedsport and Deer Head Point quadrangles, Douglas County, southern Coast Range, Oregon: U.S. Geological Survey Open File Report 2011–1150, 9 p. pamphlet, 1 sheet, scale 1:12,000.

Coe, J. A., Reid, M. E., Brien, D. L., and Michael, J. A., 2011b, Assessment of topographic and drainage network controls on debris-flow travel distance along the west coast of the United States, *in* Genevois, R., Hamilton, D. L., and Prestininzi, A. (eds.), Proceedings of the 5th International Conference on Debris Flow Hazards Mitigation, Mechanics, Prediction and Assessment, Padua, Italy, June 14-17, 2011: Italian Journal of Engineering Geology and Environment and Casa Editrice Universita La Sapienza, Rome, Italy, special issue 2011, p. 199–209. DOI: 10.4408/IJEGE.2011-03.B-024.

De Graff, J. V., Cannon, S. H., and Gartner, J. E., 2015, The timing of susceptibility to post-fire debris flows in the Western United States: Environmental and Engineering Geoscience, v. 21, no. 4, 277–292. https://doi.org/10.2113/gseegeosci.21.4.277

Fannin, R. J., and Rollerson, T. P., 1993, Debris flow: some physical characteristics and behaviour: Canadian Geotechnical Journal, v. 30, no. 1, 71–81. https://doi.org/10.1139/t93-007

Fannin, R. J., Wise, M. P., Wilkinson, J. M. T., Thomson, B., Hetherington, E. D., 1997, Debris flow hazard assessment in British Columbia, *in* Cheng-lung Chen (ed.), Debris Flow Hazard Mitigation: Mechanics, Prediction, and Assessment, Proceedings of the 1st international conference, San Francisco, Calif., August 7–9, 1997: New York, American Society of Civil Engineers, 197–206.

Franczyk, J. J., Burns, W. J., and Calhoun, N. C., 2019, Statewide Landslide Information Database for Oregon, release 4.0 (SLIDO 4.0): Oregon Department of Geology and Mineral Industries, Digital Data Series. https://www.oregongeology.org/pubs/dds/p-slido4.htm

Gallaino, G. L., and Pierson, T. C., 1984, The 1980 Polallie Creek debris flow and subsequent dam-break flood, East Fork Hood River basin, Oregon: U.S. Geological Survey Open-File Report 84-578, 59 p. https://doi.org/10.3133/ofr84578

George, D. L., R. M. Iverson, and C. M.Cannon, 2017. Newmethodology for computing tsunami generation by subaerial landslides: Application to the 2015 Tyndall Glacier landslide, Alaska, Geophys. Res. Lett., 44, 7276–7284, doi:10.1002/ 2017GL074341.

Godt, J. W., Schulz, W. H., Baum, R. L., and Savage, W. Z., 2008, Modeling rainfall conditions for shallow landsliding in Seattle, Washington, *in* Baum, R. L., Godt, J. W., and Highland, L. M. (eds.), Landslides and engineering geology of the Seattle, Washington, area: Geological Society of America Reviews in Engineering Geology, v. 20, p. 137–152. https://doi.org/10.1130/2008.4020(08)

Griswold, J. P., and Iverson, R. M., 2008 Mobility statistics and automated hazard mapping for debris flows and rock avalanches: U.S. Geological Survey Scientific Investigations Report 2007-5276, 59 p. http://pubs.usgs.gov/sir/2007/5276/

Highland, L.M., Stephenson, D.E., Christian, S.B., and Brown, W.M., 1997. Debris flow hazards in the United States, U.S. Geological Survey Fact Sheet 176-97.

Hofmeister, R. J., 2000, Slope failures in Oregon, GIS inventory for three 1996/97 storm events: Oregon Department of Geology and Mineral Industries Special Paper 34, 20 p. https://www.oregongeology.org/pubs/sp/p-SP-34.htm

Hofmeister, R. J., Miller, D. J., Mills, K. A., Hinkle, J. C., and Beier, A. E., 2002, GIS overview map of potential rapidly moving landslide hazards in western Oregon: Oregon Department of Geology and Mineral Industries Interpretive Map IMS-22, 52 p. https://www.oregongeology.org/pubs/ims/p-ims-022.htm

Hungr, O., Morgan, G. C., and Kellerhals, R., 1984, Quantitative analysis of debris torrent hazards for design of remedial measures: Canadian Geotechnical Journal, v. 21, no. 4, 663–677. https://doi.org/10.1139/t84-073

Hungr, O., McDougall, S., Wise, M., and Cullen, M., 2008, Magnitude–frequency relationships of debris flows and debris avalanches in relation to slope relief: Geomorphology, v. 96, no. 3-4, 355–365. https://doi.org/10.1016/j.geomorph.2007.03.020

Iverson, R. M., Schilling, S. P., and Vallance, J. W., 1998, Objective delineation of lahar-inundation hazard zones: Geological Society of America Bulletin, v. 110, no. 8, p. 972–984. https://volcano.wr.usgs.gov/vsc/file_mngr/file-50/lahar_inundation_GSA_Iverson.pdf

Lukashova, S. G., Lancastera, J. T., Oakley, N. S., and Swansond, B. J., 2019, Post-fire debris flows of 9 January 2018, Thomas Fire, southern California: Initiation areas, precipitation and impacts: abstract, 7th International Conference on Debris-Flow Hazards Mitigation, June 10–13, 2019, Colorado School of Mines, Golden, Colo, p. 107. https://dfhm7.csmspace.com/docs/DFHM7ProgramFull.pdf

May, L.C., Gresswell, R.E., 2004. Spatial and temporal patterns of debris-flow deposition in the Oregon Coast Range, USA, Geomorphology, 57 p. 135-149.

Montgomery, D.R., Foufoula-Georgiou, E., 1993. Channel network source respresentation using digital elevation models. Water Resources Research, 29(12), 3925-3934.

Parker, R. N., Hales, T. C., Mudd, S. M., Stuart, W. D., Grieve, S. W. D., and José A. Constantine, J. A., 2016, Colluvium supply in humid regions limits the frequency of storm-triggered landslides: Scientific Reports, v. 6, article 34438. https://doi.org/10.1038/srep34438

Pierson, T.C., 2005, Distinguishing between debris flows and floods from field evidence in small watersheds: U.S. Geological Survey Fact Sheet 2004-3142, 4 p., (Available at: https://pubs.usgs.gov/fs/2004/3142/)

Pierson T.C. 2005. Hyperconcentrated flow; transitional process between water flow and debris flow. In Debris-flow Hazards and Related Phenomena, Jakob M, Hungr O (eds). Springer: Berlin; 159–202

Reid, M. E., Coe, J. A., and Brien, D. L., 2016, Forecasting inundation from debris flows that grow volumetrically during travel, with application to the Oregon Coast Range, USA: Geomorphology, v. 273, 396–411. https://doi.org/10.1016/j.geomorph.2016.07.039

Robison, E. G., Mills, K., J., Paul, J. T., Dent, L., and Skaugset, A., 1999, Storm Impacts Monitoring Project: Final report: Salem, Oreg., Oregon Department of Forestry, Forest Practices Technical Report 4, 141 p.

Schilling, S.P., 2014, Laharz_py—GIS tools for automated mapping of lahar inundation hazard zones: U.S. Geological Survey Open-File Report 2014-1073, 78 p., http://dx.doi.org/10.3133/ofr20141073.

Sears, T. R., Lahav, M., Burns, W. J., and McCarley, J., 2019, Preparing for landslide hazards, a land use guide for Oregon communities: Oregon Department of Land Conservation and Development (DLCD).

Strahler, A. N., 1952, Hypsometric (area-altitude) analysis of erosional topology: Geological Society of America Bulletin, v. 63, no. 11, p. 1117–1142.

Tarboton, D.G. and Ames, D.P. (2001) Advances in the Mapping of Flow Networks from Digital Elevation Data. World Water and Environmental Resources Congress, May 20-24, 2001, Orlando.

Washington Department of Natural Resources, 2004, Guidelines for evaluating potentially unstable slopes and landforms, Section 16, *in* Forest Practices Board Manual: Olympia, Wash., Washington Department of Natural Resources, Forest Practices Board. Section 16: Guidelines for Evaluating Potentially Unstable Slopes and Landforms shown in: https://www.dnr.wa.gov/publications/bc_fp_sm_presentation6.pdf and https://www.dnr.wa.gov/publications/fp_cmer_08_802.pdf https://www.dnr.wa.gov/publications/bc_fpb_bmsection16.pdf section linked from https://www.dnr.wa.gov/about/boards-and-councils/forest-practices-board/rules-and-guidelines/forest-practices-board-manual

Wiley, T. J., McClaughry, J. D., Ma, L., Mickelson, K. A., Niewendorp, C. A., Stimely, L. L., Herinckx, H. H., and Rivas, J., 2014, Geologic map of the southern Oregon coast between Port Orford and Bandon, Curry and Coos Counties, Oregon: Oregon Department of Geology and Mineral Industries Open-File Report O-14-01, 66 p., 3 map sheets, GIS data. https://www.oregongeology.org/pubs/ofr/p-O-14-01.htm

APPENDIX

Detailed Procedures for the ArcGIS Toolboxes Part 1, 2, 3, & 6

DFSM Part 1 Base Maps & Channel Lines: Introduction

This GIS Methods Section for Part 1 of the Debris Flow Susceptibility Model (DFSM) is described in Section 3.3 in the report. The starting inputs are the workspace folder and the 3-foot, lidar derived digital elevation model (DEM) of the area of interest. The output datasets will be study area base maps, hydrology maps, and channel lines, as well as the DFSM2_InitiationTransport.gdb geodatabase.

The Part 1 Base Maps tool gives the user the option of re-running the model using a hydro-conditioned dem. This hydro-conditioned dem corrects for errors in channel lines due to roads and low-slope areas. Note that replacing the initial dem with the hydro-conditioned dem and re-running the Part 1 model will overwrite the previous model outputs. The steps for hydro-conditioning a dem are in Section 3.4 of the report.

The Part 2 geodatabase includes select copies of the initial base maps. Subsequent analysis on initiation and transport potential and basin characteristics are based on the initial dem and not the hydro-conditioned dem. Select base maps will be used in Part 2 of DFSM to build the initiation raster. Select base maps and channel lines will be used in Part 2 of DFSM to analyze the transportation potential for the area of interest.

DFSM Part 1 Base Maps & Channel Lines: Methods

Check Input DEM for Correct Projection / Cell Size

To output results that are appropriate for the DFSM model design, it will only run using a dem that is projected into a projected coordinate system (PCS) that measures in feet and has a resolution of less than or equaled to 9-feet. This model section checks that both these conditions are met. If not, the model will stop and produce an error message.

Check DEM projection – Describe arcpy function: Input = inputDEM. This step returns the projection and cell size of the input dem.

Create File Geodatabase for Output Datasets, Part 1 Model

Create new geodatabase – Create File GDB tool: Input = workSpace, GDB name = DFSM1_BaseMapChannels.gdb. This step creates a new file geodatabase in the workspace directory. This will contain most of the model outputs.

Create Base Map Datasets

This section creates base map rasters from the input DEM (dem3ft). These rasters will be used for creating future datasets and running basin analysis. If there is an error, the model will stop and produce an error message.

Make Copy of Input DEM – Copy Raster tool: Input = inputDEM, output = dem3ft, pixel type = 32_BIT_FLOAT, null values = -3.402823e+38. A copy of the input dem is created in the DFSM1_BaseMapChannels.gdb.

Resample DEM – Resample tool: Input = dem3ft, output = dem9ft, output cell size = 9, resampling technique = bilinear. This step resamples the input dem to 9-feet.

Fill Resampled DEM – Fill tool: Input = dem9ft, output raster = dem9ft_fill. This step removes small imperfections in the resampled dem that might adversely impact hydrologic processes.

Create Hillshade Raster – Hillshade tool: Input = dem3ft, output = dem3ft_hillshade. This step creates a hillshade raster from the input dem.

Create Slope Raster – Slope tool: Input = dem9ft_Fill, output = dem9ft_fill_slope. This step creates a slope raster from the filled, resampled dem.

Create Channel Lines Dataset

This section starts by creating all the hydrology raster datasets and channel lines feature class from the resampled and filled input dem (dem9ft_fill) and slope raster (dem9ft_fill_slope). It uses a curvature raster as an additional "weight" to develop the final flow accumulation raster output.

Create Flow Direction Raster – Flow direction tool: Input = dem9ft_fill, output = dem9ft_fill_flowDirect. This step creates a raster whose values represent the direction of water flow, based on elevation.

Smooth the DEM – Focal Statistics and NbrCircle tools: Input = dem3ft, output = smooth_DEM, neighborhood = 32.81 (radius, in feet), statistic = MEAN. This step smooths the input dem before calculating curvature. The neighborhood value used is derived from the 10-meter default input to the USGS Pre-Processor tool (Part 4).

Create Curvature Raster – Curvature tool: Input = smooth_DEM, output = planCurv_Raster. This step creates the plan curve raster.

Smooth Curvature Raster – Focal Statistics and NbrNeighborhood tools: Input = planCurv_Raster, output = curveMean_Raster, neighborhood = 3 (rectangle, in feet), statistics = MEAN. This step smooths the plan curvature raster. The neighborhood value is derived from the resolution of the input raster.

Identify Concave Areas – Conditional tool: Input = curveMean_Raster, output = concaveDrain1_out. This step creates a conditional statement whereas the input raster values less than the concave threshold is reclassed to value = 1. All other values = 0.

Eliminate Small Concave Areas – Conditional, Region Group, Zonal Geometry tools: Input = concaveDrain1_out, output = concaveDrain3_out, geometry type = AREA. This series of steps first reclass the input to value = 1, create regional groups based on isolated zones, and calculate the area of each regional group. Finally, a conditional statement reclasses to 'NoData' all regional groups less than a minimum area.

Resample Concave Drain Raster – Resample tool: Input = concaveDrain3_out, output = concaveDrain, cell size = 9, resampling technique = NEAREST. This step resamples the concave drainage raster resolution from 3 feet to 9 feet.

Create Flow Accumulation Raster – Flow Accumulation tool: Input = dem9ft_fill_flowDirect, output = concaveRaster, in weight raster = concaveDrain, data type = INTEGER, flow direction type = D8 (default). This step created a raster whose values represent the accumulated flow to each cell. This step creates a raster that models accumulated flow to each cell with a weight added in that represents high concave areas.

Refine Drainage Network – Conditional tool: Input = flowAccum, output = dem9ft_fill_flowAccum. This series of steps first multiply all flow accumulation raster values by 81 (area of raster resolution) and then create conditional statement that reclasses all cells with a minimum flow accumulation as value = 1.

Create Stream Order Raster – Stream order tool: Stream Input = dem9ft_fill_flowAccum_str, flow direction input = dem9ft_fill_flowDirect, method = STRAHLER, output = streamlinesOrder_raster. This step reclasses the stream raster output based on stream confluence.

Create Stream Order Polylines – Stream to Feature tool: Input #1 = streamlinesOrder_raster, input #2 = dem9ft_fill_flowDirect, output = streamlinesOrder_polylines, simplify polylines = SIMPLIFY. This step will convert raster stream order and direction to polylines.

Delete All Intermediate Datasets – Delete tool. This step deletes a list of the intermediate datasets used in this section.

Clean Channel Lines and Divide into Equal Intervals

This section first determines if channel lines are created from the previous steps. If channel lines are not created, the process will end; no further processing of the study area is necessary. If channel lines are created, it removes first-order streamlines under a specific length and under a specific slope value. It then creates points along the streamlines every 100 feet and uses these points to divide the streamlines into equal length intervals.

Delete Streamlines by Length – Copy Features, Select Layer by Attribute, Delete Features tools: Input = streamlinesOrder_polylines, output = streamlinesOrder_polylines_minLines, where clause = ‘grid_code = 1’, selection type = NEW_SELECTION. New selection type = SUBSET_SELECTION, where clause = ‘Stream_Length < 27’. This step will first copy streamlinesOrder_polylines to a new dataset. The through a series of selections, select only the streamlines that are first order and less than 27 feet in length.

Delete Streamlines by Slope – Select Layer by Attribute, Zonal Statistics as Table, Join Field, Delete Feature tools: Inputs = streamlinesOrder_polylines_minLines and dem9ft_fill_slope, output = removelinesTable, where clause = ‘grid_code = 1’, selection type = NEW_SELECTION. Join ‘MEAN’ field from removelinesTable to streamlinesOrder_polylines_minLines. New selection type = SUBSET_SELECTION, where clause = ‘MEAN < 5’. Delete selection. This step will delete the first order streamlines that have a mean slope less than five degrees.

Dissolve Streamlines by Stream Order – Dissolve, Alter Field tools: Input = streamlinesOrder_polylines_minLines_joinTbl, output = streamlines_RAW_disslv, dissolve field = ‘grid_code’. This step dissolves the streamlines by stream order and renames a field.

Create Equal Distant Points Along Streamlines = Generate Points Along Lines tool: Input = streamlines_RAW_disslv, output = channelsIntervalPoints, point placement = DISTANCE, distance value = 100. This step will create a point along the streamlines feature class every 100 feet.

Split Streamlines at Points – Split Line at Point tool: Input = streamlines_RAW_disslv, output = channelsEqualLength, point features = channelsIntervalPoints, search radius = 2. This step will split the streamlines at every point and every confluence.

Delete All Intermediate Datasets – Delete tool. This step deletes a list of the intermediate datasets used in this section.

Create Inundation End Points

This section creates streamline end points and appends them to the interval points. These end points will be used to finalize the interval points created and output with the Part 3 Basins tool.

Convert Channel Vertices to Points – Feature Vertices to Points tool: Input = channelsEqualLength, output = verticesByChannel, point location = BOTH_ENDS. This step will create a point at each channel line vertex.

Isolate End Points – Generate Near Table, Add Join, Statistics, Select Layer by Attribute: Input = verticesByChannel, output = verticesEndPoints, near search radius = 2-foot, statistics field = COUNT, select SQL = 'FREQUENCY = 1'. This series of steps will first create a table that links each vertex point with all the near channel lines within the search radius. The count of near channels is determined and the points with only one near channel (channel end points) is appended to the channel interval points.

Append End of Channel Vertex Points to Interval Points – Copy Features, Append, Delete Field tools: Input = verticesEndPoints, output = channelsIntervalPoints. This step appends the End Points to the interval channel points.

Delete All Intermediate Datasets – Delete tool. This step deletes a list of the intermediate datasets used in this section.

Create File Geodatabase for Output Datasets, Part 2 Model

This section creates a new file geodatabase for Part 2 of the DFSM model and produce copies of select base map rasters in the new geodatabase. When rerunning Part 1 for including a hydro-conditioned dem, this section will pass so that the original surface rasters will be maintained in the Part 2 geodatabase for continued processing.

Create new geodatabase – Create File GDB tool: Input = workSpace, GDB name = DFSM2_InitiationTransport.gdb. This step creates a new file geodatabase in the workspace directory. This will contain the model outputs for the DFSM Part 2 model.

Copy Select Initial Raster Datasets – Copy Raster tool: Inputs = dem9ft_fill, dem9ft_fill_slope, and dem3ft_hillshade, outputs = copy of input datasets. This step makes copies of the three input rasters into the DFSM2_InitiationTransport.gdb geodatabase.

DFSM Part 2 Initiation and Transport: Introduction

This GIS Methods Section for Part 2 of the Debris Flow Susceptibility Model (DFSM) is described in Section 3.5 in the report. The Part 2 Initiation and Transport tool calculates initiation potential (Sections 3.5.1 – 3.5.4) and transport potential (Sections 3.5.5 – 3.5.8) parameters within the study area.

The Part 2 Initiation and Transport tool's only input is the workspace folder location. That folder location MUST be the folder location used in Part 1. In this way, the Part 2 model will be able to copy the final channel lines from Part 1 outputs and then produce output datasets into the geodatabase (DFSM2_InitiationTransport.gdb) created during the Part 1 model run.

DFSM Part 2 Initiation and Transport: Methods

Copy Channel Lines from Part 1 Geodatabase to Part 2 Geodatabase and Create Unique ID

This section creates a copy of the channel lines features class into the DFSM2_InitiationTransport.gdb geodatabase.

Copy channel Lines – Copy Features and Add Field tools, Update Cursor: Input = ChannelsEqualLength, output = ChannelsEqualLengthFinal, location = DFSM2_InitiationTransport.gdb. This step will copy the channel lines from the Part 1 model output into the Part 2 model geodatabase. A new field is added, and a unique channel ID is calculated.

Create Initiation Potential Raster Dataset

This section creates the initiation potential raster dataset. It produces the curvature, slope, and distance rasters, calculates local characteristics for each, and reclasses them. It then overlays them to calculate the initiation potential raster. See Sections 3.5.1 – 3.5.4 for additional explanation of these methods.

Create Curvature Raster – Curvature tool: Input = dem9ft_fill, output (Plan Curve) = dem9ft_fill_curvPlan. This step will create the curvature raster.

Determine Local Curvature Characteristics – Focal Statistics tool: Input = dem9ft_fill_curvPlan, output = dem9ft_fill_curvPlan_local, neighborhood = 'Circle 35 MAP', statistics type = MEAN. This step will calculate a mean curvature within a neighborhood for each output raster cell. The neighborhood is defined roughly as 100 square meters or 729 square feet.

Reclass Local Curvature Raster – Reclassify tool: Input = dem9ft_fill_curvPlan_local, output = dem9ft_fill_curvPlan_local_reclass, reclass field = VALUE, remap value = '-100 -0.400 4; -0.400 0.300 3; 0.300 1.100 2; 1.100 100 1'. This step reclasses the local curvature raster into four integer classes (1 – 4), based on thresholds established in Section 3.5.2. These are the final curvature values.

Determine Local Slope Characteristics – Focal Statistics tool: Input = dem9ft_fill_slope, output = dem9ft_fill_slope_local, neighborhood = 'Rectangle 35 35 MAP', statistics type = MEAN. This step will calculate a mean slope within a neighborhood for each output raster cell. The neighborhood is defined roughly as 100 square meters or 729 square feet.

Reclass Local Slope Raster – Reclassify tool: Input = dem9ft_fill_slope_local, output = dem9ft_fill_slope_local_reclass, reclass field = VALUE, remap value = '0 15 1; 15 25 2; 25 35 3; 35 90 4'. This step reclasses the local slope raster into four integer classes (1 – 4), based on thresholds established in Section 3.5.1. These are the final slope values.

Calculate Distance to Channels Raster – Euclidean Distance tool: Input = ChannelsEqualLengthFinal, output = distanceToChannel, cell size = 9, distance method = PLANAR. This step will calculate a raster where the cell values are based on the cell's distance from the nearest channel line.

Reclass Distance to Channel Raster – Reclassify tool: Input = distanceToChannel, output = distanceToChannel_reclass, reclass field = VALUE, remap value = '0 100 4;100 200 3;200 300 2;300 10000 1'. This step reclasses the local distance raster into four integer classes (1 – 4), based on thresholds established in Section 3.5.3. These are the final distance to channel values.

Calculate Raw Initiation Potential Raster – Combine tool: Inputs = dem9ft_fill_curvPlan_local_reclass + dem9ft_fill_slope_local_reclass + distanceToChannel_reclass, output raster = InitiationRaster. This step calculates 64 possible combinations from the result of overlapping reclassed local slope, curvature, and distance from channel cell values from the three input rasters.

Delete All Intermediate Datasets – Delete tool. This step deletes a list of the intermediate datasets used in this section.

Calculate Initiation Potential Scores

This section uses the slope, curvature, and distance to channel reclassed values to calculate the final Initiation Potential scores. Additional details about how the initiation potential values are calculated are in Section 3.5.4 in the report.

Reclass Raw Initiation Potential Raster – Add Field tool and Update Cursor: Input = InitiationRaster. This step adds a new field and calculates final initiation potential values in this field based on combinations of the integer fields from the Combine tool. These initiation potential values are Very Low to None, Low, Moderate, or High.

Calculate Channel Confinement Values for Transport Potential

This section calculates channel confinement by examining elevation ranges 100 feet perpendicular to the channel line intervals. Additional details about how the channel confinement is calculated are in Section 3.5.7 in the report.

Create Transects Along Channel Lines – Generate Transects Along Lines, Alter Field, and Add Field tools and Update Cursor: Input = ChannelsEqualLengthFinal, output = transects, interval = 27, transect length = 200, include ends = END_POINTS. This step creates 200 foot transect lines along each channel line interval every 27 feet. Each transect ID is copied to a new field in its attribute table. Each transects corresponding channel line interval ID is added to a new field in its attribute table.

Create Transect Sample Points – Generate Points Along Lines tool: Input = transects, output = transectPoints, point placement = DISTANCE, point distance = 3, include end points = NO. This step creates a series of sample points along each transect line at 3-foot intervals. Each point's source transect ID is written to the attribute table.

Extract Elevation Values – Sample and Join Field tools: Input raster = dem9ft, input location data = transectPoints, output = transectPointsExtract, unique ID field = 'PointsID', resampling = NEAREST. This step calculates the elevation value for each sample point, based on the input dem.

Calculate Elevation Range Per Transect – Summary Statistics and Join Field tools: Input = transectPoints, output = sstatsTableRANGEss, statistics field = RANGE, case field = 'ORIG_FID'. This step calculates the range of elevation values along each transect. It joins the table results using the transect ID existing in the transectPoints feature class.

Calculate Mean Elevation Range Per Channel Interval – Summary Statistics and Join Field tools: Input = transects, output = transectsMEANss, statistics field = MEAN, case field = 'ORIG_FID'. This step calculates the mean elevation range values along each channel interval. It joins the table results using the channel ID existing in the transects feature class. These are the raw confinement values.

Delete All Intermediate Datasets – Delete tool. This step deletes a list of the intermediate datasets used in this section.

Calculate Channel Gradient Values for Transport Potential
This section calculates channel gradient of each channel line interval based on its average underlying slope. Additional details about how the channel confinement is calculated are in Section 3.5.6 in the report.

Calculate Mean Slope – Zonal Statistics as Table tool: Input Zone = ChannelsEqualLengthFinal, input value raster = dem9ft_fill_slope, output = slopeTable, zone field = 'OBJECTID', statistics type = MEAN. This step calculates mean slope for each channel line interval. These results are then joined to the channel line intervals attribute table using common ID values.

Join Mean Slope Values – Join Field, and Alter Field tools: Input = ChannelsEqualLengthFinal, join feature = slopeTable, join field = 'MEAN'. This step joins the mean slope values from slopeTable to the channel line intervals based on common ID values. These are the raw gradient values.

Calculate Transport Potential from Channel Confinement and Channel Gradient
This section generates the transport potential for each channel line interval using the reclassed confinement and gradient values. See Section 3.5.8 of the report for additional information.

Reclass Confinement and Gradient Values – Add Field tool, Update Cursor: Input = ChannelsEqualLengthFinal. This step first adds new results fields for confinement, gradient, and transport potential values to the ChannelsEqualLengthFinal feature class. It then reclassifies both the confinement and gradient raw values into four classes (1 – 4) and puts the results in the respective new fields. Finally, it will add the reclassed confinement and gradient values and, based on the resulting added values, determine if transport potential is Very Low to None, Low, Moderate, or High.

DFSM Part 3 Basins: Introduction

This GIS Methods Section for Part 3 of the Debris Flow Susceptibility Model (DFSM) is described in Section 3.7 in the report. The Part 3 Basins tool delineates basins within the study area and calculates multiple basin characteristics. Finally, it will create a final geodatabase called DFSM4_FinalDatasets.gdb that contains copies of all final datasets. A partial list of these datasets are in Section 3.10.1 under the "Channelized Debris Flow Inventory" and "Channelized Debris Flow Susceptibility" headers.

The Part 3 Basins tool has multiple inputs. These are 1. the workspace folder location, 2. the upper/lower bounds feature class, 3. the name of the study area, 4. the debris flow fans feature class, and 5. the historic points feature class. That folder location must be the location used in Part 1 and Part 2. In this way, the Part 3 Basins model will be able to copy the final channel lines from Part 2 outputs and then produce output datasets into the DFSM3_Basins.gdb geodatabase.

DFSM Part 3 Basins: Methods

Create New Output Geodatabase

This step creates a new file geodatabase that will contain all the intermediate output datasets.

Create New File Geodatabase – Create File GDB tool: Input = workSpace, GDB name = DFSM3_Basins.gdb. This step creates a new, empty file geodatabase in the workspace folder.

Delineate Study Area Basins

This section delineates basin polygons in the study area. It requires the upper/lower bounds and channel lines feature classes to create basin pour points. Additional basin delineation methods are in Section 3.6 in the report. Methods for creating the upper/lower bounds feature class are in Section 3.6 in the report.

Create Pour Points – Intersect tool: Inputs = upper/lower bounds and channelsEqualLengthFinal feature classes, output = pourPoints, join attributes = ALL, output type = POINT. This step creates intersection points where the upper/lower bounds and channel lines feature classes overlap.

Create Pour Points Raster - Snap Pour Points tool: Input point data = pourPoints, input accumulation raster = dem9ft_fill_flowAccum, output = pourPointsSnap, snap distance = 9, pour point field = 'OBJECTID'. This step creates rasterized pour points that can move to the cell of highest accumulated flow within the snap distance.

Create Basins Raster – Watershed tool: Input flow direction raster = dem9ft_fill_flowDirect, input pour point data = pourPointsSnap, output = basinRaster, pour point field = 'Value'. This step uses the rasterized pour points and flow direction raster to create a raster dataset of delineated basins.

Convert Basins Raster to Polygons – Raster to Polygon tool: Input = basinRaster, output = basinpolysInitial, simplify = NO_SIMPLIFY, raster field = 'Value', create multipart features = SINGLE_OUTER_PART. This step creates polygons from the basin raster.

Remove Small Basins – Select, Alter Field, and Delete Field tools: Input = basinpolysInitial, output = basinpolysWorking, where clause = 'Shape_Area >= 16146'. This step selects the basins greater than 16,146 square feet and outputs a new feature class of only the selected basins.

Assign Pour Point ID to basins – Alter Field, Delete Field tools: Input = basinpolysWorking, old field name = 'gridcode', new field name = 'PourPointObjID'. This step will rename the gridcode field from the basin delineation step to PourPointObjID for clarity.

Delete All Intermediate Datasets – Delete tool. This step deletes a list of the intermediate datasets used in this section.

Calculate Basin Statistics

This section contains a series of steps that calculates all the basin statistics used for determining the final basin score.

Add Initial Fields to Basin Feature Class

This step adds multiple empty fields for future calculations.

Add fields to Basins – Add Fields tool: Input = basinpolysWorking. Field list = basin ID, HUC12 ID, Melton's Number, Max Potential Volume, High Initiatiton Volume area.

1. **Calculate Basin Relief**

This section calculates the relief value for each basin. This is the difference between the minimum and maximum elevation within the basin polygon.

Calculate Elevation Range Per Basin – Zonal Statistics as Table, Join Field, Alter Field tools: Input zone = basinpolysWorking, input raster = dem9ft_fill, zone field = 'OBJECTID', output = basinreliefTable, statistics type = RANGE. This step will calculate the range of elevation values within each basin polygon. The table field is joined to the basins polygons by common ID and renamed.

Delete All Intermediate Datasets – Delete tool. This step deletes a list of the intermediate datasets used in this section.

2. **Calculate Select Basin Characteristics**

This section compiles and calculates several different basin characteristics. It creates a unique ID and populates the user input for the watershed name for each basin. It also calculates each basin's Melton's Number and maximum potential volume.

Calculate Unique ID, Melton's Number, Maximum Potential Volume and Study Area Name Per Basin – Update Cursor: Input = basinpolysWorking. This step uses an update cursor to calculate and populate fields for a basin unique ID and the basin's Melton Number, maximum potential volume and study area name.

Determine Historic Points Per Basin

This section determines the number of historic debris flow initiation points for each basin. It also applies the unique ID of the overlaying basin to the historic points feature class. If no historic point feature class is provided as an input, the tool will pass values of '9999' to the basins feature class attribute table.

Total Historic Points Per Basin – Tabulate Intersection, Join Field, and Alter Field tools and Update Cursor: Input zone = basinpolysWorking, input features = historicPoints, output = historicPointsTable, zone fields = 'BasinID'. This step creates a table the shows the count of historic points that intersect with basins. The table point count field is joined to the basinpolysWorking feature class using the basin ID and renamed. Where there are no field joins in the basins feature class, the update cursor populates the count field with a zero.

Add Basin ID to Intersecting Historic Points – Identity and Join Field tools: Inputs = historicPoints + basinpolysWorking, output = dfHistoricPoints, join attribute = ONLY_FID. This step will identify the basins that contain historic points and add the Basin ID.

Delete All Intermediate Datasets – Delete tool. This step deletes a list of the intermediate datasets used in this section.

3. Calculate Initiation High Volume

This section calculates the total volume of high initiation potential for each basin.

Tabulate High Initiation Potential Per Basin – Tabulate Area tool: Input zone = basinpolysWorking, input values = InitiationPotential, output = initiationTabAreaTable, zone field = 'BasinID'. This step determines the area (square feet) of High initiation potential within each basin.

Calculate Volume – Update Cursor, Join Field tool: Input = basinpolysWorking. This step multiplies the area of High initiation potential by three and adds that value to the basins feature class.

Delete All Intermediate Datasets – Delete tool. This step deletes a list of the intermediate datasets used in this section.

4. Calculate Number of Initiation Sites and Initiation Potential Basin Score

This section calculates the number of initiation sites for each basin based on the basin's total high initiation potential area. It then applies a basin initiation score based on the number of initiation sites. Additional information on initiation sites and the initiation potential basin score is in Section 3.7.1 of the report.

Calculate Initiation Sites and Scores – Add Fields and Delete Field tools and Update Cursor: Input = basinpolysWorking. This step adds new results fields and then uses an update cursor to calculate the number of initiation sites (high initiation area / 1000). From the number of initiation sites, the update cursor also calculates the initiation potential score based on ranges of site amounts. Final scores are given a text value (Very Low to None, Low, Moderate, or High) and a numeric value (1 – 4).

Delete All Intermediate Datasets – Delete tool. This step deletes a list of the intermediate datasets used in this section.

5. Calculate Transport Potential Score for Each Basin

This section determines the final transport potential basin score. It first determines the percentage of high and moderate transport potential channel line length to total channel length in each basin. The final score is calculated by the percentage amount. Additional information on the transport potential basin score is in Section 3.7.2 of the report.

Assign Channel Lines with Overlay Basin ID – Identity, List Fields, and Delete Field tools: Input = ChannelsEqualLengthFinal, identity input = basinpolysWorking, output = ChannelBasinsIdentity, join attributes = ALL. This step clips the channel lines to the overlay basin and assigns them all the basin attributes. The Basin ID field is retained but all other unneeded basin fields are then removed from the channel lines, based on the field list.

Dissolve Basin Channel Lines by Transport Potential Class – Dissolve tool: Input = ChannelBasinsIdentity, output = disslvChannelsBasins, dissolve fields = 'BasinID' and 'TransportPotential' , dissolve stats = 'Shape_Length SUM'. The purpose of this step is to determine the total length of channel lines for each transport potential class within each basin.

Calculate Total Channel Length Per Basin – Statistics, Alter Field, and Join Field tool: Input = disslvChannelsBasins, output = sumstatsChannelLgthTable, statistics fields = 'Shape_Length SUM', case field = ‘BasinID’. This step calculates the total channel length within each basin. The table field is joined to the channel lines feature class using the common Basin ID.

Calculate Channel Line Percent Per Basin – Add Field tool and Update Cursor: Input = disslvChannelsBasins. This step calculates the percent of channel lines by transport potential classes within each basin. This result is added to a new field in the channel lines feature class.

Combine High and Moderate Transport Potential Channel Lines Per Basin – Select Layer by Attribute and Dissolve: Input = disslvChannelsBasins, output = disslvChannelsTransPercent, dissolve fields = ‘TransportLengthPercent’, dissolve stats = ‘TransportLengthPercent SUM’. This step combines the channel lines with High and Moderate transport potential classes by basin.

Add High and Moderate Channel Line Percent to Basins – Table to Table, Delete Features, Join Field, and Alter Field tools and Update Cursor: Input = disslvChannelsTransPercent, output = transBasinPercentLength. This step converts the dissolved channels feature class from the previous step into a table and deletes the dissolved feature class. It then joins the percent field from the table to the basins feature class (basinpolysWorking) using the common ID field. Finally, it renames the joined field and uses the update cursor to replace <Null> values with 1.

Calculate Final Transport Potential Score – Add Field tool and Update Cursor: Input = basinpolysWorking. This step will add new results fields and then use the update cursor to calculate the final transport potential scores. Final scores are given a transport potential score where 0 – 10% length = Very Low to None (1), 10 – 25% length = Low (2), 20 – 50% length = Moderate (3), and 50 – 100% length = High (4).

Delete All Intermediate Datasets – Delete tool. This step deletes a list of the intermediate datasets used in this section.

6. Debris Flow Basin Calculations

This section first applies the origin basin ID to the pour points. Next it calculates the number of debris flow fans that overlay each pour point and removes debris flow fans that do not overlay a pour point. This count is applied to the basin feature class. If no debris flow fans feature class is provided as an input, the tool will pass values of ‘9999’ to the basins feature class attribute table.

Add Basin ID to Pour Points and Remove Fields – Join Field, Fields List, Delete Field tools: Input = pourPoints, join table = basinpolysWorking, fields = BasinID. This step adds the basin ID to the origin pour point. It then creates a list of fields that should be deleted and deletes them.

Remove Unused Pour Points – Select Layers by Attribute and Delete Rows tools: Input = pourPoints, where clause = ‘BasinID IS NULL’. This step will select all the rows with no basin ID (<Null>) and delete them.

Get Count of Fans Overlaying Pour Points – Spatial Join, Join Field, Delete, and Delete Field tools: target feature = pourPoints, join feature = Debris Flow Fans, output = tempPourPoints, join operation = JOIN_ONE_TO_ONE, join type = KEEP_ALL, match option = INTERSECTS. This step will spatially join the debris flow fan attribute table to the pour points and create a temporary pour point feature class. This temporary file count field is joined to the pour points feature class using common ID and the temporary feature class is deleted.

Remove Fans Not Overlaying Pour Points – Select Layer by Location and Copy Features tools: Input = Debris Flow Fans, select features = pourPoints, overlap type = INTERSECT, copy output = dfFansFeature. This step will select the debris flow fans that overlay pour points and create a new feature class from the selection.

Determine Fan Count at Mouth of Basins – Join Field and Alter Field tools. Input = basinpolysWorking, join feature = pourPoints, fields = 'Join_Count'. This step will join the debris flow fan count field from the pour points feature class to the basins feature class and rename the joined field.

Delete All Intermediate Datasets – Delete tool. This step deletes a list of the intermediate datasets used in this section.

7. Calculate Final Debris Flow Potential Basin Score

This section adds the initiation and transport potential basin scores to determine each basin's debris flow potential. Additional information on the final debris flow potential basin score is in Section 3.7.3 of the report.

Add the Initiation and Transport Scores and Reclass – Add Field tool and Update Cursor: Input = basinpolysWorking. This step adds the numerical initiation and transport fields and reclasses them into the final basin debris flow score. Final scores are given a text value (Very Low to None, Low, Moderate, or High).

Create New Geodatabase with Final Basin Debris Flow Potential Datasets

This section compiles all the final feature classes from multiple output geodatabases and user input feature classes and outputs them into one geodatabase. In addition, working fields that are not necessary are deleted.

Create New File Geodatabase – Create File GDB tool: Input = workSpace, GDB name = DFSM4_FinalDatasets.gdb. This step creates a new, empty file geodatabase in the workspace folder.

Copy Basins Feature Class – Copy Features and Delete Field tools: Input = basinpolysWorking, output = DF_Basins. This step will copy the working basins feature class to the final dataset geodatabase. Multiple unneeded fields are deleted.

Clip Initiation Potential Raster – Clip Raster and Add Field tools and Update Cursor: Input = InitiationPotential, output = tempInitiation. This step clips the initiation potential raster with the basin polygons and outputs it to the final dataset geodatabase. It then adds a new field and uses the update cursor to copy values from one field to the new field.

Update Initiation Potential Raster Value Field – Lookup, Delete, and Add Field tools and Update Cursor: Input = tempInitiation, output = DF_InitiationPotential. This step will set the raster 'Value' field to represent the initiation potential classes. It adds a new field is and uses the update cursor adds the classes as text to the new field. Finally, it removes unnecessary fields and then deletes the temporary initiation potential raster dataset.

Copy Channel Lines Feature Class – Copy Features and Delete Field tools: Input = ChannelsBasinsIdentity, output = DF_TransportPotential. This step copies the working channel lines feature class to the final dataset geodatabase. It then deletes unnecessary fields.

Clip Historic Points Feature Class – Clip (analysis) tools: Input = Historic Points, output = DF_HistoricPoints, clip features = basinpolysWorking. This step clips the historic points to the basin polygons and outputs to the final dataset geodatabase.

Select and Copy Fans with Basin ID – Select Layer by Attribute, Copy Features, and Delete Field tools. Input = dfFansFeature, output = DF_Fans, where clause = 'BasinID IS NULL', selection type = 'SWITCH_SELECTION'. This step selects the debris flow fans that are not associated with a basin, switches the selection, and copies the selected features to a new feature class. Finally, unnecessary fields are deleted.

Copy 9-Foot Resolution DEM – CopyRaster tool: Input = dem9ft_fill, output = DF_DEM9ftFilled. This step copies the filled, 9-foot resolution dem to the final geodatabase.

Create 9-Foot Resolution Hillshade – Hillshade tool: Input = dem9ft, output = DF_Hillshade. This step creates a hillshade raster from the 9-foot resolution dem and outputs to the final dataset geodatabase.

Delete All Intermediate Datasets – Delete tool. This step deletes a list of the intermediate datasets used in this section.

Create Input Datasets for Inundation Tool

This section creates the Contributing Area rasters, and Inundation Points for the typical, intermediate, and extreme scenarios. These datasets are copied into the DFSM4_FinalDatasets.gdb.

1. **Inundation Basins, Channel Lines, and Points**

Create LMH Basins Feature Class – Select Layer by Attribute, Copy tools: Input = finalBasins, output = inundationBasins, SQL = "BasinScore = 'High' OR BasinScore = 'Moderate' OR BasinScore = 'Low'". This step selects the basins with a basin susceptibility score of Low, Moderate, or High and copy the selection to a new feature class.

Clip Channel Lines to Inundation Basins – Add Join, Copy Features, Select Layer by Attribute tools: Input = DF_TransportPotential, output = inundationChannelLines, join features = inundationBasins. This step clips the interval channel lines to the Inundation Basins and remove channel lines that have a susceptibility score of 'Very Low to None.'

Create Final Inundation Points (Intermediate and Extreme scenarios) – Dissolve, Generate Points Along Lines, Select Layer by Attribute, Select Layer by Location, Merge tools: Input = inundationChannelLines, distance value = "25 Feet", output = inundationPoints, This series of steps dissolves the inundation channel lines and then generates points along the lines every 25 feet. It then selects the inundation End Points based on location relative to the inundation basins and then merges the selection with the generated points.

Reclass Initiation Potential Raster – Reclassify tool: Input = DF_InitiationPotential, output = ID_contributingArea_TempIE, remap table = RemapValue([[1, 0], [2, 0],[3, 1],[4, 1],["NoData", 0]]). This step reclasses the final Initiation Potential raster to give the Moderate and High classes a new value of 1 and the other classes, including No Data, a new value of 0. The output is a temporary raster.

2. **Create Final Contributing Areas Rasters (Three Scenarios) and Inundation Points (Typical)**

Create Final Inundation Points (Typical scenario) – Select Layer by Attribute, Select Layer by Location, Copy Features tools: Inputs = inundationBasins and ID_InundationPoints_IE, output ID_inundationPoints_T, SQL statement = "InitiationSites >= 1". This step clips the Intermediate/Extreme inundation points to the inundation basins that have at least one initiation site.

Clip Transect Points (from DFSM Part 2) to inundation Basins – Select Layer by Location and Copy Features tools: Inputs = transectPoints and inuncationBasins, output = transectTPoints. This step selects the transect points that fall within the inundation basins and create a new feature from the selection.

Reclass Initiation Potential Raster – Reclassify tool: Input = DF_InitiationPotential, output = highTempContribArea, remap table = RemapValue([[1, 0], [2, 0],[3, 0],[4, 1],["NoData", 0]]). This step reclasses the final Initiation Potential raster to give the High class a new value of 1 and the other classes, including No Data, a new value of 0. The output is a temporary raster.

Extract Distance to channel and High Initiation – Extract Multi Values to Points: In point features = transectTPoints, in rasters = [distanceToChannel, highTempContribArea]. This step, for each transect point, extracts the distance to channel and high initiation (reclassed to 1).

Determine the Maximum Distance of High Initiation – Select Layer by Attribute and Summary Statistics tools: Input = transectTPoints, output = transectTPoints_ssTable, field statistics = "distanceToChannel MAX". This step will use a method like calculating channel confinement (DFSM Part 2). It creates a table that calculates the MAXIMUM distance of transect points for each channel line interval.

Calculate Mean MAX value for remaining channel lines – Add Field, Summary Statistics, Join Field, Select Layer By Location, Select Layer By Attribute tools, and Update Cursor: Input = inundationChannelLines, output = inundationChannelLines_ssTable, field statistics = "BufferDistance MEAN". These steps calculate the MEAN Maximum distance for High Initiation for each channel line segment, based on transport class and basin location. It then updates the buffer distance to the correct channel line segments that fall within basins with at least one initiation site.

Buffer Channel Lines – Select Layer by Attribute, Buffer, Clip Raster, Delete Features tools: Input = inundationChannelLines and inundationBasins, output = inundationTempBuffer, where clause = "BufferDistance IS NOT NULL". These steps first select the channel lines that have a buffer distance value and then buffer the selected lines by their corresponding buffer distance field values. The buffers are then clipped to the inundation basins.

Buffer to Raster and Mosaic – Polygon to Raster, Mosaic to New Raster: Input = inundationBuffer, output = ID_ContributingArea_T. These steps will first convert the channel lines buffer to a raster. This raster is then mosaiced first to the temporary inundation contributing area raster (typical scenario) to create the final typical scenario contributing area raster (ID_ContributingArea_T). Finally, it is mosaiced to the temporary inundation contributing area raster (intermediate and extreme scenarios) to create the final intermediate and extreme scenario contributing area raster (ID_ContributingArea_IE).

Delete All Intermediate Datasets – Delete tool. This step deletes a list of the intermediate datasets used in this section.

DFSM Part 6 Post-Processing: Introduction

This GIS Methods Section for Part 6 of the Debris Flow Susceptibility Model (DFSM) will take us from Section 3.10 in the report. The Part 6 Inundation Zones Post-Processing tool processes the inundation outputs from the USGS model, Part 5_Multi-Point Laharz_py and is considered the sixth in the sequence of steps to complete the modeling analysis.

The Part 6 Inundation Zones Post-Processing tool inputs one inundation output at a time. The tool inputs include 1. the workspace folder location, 2. the watershed name, 3. final debris flow basins, 4. the inundation raster, 5. the debris flow scenario (drop-down menu; A, B, or C), 6. the zone (drop-down menu; Typical, Intermediate, or Extreme), and 7. an optional mask. The folder location does not have to be the location used in DFSM Parts 1, 2, or 3.

This tool will produce a geodatabase called DFSM5_FinalInundation.gdb to contain the processed inundation outputs. The inundation output will be classed into transport/erosion and deposition. Multiple raster outputs of the model can be produced in the same output geodatabase if they are not similarly named. Similarly named outputs will be overwritten.

DFSM Part 6 Post-Processing: Methods

Create New Output Geodatabase and Temporary Folder

This step creates a temporary folder the contains all the intermediate datasets and a new file geodatabase that contains all the output datasets.

Create New File Geodatabase – Create File GDB tool: Input = workSpace, GDB name = DFSM5_FinalInundation.gdb. This step creates a new, empty file geodatabase in the workspace folder.

Create Temporary Working Folder – Python coding: Output = workFolder. This step first checks if the temporary folder exists. If it does, it will delete it and create a new, empty folder. The temporary folder contains all the intermediate outputs.

Inundation Post-Processing

Remove Slivers and Holes

The first series of steps removes slivers and holes in the raw inundation raster output from the USGS Inundation Tools.

Reclass Inundation Raster – Reclassify tool: Input = Inundation Raster, output = rasterReclass1, remap = "0 NODATA;0 1000 1", field = “Value”. Because the USGS inundation tool raster output contains multiple values, this step reclasses the inundation raster input into 0 = no data and all other values into 1.

Remove Slivers and Holes – Focal Statistics tool: Input = rasterReclass1, output = rasterFocStats, neighborhood = "Rectangle 3 3 CELL", statistics = “SUM”. This step reclasses raster cells that do not have surrounding cells of value (slivers) into ‘no data’ and ‘no data’ cells (holes) that are surrounded by cells of value into that surrounding value.

Reclass Focal Statistics Output – Reclassify tool: Input = rasterFocStats, output = rasterReclass2, remap = "1 3 NODATA;3 1000 2", field = “Value”. This step reclasses all cells with values of 1 – 3 into ‘no data’ and all other cells into value = 2.

Remove Inundation within a Mask (Water Bodies)

The next series of steps first reclass raster values inside of a water body polygon mask. It then combines mask raster with cleaned inundation raster. The mask is an optional input to the tool. If no mask is input in the tool, these steps will be passed over.

Extract Raster within Polygon Mask – Extract by Mask tool: Input = rasterReclass2, output = maskExtract, mask = Polygon. This step extracts raster values that fall within the polygon mask and output as a new raster.

Reclass Extracted Raster – Reclassify tool: Input = maskExtract, output = reclassifyMask, remap = "2 0", field = “Value”. This step reclasses the extracted raster from value = 2 to value = 0.

Mosaic Inundation and Extracted Rasters – Mosaic to New Raster tool: Inputs = maskNull and rasterReclass2, output = mosaicRasterRaw, pixel type = "8_BIT_UNSIGNED", cell size = "9", number of bands = "1", mosaic method = "FIRST". This step mosaics the reclassed, extracted raster on top of the cleaned inundation raster input.

Reclass Mosaic Raster – Reclassify tool: Input = mosaicRasterRaw, output = mosaicRasterNull remap = "0 NODATA;2 2", field = “Value”. This step reclasses all values = 0 (from extracted raster) to “no data” and all other raster values remain the same.

Reclass Inundation Raster into Transport/Erosion and Deposition

The next series of steps will reclass the inundation raster into no inundation, transport/erosion, and deposition. No inundation values may include raster values within a water body mask if that mask was included as an input.

Extract Inundation Raster by Basins – Extract by Mask tool: Input = rasterReclass2, output = extractRaster, mask = basins. This step extracts the cleaned inundation raster within the final basins.

Reclass Extracted Raster – Reclassify tool: Input = extractRaster, output = rasterReclass3, remap = “2 1”, field = “Value”. This step reclasses extracted inundation raster (within basins) from value = 2 to value = 1.

Mosaic Inundation Rasters – Mosaic to New Raster and Build Raster Attribute Table tool: Input = rasterReclass3 + mosaicRasterNull (mask included) or rasterReclass3 + rasterReclass2 (no mask included), output = mosaicRaster, pixel type = "8_BIT_UNSIGNED", cell size = "9", number of bands = "1", mosaic method = "FIRST". This step mosaics the value = 2 raster (deposition) and the value = 1 raster (transport/erosion) and build the raster table. This is the final inundation raster dataset.

Rename Final Inundation Raster – Exists and Rename tools: Input = mosaicRaster, output = newRaster, newname = watershedName + "_" + scenario + "_" + zone. This step renames the final raster dataset based on the watershed name, scenario type, and zone type tool inputs.